Hyperthermic applications and issues relating to the assessment of technical quality and its clinical verification

Hypertherme applicaties en vraagstukken met betrekking tot de bepaling van technische kwaliteit en haar klinische verificatie

Proefschrift

ter verkrijging van de graad van doctor

aan de Erasmus Universiteit Rotterdam,

op gezag van de Rector Magnificus,

Prof. dr. P.W.C. Akkermans M.A.

en volgens besluit van het College voor Promoties.

De openbare verdediging zal plaatsvinden op

donderdag 29 juni 2000 om 11^{00} uur

door

Paulus Johannes Maria RIETVELD

geboren te Rotterdam

Promotiecommisie

Promotor: Prof. dr. P.C. Levendag

Overige leden: Prof. dr. ir. P.M. van den Berg

                              Prof. dr. D. González González

                              Prof. dr. J.G.M. Klijn

                              Dr. ing. G.C. van Rhoon, tevens copromotor

Immervoort en nimmerpoos

Opgetoerd en stripbeloerd
fieber ik een inktselploert,
en brouw het fabelsoort
waaraan geen einder gloort,
want toefselwalm geeft luierroos.
Immervoort en nimmerpoos.

De fantadoos, die triller boort,
Smiespert grollig maar gesmoord.
En ik fieber dan een lang morso
van doening en van vermiso,
Maar prutsel pal, want toef is voos.
Immervoort en nimmerpoos.

Marten Toonder – Teksten en tekeningen

CONTENTS

General Introduction

1.1 Brief biological rationale for hyperthermia

Hyperthermia is defined as a temperature elevation by several degrees (3-7 °C) above the normal physiological level. *In vitro* and *in vivo* experiments have shown that a cell kill response to hyperthermia in conjunction with radiotherapy exists (Harisiadis *et al.* (1975); Alfieri and Hahn, (1978); Dewey *et al.* (1977); Bhuyan, (1979)). Harisiadis *et al.* also report on the increased sensitivity to hyperthermia of tumour parts that are normally less sensitive to radiation alone.

Tumour tissue differs from normal tissue in that it has a chaotic structure of the vascularisation. Due to this inferior vasculature structure, areas exist in the tumour with insufficient blood perfusion, which, in turn, causes local hypoxia and a low pH. Tumour cells in these hypoxic areas are relatively insensitive to radiation and because of the poor blood perfusion, a systemic chemotherapeutic approach for these areas has also less effect. One approach used to attack the cells in insufficiently perfused areas is hyperthermia in combination with radiotherapy or chemotherapy since hypoxic areas are relatively sensitive to hyperthermia. This makes hyperthermia an ideal complementary treatment modality to both radiotherapy and/or chemotherapy, taking into account that normal tissue in general tolerates a hyperthermic treatment of one hour with temperatures of up to 44 °C without relevant clinical damage, i.e. no negative side-effects.

1.2 Clinical experience with hyperthermia

The combination of radiotherapy and hyperthermia has proven its clinical efficacy providing that the combined therapy is applied adequately. The relative value of hyperthermia as an adjunct to either radiotherapy or chemotherapy has been investigated in a number of

phase I-II and phase III studies. Without providing a complete overview of all (recently) published clinical studies including hyperthermia, I will summarise and comment on a few studies, which have had an impact on the credibility of hyperthermia in the last decade.

Perez *et al.* (1991) published a devastating report on the efficacy of hyperthermia in the treatment of superficially measurable tumours. They found no significant difference in overall complete response (**CR**) between radiotherapy alone and radiotherapy plus hyperthermia (307 pts.). The authors concluded that the most important reason that the CR rate did not improve with hyperthermia was because of the poor quality of the hyperthermia treatments. Emami *et al.* (1996) came to the same conclusion in their evaluation of interstitial hyperthermia added to interstitial radiotherapy (184 pts.): no gain in CR due to poor hyperthermic quality. Although these two studies found no beneficial effect due to hyperthermia, neither did they show any negative effects of the addition of hyperthermia.

A more recent study by Vernon *et al.* (1996) showed in a combined analysis of five randomised phase III studies that the addition of hyperthermia to radiotherapy was beneficial for the treatment of advanced primary and recurrent breast cancer (CR rate radiotherapy alone 41% versus 59% for radiotherapy plus hyperthermia (306 pts.)), which difference in local control lasted throughout the 3 years follow-up. Overgaard *et al.* (1995) reported from a phase III study on the addition of hyperthermia to radiotherapy in the treatment of recurrent or metastatic malignant melanoma a significantly improved local tumour control (CR rate radiotherapy alone: 35% versus 62% for radiotherapy plus hyperthermia (68 pts.); 2-year control (SE) 28 (6)% versus 46 (8)%). In the treatment of glioblastoma, Sneed *et al.* (1998) showed in their prospective randomised trial that the addition of interstitial hyperthermia to radiotherapy improved the time to progression and 2-years survival (15% radiotherapy alone versus 31% radiotherapy plus interstitial hyperthermia (79 pts.)). In a multi-centre randomised phase III trial comparing radiotherapy alone with radiotherapy plus hyperthermia in the treatment of primary cervical cancer (stage 2b lateral, 3b and 4a). Van der Zee *et al.* (2000) proved that the combined treatment was significantly more effective than radiotherapy alone: in CR 57% for radiotherapy alone versus 83% radiotherapy plus hyperthermia (114 pts.). This study also showed an improved 3-years survival: 27% versus 51%. Based on the results of the phase III trials for the combined modality of radiotherapy plus hyperthermia in the palliative treatment of cancer (Van der Zee *et al.* (1988); Overgaard *et al.* (1995); Valdagni and Amichetti, (1994)) and curative treatment of primary cervical cancer (Van der Zee *et al.* (2000)), the Dutch minister of Health, Welfare and Sport has decided to acknowledge the

addition of hyperthermia to radiotherapy as standard in the palliative treatment of superficial tumours and curative treatment of primary cervical cancer (stage 2b lateral, 3b and 4a).

The data used by Perez *et al.* (1991) and Emami *et al.* (1996) was obtained in the period of February 1981 till June 1992 while the data analysed by Vernon *et al.* (1996), Overgaard *et al.* (1995), Sneed *et al.* (1998) and Van der Zee *et al.* (2000) was obtained between January 1986 and September 1996. Although there is a large overlap in time, general insight in the hyperthermic mechanisms and continuous technical progress in hyperthermia equipment will have contributed to the different outcome in these studies, indicating strongly that the technical quality of the hyperthermia equipment is of crucial importance to clinical efficacy (and acceptance).

1.3 Quality in hyperthermia

Quality in hyperthermia is defined by the ESHO Quality Assurance (**QA**) guidelines (Hand *et al.* (1989)) and RTOG QA guidelines (Dewhirst *et al.* (1990)). These guidelines cover basic *technical* properties of hyperthermia equipment. However, the effectiveness of hyperthermia, i.e. *clinical* quality, especially in a combined treatment modality, can only be investigated in a phase III study. This often requires large numbers of patients and can be a lengthy process.

The effectiveness of combining radiotherapy or chemotherapy with hyperthermia is defined by a broad spectrum of (prognostic) factors of which the radiotherapy /chemotherapy dose and thermal dose (based on the minimum temperatures) are known entities. Besides these parameters, other (confounding) factors like tumour histology, thermotolerance, volume or location, timing of hyperthermia in relation to radiotherapy or chemotherapy and further treatment-related factors like SAR coverage and the number of hyperthermia treatments play an important role in the effectiveness of the combined treatment (Raaphorst *et al.* (1998); Sakurai *et al.* (1998); Engin *et al.* (1995); Kapp and Cox (1995); Hand *et al.* (1997); Lee *et al.* (1998)). The complexity of these factors and their (non-linear) interactions make the assessment of the clinical quality of hyperthermia treatments (for each specific tumour group) in the combined treatment modality a cumbersome and difficult subject.

If the effectiveness of two concurrent hyperthermia techniques have to be investigated, a relatively quick way to demonstrate their difference can be an intra-patient comparison. In this set-up, both hyperthermic applications are used alternately during one treatment series of a patient and with the well-defined and technically measurable temperature, a more limited

assessment i.e. technical assessment of hyperthermia quality can be achieved for both types of applications under otherwise constant circumstances.

A major drawback in the use of invasive thermometry is the relatively poor quality of spatial resolution as the measurement of a true 3D-representative temperature data set is clinically not feasible. Only recently is 3D-treatment planning starting to emerge on a more routine basis (for deep and interstitial hyperthermia) in which a full 3D-SAR distribution is generated. From this, a 3D-temperature distribution can be calculated given a static blood perfusion. However, there are no guidelines concerning the evaluation of a patient-based SAR distribution obtained from antennae in array configurations. Neither is it possible to obtain and correlate an invasively measured SAR distribution to the calculated SAR values. It is also not possible to correlate a coarse-measured temperature distribution to a fine-meshed treatment-model-calculated temperature distribution in a patient due to large variations in blood flow and strong dynamic changes in blood flow during a hyperthermia treatment. In conclusion, a full assessment of the technical quality of a hyperthermia treatment can not be obtained from clinical data yet.

Although full assessment of the technical quality is not feasible, the ESHO Quality Assurance guidelines (Hand *et al.* (1989)) on the *basic technical* qualities of an antenna can be used: the effective field size (EFS), i.e. surface at 1 cm depth in muscle-equivalent tissue with a SAR of more than 50% with the SAR normalised to the absolute maximum at that depth, and penetration depth (PD, defined as the depth under 1 cm with 50% SAR level). Evaluation of SAR data in a muscle-equivalent tissue phantom is the best alternative for technical hyperthermic quality assessment. These measurements and/or calculations can be performed with either one antenna or multiple antennae in a clinically relevant array application.

For evaluation of superficial hyperthermia antennae, the development of a thermographical measuring device existing of an Infra Red camera interfaced to a PC made it possible to obtain (coarse) 3D-SAR information using a flat multi-layered phantom (Van Deursen and Van Rhoon, (1987)). However, the time-interval between measurements to reinstate the phantom properties slows down the process of measurements. Also, the heat conduction in the phantom during the power pulse (60 to 90 seconds) causes extra inaccuracy. Another drawback of measuring SAR distributions from muscle-equivalent phantoms this way, is the initial variation in the structure of the phantom and the varying electro-magnetic properties in

time of the phantom. Only with computer planning models, a better-controlled method of generating SAR distributions have become available.

The efficacy of these computer generated SAR distributions depends on the accuracy of the models used and experimental verification was used to validate the models. The Gaussian beam model as introduced by Bach Andersen (1987) and further developed Lumori *et al.* (1990a) has proven to be reliable to predict SAR distributions in layered water-fat-muscle phantoms from Current Sheet Applicators (CSA) in an array application (Lumori *et al.* (1990b)). The experimental verification of the model showed an error less than 3% (Lumori *et al.* (1990a)). This model played an important role in the technical evaluation and comparison of superficial hyperthermia antennae under development in the University Hospital Rotterdam-Daniel. Presently, other, more sophisticated, models have proven their reliability in predicting SAR distributions from antennae especially in the application of deep regional hyperthermia (Sullivan (1991); Sullivan *et al.* (1993); Wust *et al.* (1996); Wust *et al.* (1999)). They either used a FDTD algorithm or IE algorithm to calculate SAR distributions in 3D patient representations. Basis for these 'clinical' calculus techniques was provided by Van den Berg *et al.* (1983) and Zwamborn (1991).

Through the use of the same FDTD algorithm, the first preliminary results of modelling a superficial Lucite Cone Applicator have become available (Samaras *et al.* (2000)).

1.4 Aim of this study

The main object of this thesis is to address the problem of *technical quality* in superficial hyperthermia. Since 1978, the clinical application of hyperthermia has been the subject of various research projects in Rotterdam. Initially, research was done into the application of whole body hyperthermia (Van der Zee, (1987)) and since 1983 research has been concentrated on the application of local superficial hyperthermia and (loco-) regional deep hyperthermia as an adjuvant to radiotherapy. This research has resulted in the development of a 433 MHz waterfilled waveguide antenna, used in an incoherent multi-element array for superficial hyperthermia applications, a 27 MHz capacitive coupling system for interstitial hyperthermia (Kaatee, (2000)) and a 27 MHz ring capacitor applicator for deep regional hyperthermia (Van Rhoon, (1995)).

In general, CR rates in the treatment of recurrent breast cancer by radiotherapy plus hyperthermia are found to be lower in the case of large tumours than in small tumours.

Through clinical evaluation, we found that technical improvement (i.e. changing the frequency from 2450 MHz to 433 MHz and designing the waterfilled waveguide applicator (**WGA**),) resulted in an increase of CR for tumours with a diameter larger than 3 cm from 31% to 65% (Van der Zee *et al.* (1999)), **chapter 2**. However, a difference between CR rates of large tumours and in small tumours (< 3 cm) remained, 65% respectively 87%. To further improve the technical quality of the superficial hyperthermia treatment, research concentrated on the development of an antenna capable of adequately heating a large tumour volume. To clinically verify the technical quality of a hyperthermia treatment, the temperature distribution must be monitored throughout the treatment. The use of *interstitial* thermometry in clinical practice and for research purposes is discussed in **chapter 3**.

Since the 433 MHz driven WGA has a limited effective field size (**EFS**, 33% of the aperture), it is not suitable for the heating of a large tumour volume. Therefore, an antenna had to be developed with an EFS that covered the *entire* aperture of the antenna. The new antenna, the Lucite Cone Applicator (**LCA**) is based on the WGA and has an EFS that is about three times larger than that of the WGA. The basic properties of this antenna are reported in **chapter 4**.

In clinical application, an array of antennae is often needed to cover the entire tumour area. To study the basic technical properties of the newly developed LCA, a simple 2D beam profile model (Gaussian beam (**GB**) model) was tested on its usability to predict SAR distribution from a 2*1 array of LCA (**chapter 5**). Finally, in **chapter 6**, more clinically relevant 2*2 array applications of the LCA were quantitatively evaluated using the GB model and verified by thermographically obtained SAR images.

In theory, arrays of antennae with individual power control of each element are capable of heating a treatment volume if two conditions are fulfilled: a) the overall treatment volume needs a certain minimum dose and b) normal tissue in the treatment volume must not be damaged. Since the tissue properties in the treatment volume can vary greatly either initially or during the treatment, individual power adjustments are essential in optimising the hyperthermia treatment. An array constructed from small antennae provides a high spatial resolution of power deposition, which can counteract small unwanted hot spots in the treatment volume adequately. However, major drawbacks of a small aperture antenna array are a) the (potential) loss of penetration depth and thus a decrease in CR and b) a strict demand of spatial resolution of thermometry to exploit the feasibility of power steering. In contrast, arrays of large aperture antennae are more difficult to conform to the body contours.

A small hot spot (in normal tissue) causes the reduction of local power output in the whole area under the aperture with the risk of local underdosage in that part of the treatment volume, and thus may decrease the CR. Both systems therefore have their specific technical advantages and disadvantages. To investigate the pros and cons of large and small aperture antennae, a theoretical comparison of the SAR distribution from arrays of large LCA and small Current Sheet Applicators (**CSAs**) using the GB model was performed (**chapter 7**). In this study, an attempt has been made to find a quantitative measure to evaluate arrays of antennae to be used for superficial hyperthermic treatments. The currently available QA guidelines do not provide any such measure for these purposes.

The remaining (and perhaps the most burning) question to be answered, having acknowledged technical progress made in the laboratory, is:

Does technical improvement in a hyperthermic application actually result in a quantifiable improvement in the clinical hyperthermia treatment?

Only a clinically orientated study will make clear which technical improvement is most significant under which clinical circumstances. Therefore, we set up a paired comparison of the temperature distributions achieved by either WGA or LCA arrays within several patient treatment series (**chapter 8**). From this comparison, we calculated to what extent laboratory-obtained improved SAR distributions resulted in an improved temperature distribution under clinical conditions.

Since the Gaussian beam model is a simple 2D model that does not take into account mutual interaction between antennae and 3D tissue load properties, the more complex FDTD-modelling was tested on its capability to predict SAR distributions from an LCA. FDTD-modelling has proven its efficacy as 3D SAR distribution calculator in regional and interstitial hyperthermia. In **chapter 9** we show the first results of basic FDTD-modelled SAR distributions from the LCA, which are correlated with thermographically obtained data.

Chapter 10 concludes this study with a general discussion. Furthermore, some directives are formulated for future research.

1.5 References

ALFIERI, A.A. AND HAHN, E.W. 1978, An in situ method for estimating cell survival in a solid tumor. *Cancer Research*, **38**, 3006-3011.

BACH ANDERSEN, J. 1987, Electromagnetic power depostion: inhomogeneous media, applicators and phased arrays. *Physics and Technology of Hyperthermia.* edited by S.B. Field and C. Franconi (Dordrecht / Boston / Lancaster: Martinus Nijhoff Publishers), pp. 159-188.

BHUYAN, B.K. 1979, Kinetics of cell kill by hyperthermia. *Cancer Research*, **39**, 2277-2284.

DEWEY, W.C., HOPWOOD, L.E., SAPARETO, S.A. AND GERWECK, L.E. 1977, Cellular responses to combinations of hyperthermia and radiation. *Radiology*, **123**, 463-474.

DEWHIRST, M.W., PHILLIPS, T.L., SAMULSKI, T.V., STAUFFER, P., SHRIVASTAVA, P., PALIWAL, B., PAJAK, T., GILLIM, M., SAPOZINK, M., MYERSON, R. AND ET AL, 1990, RTOG quality assurance guidelines for clinical trials using hyperthermia. *International Journal of Radiation Oncology Biology Physics*, **18**, 1249-1259.

EMAMI, B., SCOTT, C., PEREZ, C.A., ASBELL, S., SWIFT, P., GRIGSBY, P., MONTESANO, A., RUBIN, P., CURRAN, W., DELROWE, J., ARASTU, H., FU, K. AND MOROS, E. 1996, Phase III study of interstitial thermoradiotherapy compared with interstitial radiotherapy alone in the treatment of recurrent or persistent human tumors: a prospectively controlled randomized study by the radiation therapy oncology group. *International Journal of Radiation Oncology Biology Physics*, **34**, 1097-1104.

ENGIN, K., LEEPER, D.B., TUPCHONG, L. AND WATERMAN, F.M. 1995, Thermoradiotherapy in the management of superficial malignant tumors. *Clinical Cancer Research*, **1**, 139-145.

HAND, J.W., LAGENDIJK, J.W., BACH ANDERSEN, J. AND BOLOMEY, J.C. 1989, Quality assurance guidelines for ESHO protocols. *International Journal of Hyperthermia*, **5**, 421-428.

HAND, J.W., MACHIN, D., VERNON, C.C. AND WHALEY, J.B. 1997, Analysis of thermal parameters obtained during Phase III trials of hyperthermia as an adjunct to radiotherapy in the treatment of breast carcinoma. *International Journal of Hyperthermia*, **13**, 343-364.

HARISIADIS, L., HALL, E.J., KRALJEVIC, U. AND BOREK, C. 1975, Hyperthermia: biological studies at the cellular level. *Radiology*, **117**, 447-452.

KAATEE, R.S.J.P. 2000, Development and evaluation of a 27 MHz-multi-electrode current-source interstitial hyperthermia system. 1-139. Thesis

KAPP, D.S. AND COX, R.S. 1995, Thermal treatment parameters are most predictive of outcome in patients with single tumor nodules per treatment field in recurrent adenocarcinoma of the breast. *International Journal of Radiation Oncology Biology Physics*, **33**, 887-899.

LEE, H.K., ANTELL, A.G., PEREZ, C.A., STRAUBE, W.L., RAMACHANDRAN, G., MYERSON, R.J., EMAMI, B., MOLMENTI, E.P., BUCKNER, A. AND LOCKETT, M.A. 1998, Superficial hyperthermia and irradiation for recurrent breast carcinoma of the chest wall: prognostic factors in 196 tumors. *International Journal of Radiation Oncology Biology Physics*, **40**, 365-375.

LUMORI, M.L.D., BACH ANDERSEN, J., GOPAL, M.K. AND CETAS, T.C. 1990a, Gaussian beam representation of aperture fields in layered, lossy media: simulation and experiment. *IEEE Transactions on Microwave Theory and Techniques*, 38, 1623-1630.

LUMORI, M.L.D., HAND, J.W., GOPAL, M.K. AND CETAS, T.C. 1990b, Use of Gaussian beam model in predicting SAR distributions from current sheet applicators. *Physics in Medicine and Biology*, 35, 387-397.

OVERGAARD, J., GONZALEZ GONZALEZ, D., HULSHOF, M.C., ARCANGELI, G., DAHL, O., MELLA, O. AND BENTZEN, S.M. 1995, Randomised trial of hyperthermia as adjuvant to radiotherapy for recurrent or metastatic malignant melanoma. European Society for Hyperthermic Oncology. *The Lancet*, 345, 540-543.

PEREZ, C.A., PAJAK, T.F., EMAMI, B.N., HORNBACK, N.B., TUPCHONGA, L. AND RUBIN, P. 1991, Randomised phase III study comparing irradiation and hyperthermia with irradiation alone in superficial measurable tumors. *American Journal of Clinical Oncology: Cancer Clinical Trials*, 14, 133-141.

RAAPHORST, G.P., MAO, J.P. AND NG, C.E. 1998, Thermotolerance effects on thermoradiosensitization in human glioma cells. *International Journal of Hyperthermia*, 14, 85-95.

SAKURAI, H., MITSUHASHI, N., KITAMOTO, Y., NONAKA, T., HARASHIMA, K., HIGUCHI, K., MURAMATSU, H., EBARA, T., ISHIKAWA, H. AND NIIBE, H. 1998, Cytotoxic enhancement of low dose-rate irradiation in human lung cancer cells by mild hyperthermia. *Anticancer Research*, 18, 2525-2528.

SAMARAS, T., RIETVELD, P.J.M. AND VAN RHOON, G.C. 2000, Effectiveness of FDTD in predicting SAR distributions from the lucite cone applicator. *submitted*

SNEED, P.K., STAUFFER, P.R., MCDERMOTT, M.W., DIEDERICH, C.J., LAMBORN, K.R., PRADOS, M.D., CHANG, S., WEAVER, K.A., SPRY, L., MALEC, M.K., LAMB, S.A., VOSS, B., DAVIS, R.L., WARA, W.M., LARSON, D.A., PHILLIPS, T.L. AND GUTIN, P.H. 1998, Survival benefit of hyperthermia in a prospective randomized trial of brachytherapy boost hyperthermia for glioblastoma multiforme. *International Journal of Radiation Oncology Biology Physics*, 40, 287-295.

SULLIVAN, D.M. 1991, Mathematical methods for treatment planning in deep regional hyperthermia. *IEEE Transactions on Microwave Theory and Techniques*, 39, 864-872.

SULLIVAN, D.M., BEN-YOSEF, R. AND KAPP, D.S. 1993, Stanford 3D hyperthermia treatment planning system. Technical review and clinical summary. *International Journal of Hyperthermia*, 9, 627-643.

VALDAGNI, R. AND AMICHETTI, M. 1994, Report of long-term follow-up in a randomized trial comparing radiation therapy and radiation therapy plus hyperthermia to metastatic lymphnodes in stage IV head and neck patients. *International Journal of Radiation Oncology Biology Physics*, 28, 163-169.

VAN DEN BERG, P.M., HOOP, A.T., SEGAL, A. AND PRAAGMAN, N. 1983, A computational model of the electromagnetic heating of biological tissue with application to hyperthermic cancer therapy. *IEEE Transactions on Biomedical Engineering*, 30, 797-805.

VAN DER ZEE, J. 1987, Whole Body Hyperthermia. 1-205. Thesis

VAN DER ZEE, J., TREURNIET-DONKER, A.D., THE, S.K., HELLE, P.A., SELDENRATH, J.J., MEERWALDT, J.H., WIJNMAALEN, A.J., VAN DEN BERG, A.P., VAN RHOON, G.C., BROEKMEYER-REURINK, M.P. AND REINHOLD, H.S. 1988, Low dose reirradiation in combination with hyperthermia: a palliative treatment for patients with breast cancer recurring in previously irradiated areas. *International Journal of Radiation Oncology Biology Physics*, **15**, 1407-1413.

VAN DER ZEE, J., VAN DER HOLT, B., RIETVELD, P.J., HELLE, P.A., WIJNMAALEN, A.J., VAN PUTTEN, W.L. AND VAN RHOON, G.C. 1999, Reirradiation combined with hyperthermia in recurrent breast cancer results in a worthwhile local palliation. *British Journal of Cancer*, **79**, 483-490.

VAN DER ZEE, J., GONZALEZ GONZALEZ, D., VAN RHOON, G.C., VAN DIJK, J.D.P., VAN PUTTEN, W.L.J. AND HART, A.A.M. 2000, Comparison of radiotherapy alone with radiotherapy plus hyperthermia in locally advanced pelvic tumours: a prospective, randomised, multicentre trial. *The Lancet*, **355**, 1119-1125.

VAN DEURSEN, J.B.P. AND VAN RHOON, G.C. 1987, Microprocessor-controlled interface for an Aga thermograph. *Biomedical Measurements Information and Control*, **2**, 10-13.

VAN RHOON, G.C. 1995, Radiofrequency hyperthermia systems. 1-199. Thesis

VERNON, C.C., HAND, J.W., FIELD, S.B., MACHIN, D., WHALEY, J.B., VAN DER ZEE, J., VAN PUTTEN, W.L., VAN RHOON, G.C., VAN DIJK, J.D., GONZALEZ GONZALEZ, D., LIU, F.F., GOODMAN, P. AND SHERAR, M. 1996, Radiotherapy with or without hyperthermia in the treatment of superficial localized breast cancer: results from five randomized controlled trials. International Collaborative Hyperthermia Group. *International Journal of Radiation Oncology Biology Physics*, **35**, 731-744.

WUST, P., SEEBASS, M., NADOBNY, J., DEUFLHARD, P., MÖNICH, G. AND FELIX, R. 1996, Simulation studies promote technological development of radiofrequency phased array hyperthermia. *International Journal of Hyperthermia*, **12**, 477-494.

WUST, P., NADOBNY, J., SEEBASS, M., STALLING, D., GELLERMAN, J., HEGE, H.C., DEUFLHARD, P. AND FELIX, R. 1999, Influence of patient models and numerical methods on predicted power deposition patterns. *International Journal of Hyperthermia*, **15**, 519-540.

ZWAMBORN, A.P.M. 1991, Scattering by Objects with Electric Contrast. 1-165. Thesis

Reirradiation combined with hyperthermia in recurrent breast cancer results in a worthwhile local palliation

J van der Zee, B van der Holt, PJM Rietveld, PA Helle, AJ Wijnmaalen, WLJ van Putten and GC van Rhoon

Reirradiation combined with hyperthermia in recurrent breast cancer results in a worthwhile local palliation

J van der Zee[1], B van der Holt[2], PJM Rietveld[1], PA Helle[3], AJ Wijnmaalen[4], WLJ van Putten[2] and GC van Rhoon[1]

Department of Radiation Oncology, [1]Subdivision of Hyperthermia, and [2]Department of Statistics, University Hospital Rotterdam, Daniel den Hoed Cancer Center, Rotterdam, The Netherlands; and [3]Department of Radiation Oncology, Medisch Spectrum Twente, Enschede, The Netherlands; [4]Department of Radiation Oncology, University Hospital Rotterdam, Daniel den Hoed Cancer Center, Rotterdam, The Netherlands

Summary Both experimental and clinical research have shown that hyperthermia (HT) gives valuable additional effects when applied in combination with radiotherapy (RT). The purpose of this study was evaluation of results in patients with recurrent breast cancer, treated at the Daniel den Hoed Cancer Center (DHCC) with reirradiation (re-RT; eight fractions of 4 Gy twice weekly) combined with HT. All 134 patients for whom such treatment was planned were included in the analysis. The complete response rate in 119 patients with macroscopic tumour was 71%. Including the 15 patients with microscopic disease, the local control rate was 73%. The median duration of local control was 32 months, and toxicity was acceptable. The complete response (CR) rate was higher, and the toxicity was less with the later developed 433-MHz HT technique compared with the 2450-MHz technique used initially. With this relatively well-tolerated treatment, palliation by local tumour control of a worthwhile duration is achieved in the majority of patients. The technique used for hyperthermia appeared to influence the achieved results. The value of HT in addition to this re-RT schedule has been confirmed by a prospective randomized trial in a similar patient group. In The Netherlands, this combined treatment is offered as standard to patients with breast cancer recurring in previously irradiated areas.

Keywords: breast cancer; reirradiation; hyperthermia; local tumour control; palliation

The clinical problem

Local regional recurrences of breast cancer may be the cause of severe suffering when uncontrolled, without being life-threatening at short term. Symptoms such as ulceration, bleeding and severe pain have been seen in 62% of the patients with recurrent breast cancer referred for radiotherapy (RT) (Bedwinek et al, 1981*a*). Furthermore, watching a growing tumour at the surface of the body is a stressful experience to the patient. The survival of patients with a locoregional recurrence appears not to be related to any local treatment; in the majority of patients, distant metastasis is identified after a median follow-up time of less than 12–30 months. Nevertheless, the median survival time in this patient group may vary from 12 to 53 months, depending mainly on tumour characteristics at the time of first diagnosis, with a 5-year survival rate of 22–50% (Bedwinek et al, 1981*b*; Toonkel et al, 1983; Patanaphan et al, 1984; Aberizk et al, 1986; Deutsch et al, 1986; Hietanen et al, 1986; Stadler and Kogelnik, 1987; Blanco et al, 1990; Schwaibold et al, 1991; Halverson et al, 1992). The financial cost of treating patients with local regional breast cancer recurrences has been estimated to be around Australian $533 per month by Hurley et al (1992). Therefore, application of a treatment which can result in long-term local tumour control would be worthwhile from the perspectives of both the patient and the health care system.

In the case of a recurrent tumour within a previously irradiated area, the chance of achieving local control by either RT or chemotherapy is reduced (Okunieff et al, 1991). The radiation dose that can be given without a high risk of unacceptable toxicity is lower than considered adequate (Bedwinek et al, 1981*a*; Halverson et al, 1990; Withers et al, 1995). This poor prognosis led to the evaluation of combining re-RT and local hyperthermia (HT) in this patient group at the DHCC.

Experimental research has shown that HT is an effective cell-killing agent especially to cells in a hypoxic, nutrient deprived and low pH environment, conditions which are specifically found in malignant tumours. The combination of RT with HT should result in at least a complementary tumoricidal effect, if not a supra-additive effect (Field, 1990; Raaphorst, 1990). The existing clinical data appear to confirm the findings from experimental research. Recently, the therapeutic gain by HT in addition to RT, has been documented by randomized comparative studies in various tumour types (Valdagni et al, 1988; Overgaard et al, 1995; International Collaborative Hyperthermia Group, 1996; van der Zee et al, 1996).

At the DHCC, both treatment modalities underwent changes during the period since the combination was first applied clinically. The total re-RT dose gradually increased from about 20 to 32 Gy. The treatment schedule of eight fractions of 4 Gy, twice weekly, was first applied in 1981, and, after apparent effectiveness and tolerance (van der Zee et al, 1988), this became the protocol in 1988. Hyperthermia technique was gradually improved over the years.

MATERIALS AND METHODS

Patients and tumours

All 134 patients with recurrent adenocarcinoma of the breast, for whom reirradiation with eight fractions of 4 Gy combined with HT

Table 1 Patient and tumour characteristics in relation to treatment technique

	433 MHz $n = 107$		2450 MHz $n = 27$	
	Median (range) s.d.[a]	Patients	Median (range) s.d.[a]	Patients
Disease-free interval from start of first treatment to first relapse (months)	23 (1–158) 27		15 (2–168) 25	
Number of previously given kinds of chemotherapy				
0		57		9
1		33		13
2 or 3		17		5
Number of previously given kinds of hormonal therapy				
0		54		10
1		23		8
≥2		30		9
Number of previous surgical procedures at the same location				
0		7		1
1		49		16
≥2		51		10
Dose of radiotherapy given previously (Gy)	45 (20–66) 6		45 (15–58) 10	
Macroscopic tumour				
≤3 cm		38		11
>3 cm		57		13
Ulcerating tumour		24		6
Tumour histology: grade of differentiation				
Good		1		0
Moderate		18		1
Poor		53		12
Undifferentiated		14		7
Unknown		21		7
Number of lesions				
Single		42		9
2		19		8
3–9 or more		46		10
Haemoglobin at time of treatment (mmol l⁻¹)	8.3 0.7		8.3 0.7	
Tumour outside treatment volume		41		10
Macroscopic tumours only:				
Tumour volume (cm³)	11 (1–868) 166		6 (1–777) 39	
Tumour maximum diameter (cm)	4.9 (5–300) 6.0		4.7 (6–175) 4.8	
Maximum depth (cm)	2.0 (1–9) 1.6		2.0 (1–5) 0.7	
Continuation of hormonal therapy during local treatment		15		5

[a]s.d., standard deviation.

was planned between January 1981 and May 1992 for a total number of 143 fields, are included in this evaluation. Only the first treated field in each patient was included, leaving a total number of 134 fields in 134 patients to be analysed. Six of these patients had been included in the randomized study reported by the International Collaborative Hyperthermia Group (1996).

Patients were selected for re-RT plus HT on the following criteria: recurrent tumour, inoperable ($n = 119$) or after microscopically incomplete excision ($n = 15$); and systemic therapy was either inadequate to control the local regional tumour, or was deemed inappropriate, in the absence of (symptomatic) systemic disease.

At the time of treatment, patients were aged 28–82 years, with a median of 58 years. Performance status was generally good, with WHO scores 0 or 1 in 132 patients and 2–4 in two patients. Distant metastasis was present at the start of treatment in 38% of the patients. Seventy per cent of the patients had been treated with hormonal and/or chemotherapy in the past. Previous RT to the same area had been given 4 months (median 41 months) before the re-RT plus HT treatment. Tumour localization was on the chest wall in 130 patients. Patient and tumour characteristics known to have prognostic value are given in Table 1, in relation to the HT technique used for treatment. In case of multiple lesions, the maximum diameter and the volume of the largest lesion was used in the evaluation. Tumour volume was calculated according to the formula $1/6\pi a^*b^*c$, in which a and b are the largest diameters measured by calipers and c is the maximum extension in depth estimated by palpation and, in some cases, established by ultrasound or computerized tomography (CT) scan.

Table 2   Treatment characteristics

	n	Range	Median (s.d.ᵃ)
Total re-RT dose			
<32 (12–28) Gy	4		
=32 Gy	129		
=36 Gy	1		
Size of radiation field (cm²)		30–875	248 (184)
Size of hyperthermia field (cm²)		64–800	300 (155)
Number of HT applicator set-ups			
1	101		
2	7		
3	2		
4	2		
Received eight HT treatments	123		
Total duration of all HT treatments (min)			480 (55)
Number of thermometry points [median (range)]:	433 MHz		2450 MHz
In tumour tissue	5.4 (1–20)		2.6 (1–10)
In normal tissue	13.9 (1–44)		2.9 (1–11)
HT dose parameters [median (s.d.ᵃ)]:	433 MHz		2450 MHz
Tmaxmax$_{mean}$ in tumour (°C)	43.4 (1.3)		42.2 (1.4)
T90$_{t,c}$, in tumour (°C)	40.1 (1.2)		40.6 (1.7)
Tmaxmax$_{mean}$ in normal tissue (°C)	43.8 (1.0)		42.2 (1.2)
T90$_{t,c}$, in normal tissue (°C)	39.2 (1.1)		39.9 (1.2)
Tumour tissue T90 >40°C (min)	61 (118)		118 (137)
Normal tissue T90 >40°C (min)	0 (55)		48 (101)

ᵃs.d., standard deviation.

Treatment

All patients were treated with the same radiation schedule of 4 Gy twice weekly, each fraction followed by 1 h HT. The time interval between two re-RT + HT treatments was 3–4 days, that between the re-RT fraction and HT session was an average of 40 min. A summary of treatment characteristics is given in Table 2.

Radiotherapy

The planned treatment of eight fractions of 4 Gy was applied to 129 patients. Four patients received a lower total dose, of 12–28 Gy, as their treatment was terminated because of general deterioration by rapid progression of systemic disease. In one patient, the treatment was interrupted because of development of a urinary tract infection, and a ninth fraction was given to compensate for the delay. Radiation techniques included electrons (n = 107), photons (n = 15), a combination (n = 9) or orthovoltage (n = 2) (unknown in one) depending on the tumour location and depth. The radiation field was chosen with a margin of at least 2 cm around the macroscopic tumour.

Hyperthermia

Seven patients received less HT treatments than RT fractions. Four patients received seven instead of eight HT treatments because of logistics. In two patients, the treated area needed four HT applicator set-ups to cover the whole field, therefore only half of the field was treated during each session. In the one patient receiving nine fractions of RT, six HT treatments were applied. Standard treatment duration was 60 min with power on. For delivery of HT, the 2450-MHz technique was used in 27 patients (1981–86) and the 433-MHz technique in 107 patients (since 1986). The aim of the treatment was to achieve the highest tumour temperatures.

Power input was limited by the temperatures measured within the tumour periphery (maximum 44°C was allowed at ≤1 cm distance from normal tissue) and the normal tissue (maximum 43°C during the first 30 min, 44°C during the second 30 min), and by power-related pain expressed by the patient at a site without thermometry. The hyperthermia field size is defined as the sum of the aperture areas of the applicators used.

2450 MHz technique

Custom-built air-filled waveguide applicators, with aperture sizes of 8 × 4 and 8 × 6 cm², were used in various combinations. Up to four applicators were coupled to one power supply, without the possibility to control power supply to the individual applicators. A maximum of eight applicators could be used at the same time. Surface cooling, when necessary, was performed by directing air currents under the applicators. Interstitial thermometry was performed by thermocouples, using either single sensor probes within a needle or multi-sensor probes within a catheter. Temperatures were measured every 5 min with the power shut off.

433 MHz technique

A dipole antenna was used in three patients. Custom-built water-filled waveguide applicators (Van Rhoon et al, 1998) were used since February 1985. The maximum number of applicators used simultaneously increased, over time, from two to five. Each applicator was supplied with independent power control. Until July 1987, the aim of the treatment was to heat the macroscopic tumour but, after experiencing tumour regrowth within the radiation field, outside the margin of the HT field (van der Zee et al, 1992); the applicator set-up was chosen such that the radiation field was widely covered. Surface temperature control was performed by using a perfused water bolus. Since May 1987, temperatures have

Table 3 Parameters included in the evaluation of prognostic factors

Chemotherapy	Former chemotherapy: yes or no
Hormonal therapy	Former hormonal therapy: yes or no
Former local treatment	Two classes: either a maximum of one surgical treatment plus RT, or two or more surgical treatments plus RT
RT dose	Total (cumulative) dose of previously applied RT; continuous variable, or classes ≤42, >42–46 and ≥46 Gy
Number of lesions	Number of tumour lesions within the treatment volume; classes 1, 2 and ≥3
Log tumour volume	Logarithm of volume of (largest) tumour lesion in mm³; continuous variable, or classes ≤2, 2–4 and ≥4
Tumour maximum diameter	Maximum diameter of (largest) tumour lesion; in two classes ≤3 and >3 cm
Tmaxmax$_{mean}$ in tumour	Continuous variable, or classes ≤42.5, >42.5–43.5 and ≥43.5°C
T90$_{best}$ in tumour	Continuous variable, or classes ≤39.6, >39.6–40.6, and >40.6°C
Tmaxmax$_{mean}$ in normal tissue	Continuous variable, or classes ≤43.3, >43.3–44.3, and >44.3°C
T90$_{best}$ in normal tissue	Continuous variable, or classes ≤38.8, >38.8–39.5 and >39.5°C
HT technique	Two classes: 433 MHz and 2450 MHz

been measured continuously during treatments by a 24-channel scanning fibre-optic system (FT1210, Takaoka Japan), with which five multisensor probes (up to four sensors) and four single-sensor probes were available.

Two patients, both with a tumour extending to a depth of more than 5 cm, who were treated with other equipment (13.5 MHz capacative and 80 MHz radiative, respectively) were included in the 433-MHz technique group.

Hyperthermia dose parameters

For both normal tissue and tumour tissue, 20 parameters representative of HT dose were calculated from the temperatures measured during heating. A full description of all these dose parameters is beyond the scope of this report, but will be published elsewhere. These parameters, however, appeared highly correlated. Factor analysis was used to select the two parameters, within tumour as well as normal tissue, that contain the most information. These parameters were Tmaxmax$_{mean}$ and T90$_{best}$. *Tmaxmax* is defined as the highest temperature measured for each heat session and, for this analysis, the average of these highest temperatures was selected. *T90* is calculated from the Gaussian distribution of all temperature measurements during each heat treatment, after the heating-up phase of 10 min, and represents the value above which 90% of all measurements were observed. The T90$_{best}$ is the T90 from the treatment session during which the highest value was achieved.

End points

Response was established at the time of maximum regression which was observed 1–14 (median 2) months after start of treatment. A complete response (CR) is defined according to WHO criteria: clinically a complete tumour remission, observed twice with a time interval of at least 4 weeks. The duration of local control, in patients treated for microscopic tumour and in patients in whom a CR was achieved, was defined from the start of treatment till the first observation of progression within the treated volume, which is defined as the volume to which radiation was applied.

Acute toxicity observed can be distinguished to result from either RT or HT. Radiation-induced acute toxicity includes erythema (none, mild, moderate or severe) and moist desquamation. Thermal burns include second and third degree burns in the

Table 4 Complete tumour response and acute toxicity in relation to treatment technique

	433 MHz technique $n = 107$ (%)	2450 MHz technique $n = 27$ (%)
Complete response (macroscopic disease only)	74	58
Max. tumour diameter ≤3 cm	87	91
Max. tumour diameter >3 cm	65	31
Local control (microscopic disease included)	76	63
Burns		
No or first degree	71	33
Second degree	19	56
Third degree	7	11
Subcutaneous	3	0
Erythema		
None–mild	65	59
Moderate–marked	35	41
Moist desquamation	12	7

For both techniques, the difference in CR rate between small and larger tumours is significant ($P = 0.017$ for the 433-MHz technique and $P = 0.003$ for the 2450-MHz technique). The difference in CR rate between the two techniques is significant for the large tumours ($P = 0.024$).

skin, and subcutaneous burns. Late radiation toxicity was scored for pigmentation, telangiectasis, subcutaneous fibrosis and ulceration. Only ulcerations observed without persistent or progressive tumour, and not resulting from a third degree thermal burn, were assessed as re-RT toxicity.

Statistical methods

The parameters included in the evaluation of prognostic factors are listed in Table 3. The evaluation of factors associated with CR was restricted to the 119 patients with macroscopic tumour. Patients treated after irradical resection of recurrent tumour were included in the analysis of local tumour control. Pearson's chi-squared test was used to determine which parameters were associated with CR rate or acute toxicity caused by the treatment. Cox regression, univariate as well as multivariate, was used to investigate which variables were associated with duration of local control.
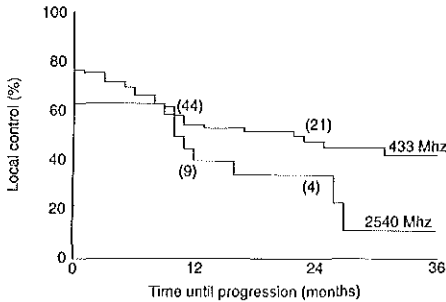
Figure 1 Duration of local control in relation to technique used for delivery of hyperthermia: 2450 MHz or 433 MHz. Actuarial local control rates at 1 and 2 years are 44% and 33% for 2450 MHz and 54% and 47% for 433 MHz respectively (log-rank test P = 0.05)
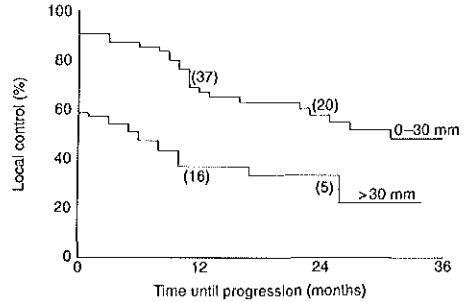
Figure 2 Duration of local tumour control in relation to tumour size: maximum tumour diameter ≤3 cm compared with >3 cm. Actuarial local control rates at 1 and 2 years are 69% and 57% for smaller tumours and 36% and 33% for larger tumours respectively (log-rank test P = 0.0001)

RESULTS

Complete response and duration of local control

The follow-up time for all patients varied from 1 to 76 months with a median of 21 months. Five patients died within 4 weeks after the last treatment, and three patients were lost to follow-up of the locally treated area because of tumour progression outside the treatment volume for which they were treated in another hospital. These eight formally non-evaluable patients were included as non-complete responders. A CR was observed in 84 out of 119 (71%) of patients with a macroscopic tumour. The probability to achieve a CR appeared higher for patients treated with the 433-MHz technique (74%) than for those treated with the 2450-MHz technique (58%) (Table 4).

In 26% (n = 35) of all patients, local tumour control was not achieved. Within the group of 99 patients with CR, or treated after microscopically incomplete resection, in-field tumour regrowth was observed in 36, after a follow-up time of 2 months to 5 years (median 11 months). The median overall survival in these patients was 20 months. Thirty-six patients have died with local tumour control after a median survival of 15 months, whereas 27 patients are still alive with local tumour control after a follow-up period of 5–76 months (median 31 months). Overall, the median duration of local control, censored for death, is 32 months.

The median overall survival time for the whole group of patients is 21 months. In the 99 patients in whom local control was achieved, the median overall survival is 31 months.

Local tumour control in patients with microscopic disease

Fifteen patients with microscopic disease after incomplete excision were all treated with the planned re-RT of eight fractions of 4 Gy. Three of these patients were treated with the 2450-MHz technique. In all three patients, in-field tumour regrowth was observed 10–12 months after the start of treatment. In the 12 patients treated with the 433-MHz technique, in-field tumour regrowth was observed only twice, 10–13 months after the start of treatment. Three patients have died with local tumour control after 4–16 (median 10) months and seven patients are still alive with local tumour control after 16–70 (median 42) months. The difference in local control probability between the two techniques is significant (P < 0.01).

Acute and late toxicity

The skin reaction resulting from re-RT was moderate to marked erythema in 48 patients, combined with moist desquamation in 15 patients. In 86 patients, the skin reaction was less severe.

Thermal burns developed in 49 patients. In three patients, all treated with the 433-MHz technique, these were located subcutaneously. There was a remarkably lower number of second and third degree thermal burns in patients treated with the 433-MHz technique (27%), compared with the patients treated with the 2450-MHz technique (67%) (Table 4). Second-degree burns generally healed within 2 months without treatment. Third-degree burns required 4–6 months of conservative treatment to heal. As these burns preferably develop at sites of limited sensitivity, they generally caused minimal symptoms.

Clinically relevant late toxicity was observed in a minority of patients. Part of the late effects of RT had been present before the start of the combined treatment, because of the previous radiation. Moderate pigmentation was observed in three patients, moderate telangiectasis in three, and subcutaneous fibrosis in 19. Ulcerations were found in 14 patients, nine of whom had this ulceration at the tumour site before treatment. Ulceration without persistent tumour was present at last follow-up in five patients. In three of these patients, this was at the site of a HT-induced burn. In two patients, the ulceration resulted from radiation damage: one in the axilla where at the start of the combined treatment severe telangiectasis was present because of previous irradiation with 50 Gy, and a second in a patient treated for an ulcerating tumour in the intact breast who had severe fibrosis because of previous RT (60 Gy). Bone necrosis, fracture or brachial plexopathy were not observed.

Prognostic factors

Influencing complete response and duration of local control
The probability of achieving a CR decreased if patients had been previously treated with chemotherapy (P < 0.01) or hormonal therapy (P < 0.02), had larger tumour volumes (P < 0.01) and had larger maximum tumour diameters (P < 0.001). Further, the CR rate increased with higher $Tmaxmax_{mean}$ in normal tissue (P < 0.04). Neither the $T90_{K-1}$ values, for both normal (P = 0.62) and tumour tissue (P = 0.30), nor the $Tmaxmax_{mean}$ in tumour tissue (P = 0.29) showed an association with CR.

Univariate Cox regression was used to determine factors that were of influence to continuous duration of local control. Factors influencing local control negatively were previous chemotherapy ($P = 0.01$), a higher number of lesions ($P = 0.02$), a larger tumour volume ($P = 0.01$) and a larger maximum tumour diameter ($P < 0.001$). A higher tumour T90$_{iso}$ ($P = 0.02$) and a higher normal tissue Tmaxmax$_{mean}$ ($P = 0.02$) improved local control duration. It is to be noted that in the univariate Cox regression there was no significant difference in local control between patients treated with 2450 MHz and 433 MHz equipment ($P = 0.08$).

All parameters significant in the univariate regression were tested in the multivariate analysis, which further included HT technique. The multivariate Cox regression analysis showed that tumour maximum diameter, divided into two classes (≤ 3 cm and >3 cm), appeared to be an independent, significant ($P < 0.001$) item with regard to local control, and that 433 MHz equipment performed better than 2450 MHz equipment ($P = 0.046$). None of the other factors was significantly associated with local control. Figures 1 and 2 show the percentages of local control for 2450 MHz compared with 433 MHz equipment, and maximum tumour diameter smaller than or equal to 30 mm compared with larger than 30 mm.

Influencing hyperthermia damage
The only parameter influencing risk of burns was the technique used for delivery of HT. Univariate logistic regression showed that 433 MHz treatments caused much less acute damage ($P < 0.001$) than 2450 MHz treatments. Neither the T90$_{iso}$ nor the Tmaxmax$_{mean}$ thermal dose parameters for both normal and tumour tissue influenced hyperthermia-induced damage (P-values varying between 0.19 and 0.52). None of the evaluated parameters were associated with late damage.

DISCUSSION

Treatment with a radiation dose of only 32 Gy in combination with hyperthermia resulted in a complete response in 71% of the patients with macroscopic tumours. With RT alone at doses of 30–40 Gy, CR rates varying from 20% to 48% have been reported for breast cancer (van der Zee and Vernon, 1996). The same RT schedule of eight fractions of 4 Gy without HT has been applied in the RTOG 81-04 study, resulting in overall 26% complete response (Perez et al, 1989). Recently, the contribution of HT to the result of the combined treatment has been confirmed by a randomized study (International Collaborative Hyperthermia Group, 1996). Within the ESHO 5-88, comparing re-RT alone (same schedule as applied in the present study) with re-RT plus HT, the CR rate after combined treatment was 78%, which was significantly higher than the 38% CR after re-RT alone. This randomized study also demonstrated that the difference in local control is durable.

We do not expect that a locally controlled chestwall recurrence will influence overall survival. Nevertheless, the absence of symptomatic local tumour can result in an improvement in quality of life (Liu et al, 1996). When a CR has been achieved, the median duration of local control was 32 months. In 27% of all patients, infield tumour regrowth was observed after a median follow-up time of 11 months. The median overall survival time in this group of patients was 20 months, which means that the local palliation was maintained for half of the remaining life span. Twenty-seven per cent of the patients have died without local tumour regrowth, after

a median follow-up time of 15 months, whereas 20% of the patients were-free of local disease at last follow-up after a median follow-up time of 31 months.

Therefore, the effect of the treatment is worthwhile for the majority of patients, whereas the treatment causes limited inconvenience. The overall duration of a treatment series is 3.5–4 weeks, during which period patients come to the hospital twice weekly for around 2 h. The HT treatment is generally well tolerated. During treatment, patients were instructed to report pain immediately; in fact this 'subjective thermometry' is a very important parameter in treatment control and should not be considered a side-effect of HT. The interstitial catheters for thermometry generally do not cause relevant problems (van der Zee et al, 1987).

The side-effects of the treatment are acceptable; the HT-induced burns generally cause no pain because of their occurrence at sites of decreased sensitivity. Side-effects other than thermal burns were no different than those expected from re-RT alone, i.e. erythema and, in about 10% of the patients, moist desquamation. Clinically relevant treatment-related late toxicity was observed in only five patients, with ulceration due to either HT or RT toxicity.

The indication to offer combined treatment to patients after incomplete resection of their recurrence was similar to that for patients with macroscopic tumours: the safe re-RT dose is inadequate for tumour control. For achievement of high local control rates with elective radiation, a dose of about 50 Gy in 2-Gy fractions is required (Bedwinek et al, 1981a; Withers et al, 1995). Our results in this subgroup demonstrate that additional HT at an adequate level is beneficial for these patients. Although the numbers are small, the percentage of patients treated with the 433-MHz technique in whom local control was maintained is significantly higher compared with patients treated with the 2450-MHz technique. This difference cannot be explained by a better patient selection. A comparison of the time interval between the primary RT and re-RT between the 2450-MHz and 433-MHz technique groups showed no difference. Another indication of a beneficial effect of HT in microscopic disease is the previous observation of re-recurrences in five patients in which HT was applied to the macroscopic tumour only, within the re-RT-alone part of the treated area (van der Zee et al, 1992).

The results achieved with the 433-MHz technique are remarkably better than those achieved with the 2450-MHz technique. Multivariate Cox regression of prognostic parameters showed only two parameters to be associated with local control duration, i.e. tumour size and HT technique. The advantage of using 433 MHz or, in two cases, lower frequencies instead of 2450 MHz is that with the lower frequencies the penetration depth, and thereby the heated volume, is larger, which can be expected to result in an adequate temperature increase in a larger part of the tumour volume. The improvement in temperature distribution cannot be deduced from the thermal dose parameters calculated, which may be explained by the higher number of intratumour temperature measurements with the 433-MHz technique compared with the 2450-MHz technique (van der Zee et al, 1993). The improvement of results with the better heating technique in tumours with a maximum diameter of >3 cm underscores that it is important to use a technique from which one can expect adequate tissue heating. In fact, the 31% CR rate achieved in the larger (≥ 3 cm maximum diameter) tumours with the 2450-MHz technique is not different from the CR rates found after re-RT alone with the same treatment schedule, i.e. 26% (Perez et al, 1989) and 38% (International Collaborative Hyperthermia Group, 1996). The importance of hyperthermia treatment

technique has been previously shown by Myerson et al, (1990). The results of the study presented here have shown that there is room for further improvement. In patients treated with the 433-MHz technique, the CR rate of 65% in patients with larger tumours is still significantly lower than that for patients with smaller tumours. We speculate that when optimum HT techniques will be available for all tumours, the overall CR rate may reach a value of about 90%. The decrease in HT-related toxicity with the use of the 433-MHz technique is another welcome improvement. Although blisters and third-degree burns generally do not result in relevant clinical problems, because of the fact that these develop at sites of decreased sensitivity, it is preferable to avoid such side-effects. The most likely explanation of the lower number of burns with the 433-MHz technique is the better control of superficial temperatures by the perfused water bolus.

This study allows a few more answers to clinically relevant questions, which have to be precautious in view of the retrospective character of the analysis. In the first place, it has been suggested that local therapy for recurrent breast cancer should be accompanied by systemic therapy (Kapp, 1996). It has been shown that systemic treatment after local treatment significantly improved disease-free survival, but had no impact on overall survival (Borner et al, 1994). In our study, continuation of chemotherapy during the local treatment series was not allowed, but in 18 patients with macroscopic tumours hormonal therapy was continued. The CR rate in patients continuing hormonal therapy was (not significantly) higher than in the remaining patients: 89% compared with 67%. However, the risk of selection bias in this comparison is obvious: 75% of the patients continuing hormonal therapy had started this more than 2 months previously, indicating that the therapy had beneficial effects. These patients, therefore, may represent a subgroup with a better prognosis. Secondly, tumour extension in depth is considered a very important selection criterion for superficial hyperthermia. We now accept patients with tumours up to 4 cm maximum depth for treatment with 433 MHz. In this study, there were 13 patients with deeper tumours. The CR rate in these patients of 62% is not significantly lower than the 72% in the remaining patients, and appears higher than observed after RT alone. This may be explained by the exceptions that we have allowed to the maximum 4-cm depth criterion. These were tumours with overlying subcutaneous fat, in which less energy is absorbed than in tissues with a high water content, and spherical tumours protruding above the skin surface, in which accumulation of energy from the various applicators can be expected at depth and in which the depth may decrease during the treatment period when the tumour regresses. A third clinically important question is whether the eight fractions of 4 Gy plus HT schedule can be applied after previous RT, up to a total dose of 60 Gy or more. In our material, the CR rate of 50% in a subgroup of eight such patients seemed lower than the 76% in the remaining patients, and a persistent ulcer developed in one patient. Further, this subgroup appeared to have a relatively short remaining lifetime compared with the other patients. Nevertheless, the 50% chance to achieve a CR may be worthwhile, depending on the symptoms of local disease and survival prognosis.

CONCLUSIONS

This study has shown that with the combination of re-RT, eight fractions of 4 Gy in 4 weeks, and HT successful palliation of local tumour recurrence of a worthwhile duration can be achieved in the

majority of patients. In addition, this treatment is well tolerated with acceptable toxicity. In The Netherlands, this combined treatment is standard therapy offered to patients with locoregional recurrent breast cancer in a previously irradiated site, providing that an adequate heating equipment is available. This study has also shown that the hyperthermia treatment technique is important for clinical outcome. The development of better HT treatment techniques, enabling a more effective treatment of larger tumours, deserves further investigations.

ACKNOWLEDGEMENTS

REFERENCES

Aberizk WJ, Silver B, Henderson IC, Cady B and Harris JR (1986) The use of radiotherapy for treatment of isolated locoregional recurrence of breast cancer after mastectomy. *Cancer* **58**: 1214–1218

Bedwinek JM, Fineberg B, Lee J and Ocwieza M (1981*a*) Analysis of failures following local treatment of isolated local-regional recurrence of breast cancer. *Int J Radiat Oncol Biol Phys* **7**: 581–585

Bedwinek JM, Lee J, Fineberg B and Ocwieza M (1981*b*) Prognostic indicators in patients with isolated local-regional recurrence of breast cancer. *Cancer* **47**: 2232–2235

Blanco G, Holli K, Heikkinen M, Kallioniemi O-P and Taskinen P (1990) Prognostic factors in recurrent breast cancer: relationships to site of recurrence, disease-free interval, female sex steroid receptors, ploidy and histological malignancy grading. *Br J Cancer* **62**: 142–146

Borner M, Bacchi M, Goldhirsch A, Greiner R, Harder F, Castiglione M, Jungi WF, Thürlimann B, Cavalli F, Obrecht JP, Leyvraz S, Alberto P, Adam H, Varini M, Lochnert T, Senn HJ, Metzger U and Brunner K (1994) First isolated locoregional recurrence following mastectomy for breast cancer: results of a phase III multicenter study comparing systemic treatment with observation after excision and radiation. *J Clin Oncol* **12**: 2071–2077

Deutsch M, Parsons JA and Mittal BB (1986) Radiation therapy for local-regional recurrent breast carcinoma. *Int J Radiat Oncol Biol Phys* **12**: 2061–2065

Field SB (1990) In vivo aspects of hyperthermic oncology. In *An Introduction to the Practical Aspects of Clinical Hyperthermia*, Field SB and Hand JW (eds), pp. 55–68. Taylor and Francis: London

Halverson KJ, Perez CA, Kuske RR, Garcia DM, Simpson JR and Fineberg B (1990) Isolated local-regional recurrence of breast cancer following mastectomy: radiotherapeutic management. *Int J Radiat Oncol Biol Phys* **19**: 851–858

Halverson KJ, Perez CA, Kuske RR, Garcia DM, Simpson JR and Fineberg B (1992) Survival following locoregional recurrence of breast cancer: univariate and multivariate analysis. *Int J Radiat Oncol Biol Phys* **23**: 285–291

Hietanen P, Miettinen M and Mäkinen J (1986) Survival after first recurrence in breast cancer. *Eur J Cancer Clin Oncol* 22: 913–919

Hurley SF, Huggins RM, Snyder RD and Bishop JF (1992) The cost of breast cancer recurrences. *Br J Cancer* 65: 449–455

International Collaborative Hyperthermia Group (1996) Hyperthermia in the treatment of superficial localized primary and recurrent breast cancer – results from five randomized controlled trials. *Int J Radiat Oncol Biol Phys* 35: 731–744

Kapp DS (1996) Efficacy of adjuvant hyperthermia in the treatment of superficial recurrent breast cancer: confirmation and future directions. *Int J Radiat Oncol Biol Phys* 35: 1117–1121

Liu F-F, Bezjak A, Levin W, Cooper B, Pintilie M and Sherar MD (1996) Letter to the Editor. Assessment of palliation in women with recurrent breast cancer. *Int J Hyperthermia* 12: 825–826

Myerson RJ, Perez CA, Emami B, Straube W, Kuske RR, Leybovich L and Von Gerichten D (1990) Tumor control in long-term survivors following superficial hyperthermia. *Int J Radiat Oncol Biol Phys* 18: 1123–1129

Okunieff P, Urano M, Kallinowski F, Vaupel P and Neuringer LJ (1991) Tumors growing in irradiated tissue: oxygenation, metabolic state, and pH. *Int J Radiat Oncol Biol Phys* 21: 667–673

Overgaard J, González González D, Hulshof MCCM, Arcangeli G, Dahl O, Mella O and Bentzen SM (1995) Randomised trial of hyperthermia as adjuvant to radiotherapy for recurrent or metastatic malignant melanoma. *Lancet* 345: 540–543

Patanaphan V, Salazar OM and Poussin-Rosillo H (1984) Prognosticators in recurrent breast cancer. A 15-year experience with irradiation. *Cancer* 54: 228–234

Perez CA, Gillespie B, Pajak T, Hornback NB, Emami B and Rubin P (1989) Quality assurance problems in clinical hyperthermia and their impact on therapeutic outcome: a report by the radiation therapy oncology group. *Int J Radiat Oncol Biol Phys* 16: 551–558

Raaphorst GP (1990) Fundamental aspects of hyperthermic biology. In *An Introduction to the Practical Aspects of Clinical Hyperthermia*. Field SB and Hand JW (eds.), pp. 10–54. Taylor and Francis: London

Schwaibold F, Fowble BL, Solin LJ, Schultz DJ and Goodman RL (1991) The results of radiation therapy for isolated local regional recurrence after mastectomy. *Int J Radiat Oncology Biol Phys* 21: 299–310

Stadler B and Kogelnik HD (1987) Local control and outcome of patients irradiated for isolated chest wall recurrences of breast cancer. *Radiother Oncol* 8: 105–111

Toonkel LM, Fix I, Jacobson LH and Wallach CB (1983) The significance of local recurrence of carcinoma of the breast. *Int J Radiat Oncol Biol Phys* 9: 33–39

Valdagni R, Amichetti M and Pani G (1988) Radical radiation alone versus radical radiation plus microwave hyperthermia for N3 (TNM-UICC) neck nodes: a prospective randomized clinical trial. *Int J Radiat Oncol Biol Phys* 15: 13–24

Van Rhoon GC, Rietveld PJM, Van der Zee J and Van den Berg AP (1998) A 433 MHz Lucite Cone waveguide applicator for superficial hyperthermia. *Int J Hyperthermia* 14: 13–27

Van der Zee J and Vernon CC (1996) Thermoradiotherapy for advanced and recurrent breast tumours. In *Medical Radiology. Thermoradiotherapy and Thermochemotherapy*, vol 2. Seegenschmiedt MH, Fessenden P and Vernon CC (eds.), pp. 35–48. Springer-Verlag: Berlin

Van der Zee J, Van Rhoon GC, Broekmeyer-Reurink MP and Reinhold HS (1987) The use of implanted closed-tip catheters for the introduction of thermometry probes during local hyperthermia treatment series. *Int J Hyperthermia* 3: 337–345

Van der Zee J, Treurniet-Donker AD, The SK, Helle PA, Seldenrath JJ, Meerwaldt JH, Wijnmaalen AJ, Van den Berg AP, Van Rhoon GC, Broekmeyer-Reurink MP and Reinhold HS (1988) Low dose reirradiation in combination with hyperthermia: a palliative treatment for patients with breast cancer recurring in previously irradiated areas. *Int J Radiat Oncol Biol Phys* 15: 1407–1413

Van der Zee J, Van Rhoon GC, Koper PCM and Van den Berg AP (1992) Clinical application and specific requirements of local hyperthermia for chest wall recurrences. *Strahlenther Onkol* 168: 653–654

Van der Zee J, Van Rhoon GC, Verloop-van 't Hof EM, Van der Ploeg SK, Rietveld PJM and Van den Berg AP (1993) The importance of adequate heating techniques for therapeutic outcome. In *Hyperthermic Oncology 1992*, vol II. Gerner EW and Cetas CT (eds.), pp. 349–352. Arizona Board of Regents: Tucson

Van der Zee J, González González D, Van Rhoon GC, Van Dijk JDP, Van Putten WLJ, Hart AAM, Koper PCM, De Wit GA and De Charro FTh (1996) Results of additional hyperthermia in inoperable pelvic tumours. In *Hyperthermic Oncology 1996*. Franconi C, Arcangeli G and Cavaliere R (eds.), pp. 215–217. Tor Vergata Post Graduate School of Medical Physics: Rome

Withers HR, Peters LJ and Taylor JMG (1995) Dose–response relationship for radiation therapy of subclinical disease. *Int J Radiat Oncol Biol Phys* 31: 353–359

Practical limitations of interstitial thermometry during deep hyperthermia

J van der Zee, JN Peer-Valstar, PJM Rietveld, L de Graaf-Strukowska and GC van Rhoon

● *Physics Contribution*

PRACTICAL LIMITATIONS OF INTERSTITIAL THERMOMETRY DURING DEEP HYPERTHERMIA

JACOBA VAN DER ZEE, M.D., PH.D., JACQUELINE N. PEER-VALSTAR, M.D.,*
PAUL J. M. RIETVELD, M.SC., LUCYNA DE GRAAF-STRUKOWSKA, M.D. AND
GERARD C. VAN RHOON, PH.D.

Department of Radiation Oncology, Subdivision of Hyperthermia, University Hospital Rotterdam/Daniel den Hoed Cancer Center,
Rotterdam, The Netherlands

Purpose: Intratumor thermometry during hyperthermia treatment is considered important for several reasons. The morbidity that we experienced from interstitially placed catheters in deep-seated tumors gave reason to weigh the advantages and disadvantages against each other.
Methods and Materials: The available thermometry in 215 patients treated with hyperthermia for deep-seated tumors was analyzed with the aim to evaluate practically feasible intratumor measurements. The influence of intratumor measurements on the treatment procedure was assessed.
Results: Total 120 catheters were placed interstitially in 78 patients. Over the years, the percentage of patients with interstitial thermometry decreased considerably. Forty-nine catheters could remain in place during the whole hyperthermia treatment series. The remaining catheters had to be removed for more or less severe complications, including one fatal event. In fact, the interstitial catheters caused the most severe treatment-related morbidity. During 188 of the total 859 treatments, at least one interstitial catheter was available for thermometry. Per treatment with catheter(s) *in situ*, the average number of intratumor measurement sites was 6.9. The value of interstitial thermometry for power steering during treatment, to both optimize intratumor temperature distribution and prevent toxicity, appeared limited. The mean volume of the tumors with interstitial thermometry was 314 cm³, SD 325. In relation to the large tumor volumes, the thermal dose parameters calculated from the available data is considered to be of limited value.
Conclusion: In view of the possible severe complications and the limited clinical value of the information achieved by interstitially placed thermometry catheters, interstitial thermometry was not found to routinely benefit the individual patient. © 1998 Elsevier Science Inc.

Deep hyperthermia, Intratumor thermometry, Toxicity.

INTRODUCTION

Intratumor thermometry during hyperthermia treatment is considered important for several reasons. The RTOG quality assurance guidelines recommend the use of at least one interstitial catheter, and preferably three in directions perpendicular to each other (1). The aim of interstitial thermometry is to verify the delivery of hyperthermia dose distribution, to allow calculating retrospectively the applied thermal dose, and to prevent toxicity. In our experience with clinically applied regional deep hyperthermia, interstitial thermometry in deep-seated tissues is the cause of the most severe treatment-related morbidity, as has been reported on previous occasions [(2, 3); Van der Ploeg *et al.*, personal communication, 1993; Peer *et al.*, personal communication, 1995]. Over the years, the number of patients treated with interstitially placed catheters decreased. In this article, the experience in the first 215 patients treated for deep-seated tumors with the BSD-2000 system is presented. The pros and contras of interstitial thermometry are discussed, and the absolute and relative contraindications listed.

METHODS AND MATERIALS

Patients

In the period June 1990 to June 1996, a total of 215 patients were treated with the BSD-2000 system (4) for deep-seated tumors. Tumor types include rectal cancer ($n = 113$), uterine cervical cancer ($n = 56$), urinary bladder cancer ($n = 26$), and various other tumor types ($n = 20$), mainly sarcoma. Patients were treated with hyperthermia in addition to radiotherapy or chemotherapy (Table 1). Radio-

---

*Current address: Radiotherapy Institute Limburg, Heerlen, The Netherlands.
 Reprint requests to: J. van der Zee, M.D., Ph.D., Department of Radiation Oncology, Subdivision of Hyperthermia, University

Hospital Rotterdam/Daniel den Hoed Cancer Center, Groene Hilledijk 301, 3075 EA Rotterdam, The Netherlands.

Table 1. Patients with interstitial thermometry related to tumor location and study

	Number of patients	Interstitial thermometry		Number of treatments*		Removed after number of treatments		Interstitial thermometry all treatments		Number of treatments if all with interstitial thermometry	
		No	Yes	Range	(Mean)	Mean	(Range)	No	Yes	Range	(Mean)
Rectum											
+RT,† Phase III	63	47	16	2–5	(4.2)	1–4	(3)	13	3	1–5	(3.3)
+RT, outside study‡ +reirradiation (40) or intraarterial	8	0	8	1–6	(3.3)	2–2	(2)	2	6	1–6	(3.2)
chemo (2)	42	18	24	1–4	(3.1)	0–3	(2)	12	12	1–4	(2.4)
Cervix											
+RT, Phase III	29	24	5	1–5	(4)	1–4	(2)	3	2	1–4	(2.5)
+RT, outside study	9	4	5	2–5	(3.8)	2–3	(2.5)	2	3	2–4	(3.3)
+chemotherapy	18	17	1	3		1		1	0	—	
Bladder											
+RT, Phase III	18	17	1	5		—		0	1	5	(5)
+RT, outside study	8	4	4	3–5	(3.8)	2–2	(2)	3	1	3	(3)
Various	20	6	14	1–5	(3.6)	1–3	(2)	7	7	1–4	(2.9)

* Only the number of treatments in patients with interstitial thermometry is given.
† RT = radiotherapy.
‡ Outside study: either treated within the pilot study preceeding the Phase III study (four patients in each tumor location group), or hyperthermia indicated by expectation of insufficient results from radiotherapy alone.

therapy and hyperthermia was given to patients randomized to combined treatment within the Phase III study on inoperable rectal cancer (primary or recurrent), cervical cancer (FIGO Stages IIB–distal, IIIB and IV), and bladder cancer (Stages T3–4N0M0). Further, this combined treatment was given to patients with recurrent rectal cancer in previously irradiated areas, and to patients with other types of advanced tumors for whom radiotherapy alone was considered inadequate. Combined chemotherapy and hyperthermia was given to patients with recurrent cervical cancer in previously irradiated areas, participating in a Phase I–II study on the effect of weekly cisplatinum and hyperthermia. Patients received one to six (mean four) deep hyperthermia treatments, to a total of 859.

Technique of catheter introduction and fixation

Catheter placement was planned at least 1 day before the first treatment. For each patient, a CT scan was either available at referral, or made specifically for deep hyperthermia treatment planning. When interstitial thermometry was not contraindicated by other factors, it was decided during CT scanning whether catheter introduction was possible. The criteria for decision to place interstitial catheters, as developed on the basis of experience over the years, are listed in Table 2. During CT scanning, the first step was to mark the skin at the site(s) from where catheter introduction appeared possible. The puncture site, and the angle under which the catheter should be inserted was selected. Following sterilization of the insertion area with 0.5% chlorhexidine in 70% alcohol and covering the area with sterile sheets, the insertion site was anesthesized with 2% procaine

hydrochloride. Thereafter the needle, with an outer diameter of 2.1 mm and a total length of 18–23 cm, was introduced. Most catheters were placed transgluteal. After the needle had reached a depth of 8–10 cm, a control CT scan was made to verify insertion angle and depth (Fig. 1). If the insertion angle was correct, the needle was introduced further to the opposite tumor margin. When the patient indicated pain, not disappearing after interruption of pushing the needle, a slightly different angle was chosen. The final direction of the needle was documented by CT scan. After completion of insertion the polyethylene closed-tip catheter (William Cook Europe ApS, Denmark, outer diameter 1.6 mm) was introduced through the needle. The catheter was

Table 2. Criteria for decision to place a catheter

Contraindications before availability of CT scan
  Use of anticoagulants
  Preexisting radiating pain
  Preoperative treatment of rectal cancer
  Puncture site not accessible during CT scanning
  Spontaneous absolute refusal by the patient
Contraindications on CT scan
  Risk of penetration of bladder or bowel lumen
  Tumor located behind bone
  Tumor too small to get at least two intratumor measuring
    sites
  Intratumor area of necrosis
  Discrimination between tumor and normal tissue not well
    possible
  Catheter fixation not possible
  Catheter introduction only possible under a steep angle to the
    skin

Fig. 1. Procedure of CT-guided catheter introduction.

protected from kinking by a nylon rod. The catheter was fixed by Histoacryl (B. Braun, Melsungen AG, Germany) and Tegaderm transparent dressing (Medical Products Division/3M, USA). First, an adhesive was amply placed over the puncture site. The remaining part of the catheter was curled up and, within a gauze, attached to the skin around the puncture site by another adhesive. This procedure allowed reaching the exterior part of the catheter while leaving the insertion site covered. Patients were instructed to see a doctor in case of increasing or otherwise severe pain, or fever, and were given an informative letter for responsible physicians outside the subdivision of Hyperthermia.

Thermometry
For thermometry, Bowman probes were available. These were calibrated once daily. Before each treatment, the probes were pulled straight in a current of hot air and sprayed with silicone to optimize the conditions for mapping within the catheters. Before each treatment, the patient was questioned about recent history of either local pain or fever. In case of fever, other possible causes such as bladder infection or pulmonary infection were excluded. The insertion site was inspected, the invasive length of the catheter verified, and the direction of the catheter derived from the form of the nylon rod. In case of symptoms of local infection, or pain, that was badly tolerated by the patient (e.g.,

causing sleeping problems), it was decided to remove the catheter after the treatment session. Patients were positioned supine. Before and after filling the water bolus, the feasibility of thermal mapping was tested. In case of disturbances, any possible cause of obstruction was corrected for, when possible. During treatment, thermal mapping was performed every 5 min; the step size was 1 cm.

Standard treatment procedure
Patients were lightly sedated with 1 mg lorazepam. Following preparations, heating was started with power output at 400 Watt. Patients were carefully instructed to mention any unpleasant sensation that might be the result of a hot spot, such as a burning sensation, a feeling of pressure, any pain, or bowel or bladder spasms. The treatment settings for frequency, amplitude distribution, and phase shifting at the start of the first treatment were chosen on the basis of the 2D pretreatment planning provided with the BSD-2000 system. Thereafter, treatment settings were adjusted depending on either information from E-field measurements or temperature distribution. Information on temperature distribution came from both intraluminally and interstitially placed thermometry probes, and from the patient. Any pain mentioned by the patient that disappeared within 1 min following power decrease was considered to indicate a too high temperature, and the treatment settings were adjusted to decrease power input at the specific location. Adjustments of treatment settings could be either changes in power output per channel, frequency or phase settings, or placement of additional water bolusses. Power output was increased to as high as the patient could tolerate without pain. Treatment duration was standard 60 min after any of the interstitially measured tumor temperatures had reached 42°C, or maximum 90 min. In cases where the intratumor catheters had to be removed before the last treatment, the time needed to reach 42°C averaged over at least two previous treatments with interstitial thermometry was chosen for subsequent treatments.

The course of each treatment was discussed within the clinical staff and the treatment settings and specific adjustments for the subsequent treatment selected on the basis of the previous experience.

RESULTS

Number of interstitial catheters
One to three catheters were placed interstitially, to a total of 120 catheters, in 78 of the 215 patients (36%) treated for deep-seated tumors (mean: 1.54/patient). Over the years, the percentage of patients with interstitial thermometry changed considerably. Of the first 40 patients, treated in the period June 1990 to January 1992, 36 (90%) had interstitial catheters. Calculated over the first 50 patients (until June 1992), the percentage was 80%. In the second (June 1992 to October 1993) and third (October 1993 to January 1995) groups of 50 patients, the percentage decreased further to 44

Table 3. Available intraluminal thermometry

	Number of intraluminal catheters:	In female	In male
Patients with interstitial thermometry ($n = 78$)	3	24	
	2	12	18
	1	2	22
	0	—	—
Patients without interstitial thermometry ($n = 137$)	3	78	
	2	8	34
	1	2	14
	0	—	1

Table 4. Morbidity from interstitial catheters

	Catheters
Subcutaneous infection	25
Intolerable pain	23
Deep infection	16
Abcess formation	2
Death due to sepsis	1
Arterial bleeding	3
Venous bleeding	1
Spontaneous loss outside the body	4
Spontaneous displacement to inside the body	2*
Continuous loss of tissue fluid	5
Tumor growth along catheter track	3[†]

* In one patient, the catheter had disappeared completely. Its intrapelvic location was later confirmed by diagnostic x-ray.
† In two patients this was confirmed histopathologically; in one patient tumor growth was strongly suggested by the clinical appearance.

and 20%, respectively. In the last group of 65 patients, treated in the period January 1995 to June 1996, the percentage of patients with interstitial catheters was only 9%. The tumor volume in the group of patients with interstitial thermometry ranged from 1 to 1562 cm³, with a mean of 314 cm³ (SD 325), the average tumor maximum diameter being 98 mm. Of the 113 patients with rectal cancer, interstitial thermometry was available in 48 (42%). This percentage was lower for cervical (11 of 56; 20%) and bladder cancer (5 of 26; 19%), and higher for patients with other tumor types (14 of 20; 70%). In four additional patients, a catheter could be placed within the tumor through a fistula before each treatment, and in one patient, an intrauterine catheter was introduced before the first treatment. Forty-nine catheters remained *in situ* until the end of the last hyperthermia treatment. The 78 patients with interstitial catheters received a total of 287 treatments. During 188 of these treatments (66%), at least one interstitial catheter was available for thermometry. Besides catheters introduced into depth, 69 catheters were placed subcutaneously in 49 patients. After experiencing that the temperature measurements achieved from these catheters gave never reason to adjust treatment setup, the use of subcuntaeous catheters was omitted.

Number of intraluminal catheters
In the 78 patients with interstitially placed catheters, one to three (mean two) additional catheters could be placed intraluminally (Table 3). Catheters could be placed within the urinary bladder in 73 patients, intravaginal in 38, and intrarectal in 46 patients. In the 137 patients without interstitial catheters, one to three (mean 2.4) catheters could be placed intraluminally in all but one. A catheter was placed in the bladder in 132 patients, in the vagina in 86 patients, and in the rectum in 110 patients.

Number of interstitial tumor thermometry sites
By multiplying the number of catheters with the number of treatments that these were *in situ*, the total number of interstitial catheters in situ during 188 treatments was 282.

Sixty-five times (in 23% of the cases) it was not possible to map the thermometry probe within the catheter. From 18 catheters (6%), no information on tumor temperature could be derived. This was either due to spontaneous displacement, to kinking, or to failure to place the catheter within the tumor during introduction, for example, when the needle get stuck against a bone, or when the needle pushed the uterus aside instead of entering it. In 57 cases (20%), only one intratumor measurement could be derived from the catheter. This was mostly the result of failure to map the probe. Overall, the total number of intratumor measurement sites was 1291. Per catheter *in situ* during treatment, the average number of intratumor measurement sites was 4.6. Per tumor with interstitial thermometry during treatment, the average number of intratumor measurements was 6.9.

Morbidity from interstitial catheters
Forty-three (36% of the total number) catheters, remaining in place during 1–33 (mean 14.7) days caused no problems. Seventy-seven catheters caused some kind of morbidity, occurring after 0–26 days, mean 10 days. Catheter removal in the first week after insertion ($n = 34$) was done for morbidity in 74% of the cases. In week 2 ($n = 47$), week 3 ($n = 18$), week 4 or later ($n = 16$) this was 73, 44, and 25%, respectively. A summary of the complications is given in Table 4. In 25 cases, the reason for catheter removal was a subcutanaeous infection. Subcutaneous infections resolved after catheter removal without further treatment. In 23 cases the catheters caused pain of such severity that the patient experienced problems to sitting or sleeping. In 13 patients (16 catheters) a deep infection developed, despite antibiotic treatment resulting in abcess formation in two, and death due to sepsis in one. In this latter patient, the same bacteria isolated from the blood were found within the tumor. In three patients, one catheter apparently had penetrated through an arterial vessel, which became clear at the time that the catheter was removed. Two

of these patients had experienced repeatedly considerable blood loss, which was reason to remove the catheter before the last treatment. In the third patient, arterial bleeding occurred after the last treatment. In all three patients, bleeding could be stopped by exerting pressure. In one patient a venous bleeding, apparent immediately after catheter insertion, could not be stopped by exerting pressure, which was reason to remove it 1 h later, before the first treatment. In three patients, all with progressive disease either during or shortly after the treatment series, tumor growth was observed along the track of the catheter. This was histopathologically confirmed in two patients with rectal cancer [the history of one of these patients has been reported previously; (5)]. In one patient with recurrent ureteral cancer, the clinical appearance of a subcutaneously growing nodule strongly suggested tumor growth. Three of four catheters inserted through the perineum were lost. Two catheters disappeared to within the body; one completely (its intrapelvic position later confirmed by diagnostic x-ray), and one almost completely and was removed for that reason. In four patients (five catheters) a continuous loss of a considerable amount of tissue fluid, resulting in loss of adhesive covering, was observed. The thereby increased risk of infection, together with the impossibility to control the patient daily, led to the decision to remove the catheter.

Reasons for not placing interstitial catheters

The decision on placement, or removal before the last treatment session, of interstitial catheters was very much influenced by the experience acquired during the first years of applying deep hyperthermia. Patients with tumors showing necrotic areas on CT scan appeared to have a larger risk on development of deep infection, unresponsive to antibiotic treatment. For patients with cervical cancer, it appeared difficult to discriminate between normal tissue and tumor tissue and further, insertion of the needle within the cervical tissue appeared not always feasible: the needle easier brushed the tissue instead of penetrating it. Furthermore, interstitial catheters in cervical cancer often cause a dull type of pain. In patients with preexisting radiating pain, caused by tumor exerting pressure on nervous tissue, the intratumor catheter appeared to aggravate the pain. In cases where the catheter entered the body under a steep angle to the skin, thermal mapping often failed. This experience, together with the finding that the value of interstitial thermometry was limited with regard to improvement in temperature distribution (see below), has led to increasing acceptance of applying treatments without interstitial thermometry. In the most recent years, the availability of two or three intraluminal sites for thermometry has eased the decision on not placing interstitial catheters. A list of reasons for not placing interstitial thermometry is given in Table 2. Ten patients used anticoagulants that could not be interrupted. Six patients were treated preoperatively for rectal cancer. In rectal cancer, implantation and growth of tumor cells in damaged tissues is not hypothetical, and it

was agreed with the surgeons that interstitial thermometry in these cases would be omitted. The most frequent reason ($n = 35$) for not placing interstitial catheters was anatomy: the presence of either bone, or bowel, or bladder lumina between possible puncture site and tumor. In 29 of 56 patients with cervical cancer and in 19 of 27 patients with bladder cancer no interstitial catheter was placed. In 20 patients, preexisting radiating pain was the reason for not introducing a catheter. The other contraindications played a role in the remaining 18 patients.

Steering possibilities

Generally, the clinical impression is that effective steering within the target volume is not very well possible. Treatment setup is adjusted in response to an observed temperature distribution in disagreement with the desired one, or to a too high temperature experienced by the patient. Within the group of patients with interstitial thermometry, it was almost never necessary to adjust power on the basis of too high measured temperatures. Further, it appeared that the temperature distribution within the target volume showed negligible effects of power distribution adaptation. Examples of temperature distribution during treatment are given in Fig. 2A–D. From each tumor group, the patient with the highest number of interstitial measurements was selected. In each case, changes in treatment setup do not decrease the gap between minimum and maximum intratumor temperature. The effect of steering is that higher power levels can be maintained or achieved than without treatment adjustment, resulting in overall higher temperatures. This figure also shows that the intraluminal temperature is in most cases within the range of interstitial temperatures, and that the course of the intraluminal temperature in most cases reflects the course of the interstitial temperatures. By the way, these four patients were all treated in combination with radiotherapy to a total dose of ≥ 50 Gy. In the patients with bladder, rectal and cervical cancer a local tumor control was achieved for a duration of 18+ months, 5+, and 6+ years, respectively. The patient with a sarcoma died 3 months following treatment due to pulmonary metastases, with a partial response in the intrapelvic tumor. A possible advantage of interstitial thermometry is that the total treatment duration can be shorter than total 90 min, when an intratumor temperature of 42°C is reached within 30 min from start heating. This was the case in only 39 of 287 (14%) treatments in patients with interstitial thermometry during at least two treatments. The treatment procedure as described above has shown to be effective in avoiding hyperthermia induced toxicity. In 215 patients, only one second-degree skin burn, healed after 1 week, and one third-degree skin burn, healed following conservative treatment after 2 months, has developed. Subcutaneous burns were observed in less than 10% of the patients, generally located in the upper leg, causing tenderness for 1–2 days and thereafter spontaneously resolving. In one patient a larger subcutaneous fat burn developed in the suprapubic region and caused

Table 5. Possible advantages and disadvantages of interstitial thermometry

Advantages	Disadvantages
For the individual patient:	
During clinical treatment: optimization of intratumor temperature distribution	Unpleasant procedure
	Negative influence on quality of life
Prevention of toxicity	Risk of bleeding
For scientific reasons:	Risk of infection
Retrospective assessment of treatment quality	Risk of penetrating bowel or bladder lumen
Learning how to use the equipment	Risk of tumor seeding
Useful in intertechnique comparison	Time consuming
Verification of noninvasive thermometry and 3D planning	Increased expense

tenderness for 6 weeks. In two patients a painful spot at the hip bone, probably caused by heat induced bone damage, necessitated to delay subsequent treatment with one week. In none of these patients, interstitial thermometry would have yielded information on temperature distribution in the burned area.

DISCUSSION AND CONCLUSIONS

In our experience, the reluctance by the clinicians in our staff to place interstitial thermometry catheters increased over the years. This reluctance can be explained by the observation that interstitial catheters caused the most relevant treatment-related morbidity, including death, combined with the experienced lack of beneficial effects. When the department started applying hyperthermia for deep seated tumors, the intention was to have interstitial thermometry in every patient. In the first 40 patients, exception was made only for 3 patients with bladder cancer and 1 patient with cervical cancer using anticoagulants. In the latter patient, an intrauterine catheter was placed before the first treatment. Thereafter, the percentage of patients with interstitial thermometry continually decreased. Intratumor temperature measurements are considered important for several reasons (Table 5). Two types of arguments in favor of interstitial thermometry can be distinguished: first, that it is in the benefit of the individual patient under treatment, and secondly, that it is of scientific value—which is in the benefit of future patients.

For the individual patient, the most important consideration is that the treatment is applied optimally. This means that the intratumor temperatures are increased to as high and as homogeneous as possible to achieve maximum tumor cell kill, and that at the same time toxicity is avoided. With the presently available equipment the reality is that we are able to move around a relative large volume with maximum energy disposition. If the aim is more specific, such as to change the temperature distribution within the tumor, the steering tools appear ineffective, as illustrated in Fig. 2. The influence of steering on intratumor temperature distribution for all patients will be the subject of a quantitative investigation, to be published separately. Our clinical experience has been confirmed by others using the BSD-2000 system

(6–8). The energy distribution within the Sigma 60 applicator has been found to be influenced by anatomical and clinical factors and the resulting temperature distribution by tissue perfusion (7). In clinical practice, the steering possibilities are used, together with placement of additional water bolusses, to eliminate power limiting local hot spots, which then allows to increase the total power output and thereby the overall regional temperature level. Interstitial thermometry was neither an important requirement for prevention of toxicity. Well instructed patients do indicate hot spots rather adequately, as demonstrated by the relatively low percentage of thermal burns. Similar experience was reported by Gellerman *et al.* (9). The disadvantages of interstitial thermometry were experienced to be many (Tables 4 and 5). CT-guided insertion of catheters is an unpleasant procedure and time consuming. It increases the total costs of a series of hyperthermia treatments with about Hfl. 900,-. (10). In many patients intolerable pain was reason to remove the catheter. Bleeding, severe infection, and tumor seeding have been observed, and one patient even died due to sepsis in relation to an intratumorally placed catheter. The incidence of morbidity in our patient material is twice as high as that reported by Feldman *et al.* (11). They report problems in 26 of 80 catheters placed in intrapelvic and intraabdominal tumors, with a severe complication in only 2. We have no explanation for this difference. We have not seen a higher incidence of complications with longer indwelling times, such as was observed by Wust *et al.* (12). The incidence of catheter-related morbidity may be lower when catheters are inserted before each treatment. However, even when this would be practically feasible, the advantages must outweigh the disadvantages. Altogether, in our experience the cost of interstitial thermometry far outweighs the benefit when the individual patient is concerned. Our rather negative experience with interstitial thermometry for deep seated tumors is completely different from that with interstitial thermometry in superficially located tumors. In the first place, the incidence of morbidity from superficially implanted catheters is very low; our recent experience is not different from that previously published (13). Second, power distribution steering during superficial hyperthermia is possible with the multiapplicator multiamplifier microwave system used by us (14).

A HTNR 481, bladder cancer, 1st treatment

B HTNR 447, rectal cancer, 2nd treatment

C HTNR 403, cervical cancer, 1st treatment

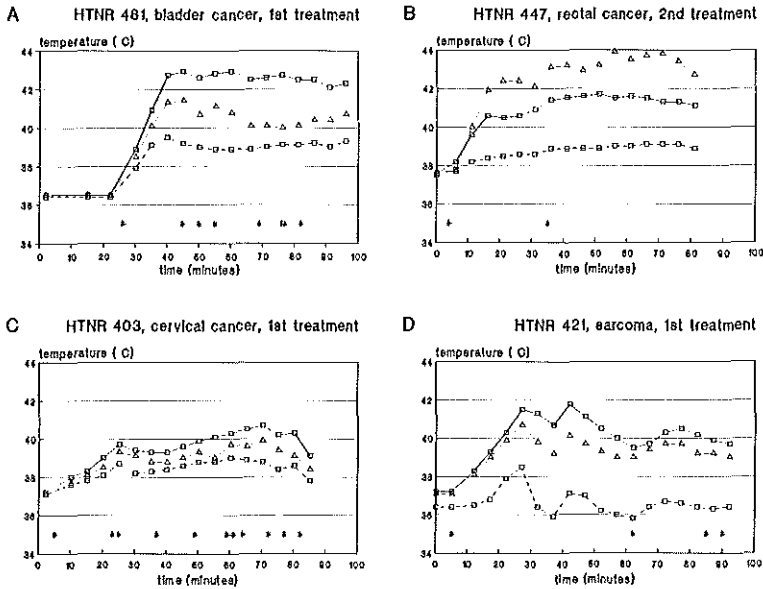**D** HTNR 421, sarcoma, 1st treatment

Fig. 2. Intratumor temperature distribution during deep hyperthermia in four patients, in each patient measured within two interstitial catheters, and in a lumen in close relation to the tumor. —□—: intratumor T_{max}; —△—: intraluminal T_{max}; –□–: intratumor T_{min}; *: start/steering. (A) Patient with stage T4 bladder cancer, with a total of 10 intratumor measurements. (B) Patient with large recurrent rectal cancer, with a total of 16 intratumor measurements. For this patient the temperature distribution during the second treatment is given, because thermal mapping during the first treatment was possible in only one catheter. Power distribution was changed only once, based upon the experience during the first treatment. (C) Patient with Stage IIIB uterine cervical cancer, with a total of 12 intratumor measurements. (D) Patient with recurrent sarcoma, with a total of 29 intratumor measurements.

The second type of arguments in favor of intratumor temperature information concerns scientific issues. The information can be used to assess, retrospectively, the treatment quality in terms of thermal dose. It is clear that higher temperatures will result in more cell kill (15). Thermal dose–response relationships have been found in many clinical studies (16). However, clinically found relationships for thermal dose parameters are complicated. These are retrospectively defined, and not prescribed, thermal doses, and as such may be just a representative of a tumor characteristic, which by itself is of prognostic value. Such is suggested by the negative relation between parameters for thermal dose and the number of thermometry points, together with the positive relation between the number of thermometry points and tumor size (17–19). Further the recent findings of angiogenesis being an independant prognostic factor for several types of cancer support this hypothesis (20). Dose-response relationships have also been found for intraluminally measured temperatures (21, 22) and even for total power output (23, 24). Wust *et al.* (12) found a positive correlation between endoluminally and intratumorally measured power densities. Whether these relationships do exist in our patients will be subject of further analysis. There are situations where the value of interstitial thermometry will

easier outweigh the possible risks. In the first place, in learning how to use newly installed equipment. Any information on how changes in treatment settings influence temperature distribution are helpful in getting experienced. In the second place, when the intratumor distribution is subject of investigation, such as when two heating techniques are compared, or when either noninvasive thermometry or 3D treatment planning is verified. However, these goals are not in the benefit of the individual patient. To address these questions, separate studies should be developed with strict demands on standardized thermometry, and patients will have to give informed consent for participation in such studies. The limited value of interstitial thermometry will remain to exist when new equipment, allowing small-scale SAR steering will become available for clinical use. The number of invasive thermometry sites within the treated volume is relatively small and the criteria as formulated by the RTOG guidelines (1) can hardly ever be met. The information that can be achieved with interstitial measurements on intratumor temperature distribution in deep-seated tumors is limited. In our patients with interstitial thermometry, the number of measuring points per treatment was only 6.9, which is rather low for tumors with an average volume of 314 cm^3. Decreasing the thermal mapping step size to,

for example, 0.5 cm would have doubled the number of measurements, but in our opinion not resulted in a relevant improvement of thermometry quality. We must realize that even if technology is no longer a limitation for small-scale

SAR steering, we will need considerable progress in other fields, such as noninvasive thermometry, and real-time information on anatomy, tissue characteristics and blood flow within the patient under treatment.

REFERENCES

1. Sapozink, M. D.; Corry, P. M.; Kapp, D. S.; Myerson, R. J.; Dewhirst, M. W.; Emami, B.; Herman, T.; Prionas, S.; Ryan, T.; Samulski, T.; Sapareto, S.; Shrivastava, P.; Stauffer, P.; Waterman, F. RTOG quality assurance guidelines for clinical trials using hyperthermia for deep-seated malignancy. Int. J. Radiat. Oncol. Biol. Phys. 20:1109–1115; 1991.
2. van der Zee, J.; van Rhoon, G. C.; Koper, P. C. M.; Treurniet-Donker, A. D.; Wijnmaalen, A. J. First clinical experience with deep regional hyperthermia. Strahlenther. Onkol. 167: 349; 1991.
3. van der Ploeg, S. K.; Verloop-van 't Hof, E. M.; van Rhoon, G. C.; Koper, P. C. M.; Treurniet-Donker, A. D.; Wijnmaalen, A. J.; van der Zee, J. First clinical experience with deep regional hyperthermia in Rotterdam. In: Gerner, E. W., ed. Hyperthermic oncology 1992, vol. I, Summary papers. Phoenix, AZ: Arizona Board of Regents; 1992:403.
4. Turner, P. F.; Schaefermeyer, T. BSD-2000 approach for deep local and regional hyperthermia: Clinical utility. Strahlenther. Onkol. 165:700–704; 1989.
5. van der Zee, J.; Veeze-Kuijpers, B.; Wiggers, T.; Treurniet-Donker, A. D. Risk of tumour growth along thermometry catheter trace: A case report. Int. J. Hyperthermia 8:621–624; 1992.
6. Anscher, M. S.; Samulski, T. V.; Leopold, K. A.; Oleson, J. R. Phase I/II study of external radio frequency phased array hyperthermia and external beam radiotherapy in the treatment of prostate cancer: Technique and results of intraprostatic temperature measurements. Int. J. Radiat. Oncol. Biol. Phys. 24:489–495; 1992.
7. Wust, P.; Stahl, H.; Löffel, J.; Seebass, M.; Riess, H.; Felix, R. Clinical, physiological and anatomical determinants for radio-frequency hyperthermia. Int. J. Hyperthermia 11:151–167; 1995.
8. Myerson, R. J.; Scott, C. B.; Emami, B.; Sapozink, M. D.; Samulski, T. V. A phase I/II study to evaluate radiation therapy and hyperthermia for deep-seated tumours: A report of RTOG 89-08. Int. J. Hyperthermia 12:449–459; 1996.
9. Gellermann, J.; Wust, P.; Stalling, D.; Nadobny, J.; Seebass, M.; Beier, J.; Hege, H. C.; Deuflhard, P.; Budach, V; Felix, R. Clinical evaluation and verification of the hyperthermia treatment planning system HyperPlan™. Int. J. Radiation Oncology Biol. Phys. (1998), submitted.
10. van der Zee, J.; van Rhoon, G. C.; de Wit, G. A.; de Charro, F. Th. Report of developmental medicine project OG 89-32 "The value of hyperthermia in addition to radiotherapy in the treatment of inoperable and radioresistant tumours." Dutch Health Insurance Fund Council; 1997.
11. Feldmann, H. J.; Hoederath, A.'; Molls, M.; Sack, H. Problems associated with CT-guided catheter insertions. Int. J. Hyperthermia 9:219–225; 1993.
12. Wust, P.; Gellermann, J.; Harder, W.; Tilly, W.; Rau, B.; Dinges, S.; Schlag, P.; Budach, V.; Felix, R. Rationale for using invasive thermometry for regional hyperthermia of pelvic tumors. Int. J. Radiation Oncology Biol. Phys. (1998) in review.
13. van der Zee, J.; van Rhoon, G. C.; Broekmeyer-Reurink, M. P.; Reinhold, H. S. The use of implanted closed-tip cath-

eters for the introduction of thermometry probes during local hyperthermia treatment sessions. Int. J. Hyperthermia 3:337–345; 1987.
14. van Rhoon, G. C.; Rietveld, P. J. M.; Broekmeyer-Reurink, M. P.; Verloop-van 't Hof, E. M.; van der Ploeg, S. K.; van der Zee, J. 433 MHz waveguide applicator system with an improved effective field size for hyperthermia treatment of superficial tumors on the chest wall. In: Gerner, E. W.; Cetas, T. C., eds. Hyperthermia oncology 1992, vol. 2. Phoenix, AZ: Arizona Board of Regents; 1993:187–190.
15. Field, S. B. In vivo aspects of hyperthermic oncology. In: Field, S. B.; Hand, J. W., eds. An introduction to the practical aspects of clinical hyperthermia. London: Taylor & Francis; 1990:55–68.
16. Dewhirst, M. W. Thermal dosimetry. In: Seegenschmiedt, M. H.; Fessenden, P.; Vernon, C. C., eds. Thermoradiotherapy and thermochemotherapy, volume 1: Biology, physiology, physics. Berlin: Springer; 1996:123–136.
17. Perez, C. A.; Emami, B. Clinical trials with local (external and interstitial) irradiation and hyperthermia. Current and future perspectives. Radiol. Clin. North Am. 27:525–542; 1989.
18. Overgaard, J.; González González, D.; Hulshof, M. C. C. H.; Arcangeli, G.; Dahl, O.; Mella, O.; Bentzen, S. M. Hyperthermia as an adjuvant to radiation therapy of recurrent or metastatic melanoma. A multicentre randomized trial by the European Society for Hyperthermic Oncology. Int. J. Hyperthermia 12:3–20; 1996.
19. van der Zee, J.; van Rhoon, G. C.; Verloop-van 't Hof, E. M.; van der Ploeg, S. K.; Rietveld, P. J. M.; van den Berg, A. P. The importance of adequate heating techniques for therapeutic outcome. In: Gerner, E. W.; Cetas, T. C., eds. Hyperthermic oncology 1992, vol. 2. Phoenix, AZ: Arizona Board of Regents; 1993:349–352..
20. Craft, P. S.; Harris, A. L. Clinical prognostic significance of tumour angiogenesis. Ann. Oncol. 5:305–311; 1994.
21. Rau, B. P.; Wust, P.; Löffel, J.; Hünerbein, M.; Below, C.; Gellerman, J.; Speidel, A.; Vogl, T.; Riess, H.; Felix, R.; Schlag, P. M. Preoperative hyperthermia in combination with radiochemotherapy in locally advanced rectal cancer. A phase III clinical study. Annals Surg. 227, 1, (1998) in press.
22. Dinges, S.; Harder, C.; Wurm, R.; Buchali, A.; Blohmer, J.; Wust, P.; Budach, V. Combined treatment of inoperable carcinomas of the uterine cervix with radiotherapy and regional hyperthermia—Results of a phase II trial. Radioth. Oncol. (1998), in press.
23. Steindorfer, P.; Germann, R.; Klimpfinger, M. Experience with an annular phased array hyperthermia system in the treatment of advanced recurrences of the pelvis. Recent Results Cancer Res. 107:226–235; 1988.
24. Terashima, H.; Imada, H.; Hiraoka, M.; Nishimura, Y.; Imajo, Y.; Hiratsuka, J.; Karasawa, K.; Kitahara, T.; Kataoka, M.; Wada, S.; Hashida, I. Multi-institutional clinical study on hyperthermia combined with radiotherapy in lung cancer. A retrospective analysis by JASTRO. In: Franconi, C.; Arcangeli, G.; Cavaliere, R., eds. Hyperthermic oncology 1996 vol. 2. Rome: Tor Vergata Post Graduate School of Medical Physics; 1996:81–82.

Chapter 4

A 433 MHz Lucite Cone waveguide applicator for

superficial hyperthermia

GC van Rhoon, PJM Rietveld and J van der Zee

A 433 MHz Lucite Cone waveguide applicator for superficial hyperthermia

G. C. VAN RHOON†, P. J. M. RIETVELD and J. VAN DER ZEE

University Hospital Rotterdam, Daniel den Hoed Cancer Center, Department of Radiation Oncology, Section Hyperthermia, PO Box 5021, NL 3008 AE, Rotterdam, The Netherlands

The effective field size (EFS, SAR $\geq$ 50% of the maximum SAR at 1 cm depth) of a conventional 433 MHz water filled waveguide applicator ($32\,cm^2$, aperture area $100\,cm^2$) has been increased by: (1) replacement of the two diverging brass side walls which are parallel to the direction of the electric field by Lucite walls; and (2) Placement of a heterogeneous permittivity in the centre of the aperture. SAR distributions were measured at several depths in layered fat-muscle phantoms. With Lucite side walls the SAR distribution becomes wider in the H-plane of the aperture, resulting in a circular SAR distribution. In this situation the EFS is $67\,cm^2$. Additional insertion of a PVC cone with a top angle of $15°$ at the centre of the aperture increases the EFS to $91 \pm 6\,cm^2$ for a waterbolus of $18 \times 18 \times 1\,cm^3$. The experiments also demonstrated that the resulting EFS is affected by the waterbolus size and shape. Calorimetric measurements showed that the efficiency of the improved applicator is comparable to the efficiency of the conventional water filled waveguide applicator, 50 and 56% respectively. The modifications reported provide a simple and inexpensive means to increase the EFS and can be easily implemented in water filled waveguide applicators.

Key words: Superficial hyperthermia, microwaves, SAR distribution, water filled waveguide applicator, MW applicator arrays

1. Introduction

Superficial hyperthermia of chest wall recurrences of breast cancer is a frequently used modality in the clinical application of hyperthermia (HT). With the publication of the results of five randomized trials comparing radiotherapy (RT) versus RT + HT in the treatment of superficial located breast cancer by the International Collaborative Hyperthermia Group (ICHG 1961) it is also one of the sites for which the combined treatment of RT + HT has been proven to be effective and, in several institutes, has become standard treatment. Unfortunately, as in other randomized (Perez *et al.* 1989, Overgaard *et al.* 1995) and non-randomized trials (Meyerson *et al.* 1990, van der Zee *et al.* 1992, van der Zee and Vernon 1996), it was also indicated in the studies reported by the ICHG (1996) that tumour depth is negatively associated with clinical outcome. For the same study material Sherar *et al.* (1997) found a significant dose response relationship between minimum thermal dose parameters and clinical outcome. Hence, it is generally expected that patients with large tumour volumes may benefit substantially from an improved quality of the superficial hyperthermia treatment of chest wall recurrences.

Improvement of the quality of the SAR distribution should aim for a large effective field size (EFS as defined by Hand *et al.* [1989]), good spatial control of the SAR distribution and sufficient penetration depth. In practice this can only be achieved with the use of multi-element HT applicator arrays. However, despite the ample clinical experience with superficial heating, the exact demands on spatial control, penetration depth and SAR converage are still unknown.

Currently, several applicator arrays with individual power control of each element (Lee 1995) have been developed and are in clinical use. All these systems are constructed by using numerous (up to 25) conventional applicator elements. Characteristic for these conventional applicators is the relative low ratio of EFS to the aperture area (commonly 30–50%). By close packing of the elements a contiguous EFS can be obtained. If special techniques are used (placing these elements at sufficient distance to the skin or overlapping of elements) it is possible to limit SAR variations within the effective field to 10%.

Conceptually such small elements may provide the best spatial resolution of SAR control and conformation to the body contour, however they also have some disadvantages. Firstly, small elements carry the risk of a loss in penetration depth (Hand 1990). A larger aperture to skin distance may reduce this risk but due to the divergence of the electric field this has the consequence of a reduced spatial control. Secondly and probably more important the use of complex applicator arrays with many small elements will put strict demands on information about the temperature distribution under each array element and automatic control algorithms in order to exploit the feasibility of SAR steering during clinical HT treatments. If power control is performed manually, as is still the case in most HT departments, the number of elements is clearly limited by the comprehension of the HT technician and practical limitations of thermometry. The relevance of these demands for the final quality of the HT-treatment should not be underestimated, as HT is still an empirical treatment with the final quality depending strongly on the experience and abilities of the HT technician.

Based upon our clinical experience our approach to improve the quality of the SAR distribution differs in the sense that we prefer to limit the number of elements of the array. This of course will affect the resolution of spatial control. To obtain a contiguous EFS under the array aperture using a limited number of elements it is essential to develop a waveguide applicator with an improved EFS preferable comparable to the aperture size. In this paper we describe our method to increase the small effective treatment area of our conventional 433 MHz water filled waveguide applicator. The performance of the improved applicator in an array configuration will be reported elsewhere.

2. Materials and methods

2.1. *Waveguide modifications*

Two types of waveguide applicators are used in the experiments, which are refered to as :

2.1.1. *Conventional waveguide applicator.* A water filled, rectangular waveguide applicator made of brass and operating in the TE_{10} mode. The dimensions of the first part of the waveguide, that is at the dipole antenna, are 3.0 by 5.0 cm. Dipole dimensions: diameter 0.3 cm, insertion depth 2.5 cm, and distance to the reflective
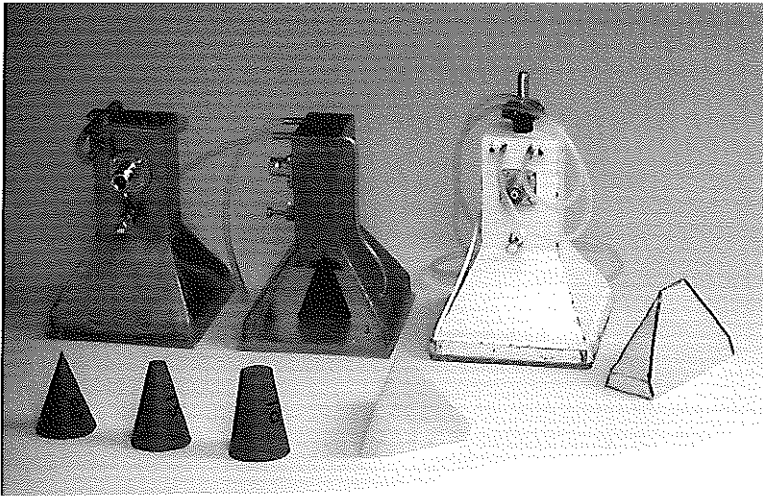
Figure 1.   Photograph of the various applicators and the different field adapters: (right) the conventional waveguide applicator; (centre) Lucite Cone waveguide applicator, note the PVC cone at the centre of the aperture; (left) Lucite waveguide applicator.

back-plane of the waveguide 2.4 cm. The second part of the applicator starts at approximately 0.5λ from the dipole. From this point the waveguide cross-section diverges to the final aperture size of $10.0 \times 10.0 \, cm^2$ (inner dimensions). As is well known the electrical (E) field of a TE_{10} waveguide varies sinusoidally over the aperture, with a zero E-field at the metal sides, which results in the reported small EFS.

2.1.2. *Lucite waveguide applicator.* Basically, this is the same water filled, rectangular waveguide applicator operating in the TE_{10} mode. The first part is identical with the conventional applicator. The second part is modified with the objective to increase the EFS. The modifications applied are:

(1)   Replacement of the two diverging brass side walls which are parallel to the direction of the E-field, by Lucite (thickness 0.28 cm). In this way a nonzero E-field condition at the boundaries is created;

(2)   Use of an heterogeneous permittivity in the horn of the applicator. Two types of field adapters were tested: (A) a PVC cone with a basediameter of 4.0 cm, height 5.5 cm, and top angle of 10, 15 or 20°, and (B) a foam insert with a base of $4.0 \times 10.0 \times 1.0 \, cm^3$ and on top of that a wedge of $4.0 \times 10.0 \times 4.5 \, cm^3$, with a top angle of 15° and a width of 5 cm at the top. The base of the cone and the foam insert are positioned centrally in the plane of the aperture. The foam insert has its long axis parallel to the E-field.

The applicators: conventional, Lucite and Lucite with field adapters are shown in figure 1.

2.2. *SAR measurements for applicator modifications*

Relative SAR distributions of each applicator configuration are measured at 1 cm depth using a flat ($50 \times 50 \times 10$ cm^3) muscle equivalent phantom (Guy 1971). In all experiments a water bolus (plastic bag filled with deionized water at room temperature) is placed between the applicator and the phantom. To measure the SAR distribution according to the ESHO quality assurance guidelines (Hand *et al.* 1989) the phantom is constructed in layers of 1 and 2 cm thickness for the first 5 cm. To ease separation, each layer of phantom material is covered by a 0.005 cm thick PVC mylar which has no influence on the resulting SAR distribution. The maximum duration of heating was limited to 1.5 minutes. In this time a temperature increase of 3–6°C was obtained at the location of maximum energy absorption. After removal of the applicator, waterbolus and the first (1 or 2 cm) layer of phantom material the temperature distribution of the exposed surface was measured by an AGA infrared camera interfaced to a personal computer (Deursen and van Rhoon 1987) within 15 s after power off. Effectively, the measured temperature distribution represents the SAR distribution. During the experiments the applicator was connected to a 433 MHz generator. Power was measured using Bird power meters and the average net power used ranged from 100 to 300 W. Following the temperature measurement, isocontour grey-scale plots of the SAR distribution were made for each applicator using in-house written software. The area within the 50% iso-SAR contour, the EFS, is determined by this software.

2.3. *Specific experiments for the Lucite Cone applicator*

The Lucite applicator containing the PVC cone (top angle 15°), hereafter called the Lucite Cone applicator (LCA), showed the largest EFS most promising for clinical applications. Therefore, a number of additional experiments, as described below, have been performed specifically for this applicator. SAR distributions have been measured at various depths in a homogeneous muscle equivalent phantom with and without a 1 cm thick layer of fat-equivalent tissue (Guy 1971) in front of the aperture. Additionally, the influence of various thicknesses (range 0–3 cm) and sizes (18×18 and 25×30 cm^2) of the waterbolus on the resulting EFS was investigated.

To mimic clinical circumstances the magnitude of SAR distortion by placing the applicator with an angle of 20° on the flat phantom surface has also been investigated.

The efficiency of the LCA has been measured calorimetrically. Hereto, the LCA is placed above a Styrofoam box ($20 \times 20 \times 20$ cm^3) with 5 cm thick walls, which was filled with saline water (9 gram NaCl per litre water). In this experiment no waterbolus is used and the aperture of the applicator is placed in close contact with the saline water surface. The temperature increase of the saline water is measured after 1 h microwave heating at 200 W net input power to the LCA. To correct for heat exchange of the water with the environment and the applicator the temperature change of the calorimeter was recorded for 30 min before and after the microwave heating. The efficiency of the applicator is defined as the ratio between the power absorbed in the saline water (corrected for all heat losses) and the net RF-power delivered to the applicator at the connecting N-plug.

Finally, the stray radiation level was measured for both the LCA and conventional applicator radiating in the muscle equivalent phantom using a waterbolus of $18 \times 18 \times 1$ cm^3. Stray radiation patterns were measured using an isotropic monitor (Narda 8662). The normal frequency band of this monitor is from 0.3 to 300 MHz

with full-scale meter ranges of 2.0, 20.0 and 200.0 mW/cm^2. For this occasion the meter has been calibrated specifically at 433 MHz (van Swinden Laboratorium, Netherlands Measure Institute).

3. Results

The heating time of 1.5 min is longer than that recommended in the ESHO QA guidelines and may give some concern regarding thermal conduction errors. Therefore, figure 2 provide a comparison of the SAR-distribution of a Lucite Cone Applicator at 1 cm depth in a muscle-equivalent phantom obtained by both the infrared thermograph method or by an E-field scanning method.[1] Special care was taken to have identical set-ups in both experiments. As is shown, the SAR distributions are in good agreement: half beam widths as measured with the infrared and E-field scanning method are 84 versus 85 mm along the E-field direction and 100 versus 99 mm for the direction perpendicular on the E-field, respectively. These differences are well within the accuracy (±10%) of each method and, in our opinion, validates the further use of the infrared thermographic method with a heating time of 1.5 min.

3.1. *Conventional applicator*

The SAR distribution as obtained for the conventional applicator is presented in figure 3a. As expected, the SAR distribution has an elliptical shape, with the major axis parallel to the direction of the electrical field. The profiles shown in figure 3b provide more detailed information about the change of the relative SAR along the major axes, parallel with, and perpendicular to the E-field, of the applicator. Each point of the curves represent a spatial mean of the SAR of 4 pixels (total width 1 cm) at the axis. The EFS measured for the conventional applicator is 32 cm^2.

Placement of the PVC cone or foam insert in the aperture of the conventional applicator did not result in a marked increase of the EFS. These results are summarized in table 1.

3.2. *Lucite applicator*

Replacing the brass side walls of the waveguide by Lucite walls made the SAR distribution at 1 cm depth in the muscle equivalent phantom circular instead of elliptical and the width of the 50% iso-SAR contour is almost the same for both axes 79 and 87 mm^2, parallel with—and perpendicular to the direction of the E-field respectively. For this applicator design the EFS is 67 cm^2, approximately 2× as large as the EFS of the conventional applicator.

3.3. *Lucite applicator with field adapters*

Adding the field adapters in the aperture of the Lucite applicator results in a further increase of the EFS. With the foam insert the EFS increases to 106 cm^2. The resulting SAR distribution (figure 4a) has the shape of an '8' with a constriction at the location of the wedge. As can be seen in figure 4b the foam insert results in a large improvement of the SAR distribution along the axis perpendicular to the E-field

---

[1] In the E-field scanning method the applicator and a receiving dipole antenna (made of semi-ridged coaxial cable, dipole arm 5 mm) were connected to a network analyser (HP8751A). A liquid muscle-equivalent phantom was used (35.6% ethyl-alcohol, 63.2% distilled water and 1.2% NaCl; $\varepsilon_r = 57$ and $\sigma = 1.2$ S/m).

RELATIVE SAR

dipole(HBW = 99 mm)   IR(HBW = 100 mm)

(a)

RELATIVE SAR

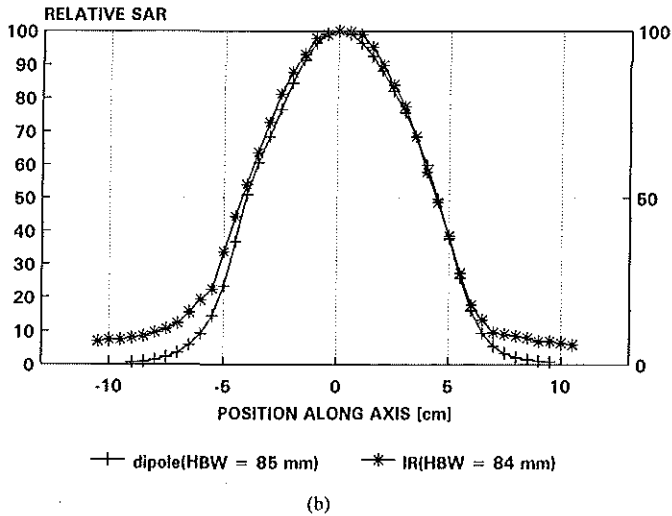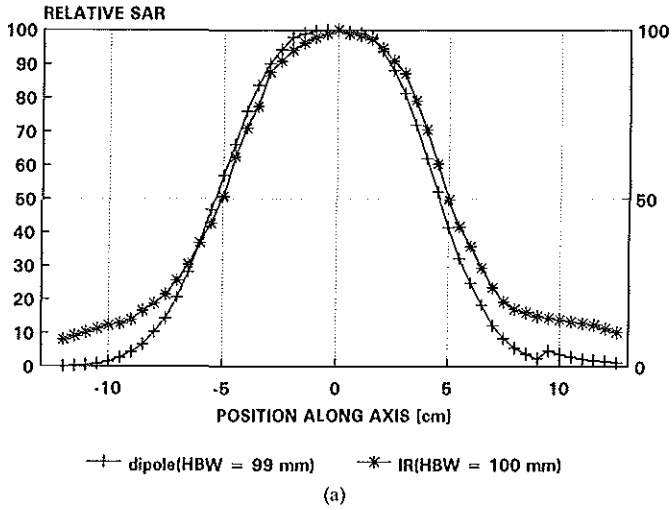dipole(HBW = 85 mm)   IR(HBW = 84 mm)

(b)

Figure 2.   Relative SAR distribution at 1 cm depth in a homogeneous muscle equivalent phantom measured with either the infrared thermographic method or with the E-field scanning method using a small dipole: (a) along the axis perpendicular to; and (b) along the axis parallel with the E-field direction. HBW: half beam width.
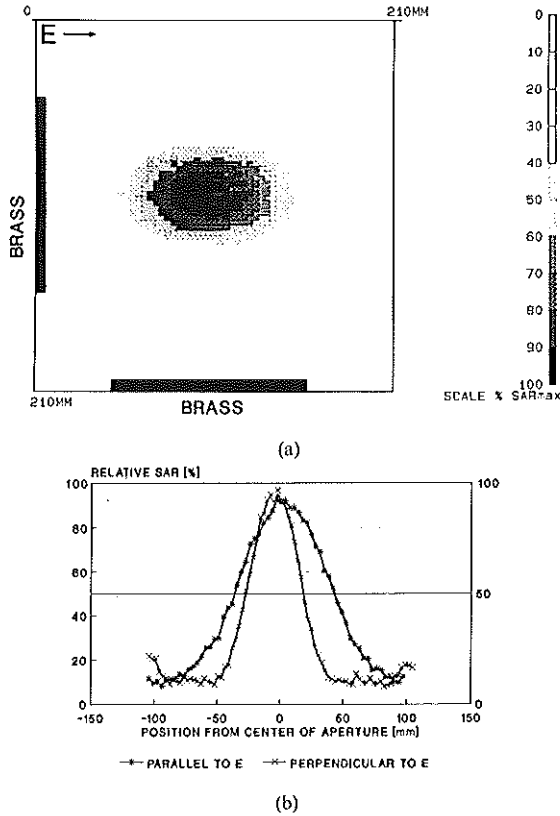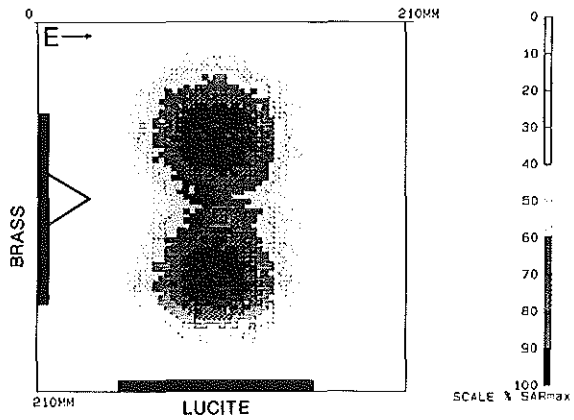
(a)

(b)

Figure 3.   (a) SAR distribution at 1 cm depth of a flat, homogeneous muscle equivalent
phantom for the conventional applicator and a water bolus thickness of 1 cm; (b)
Relative SAR along the central axes, parallel and perpendicular to the E-field, of the
conventional applicator. Each point of the curves represents a spatial mean of the SAR of
four pixels (total width 1 cm).

direction. Similar, for the PVC cone the EFS increases to $99 \, cm^2$ (for six different
LCAs $91 \pm 6 \, cm^2$ average ± 1 s.d.). For this applicator configuration the SAR dis-
tribution has an elliptical shape (figure 5a). Again, as can be seen in figure 5b the
improvement of the SAR distribution is mainly along the axis perpendicular to the
direction of the E-field. The experiments using the PVC cones with top angle of 10 or
20° showed worse results. That is with a top angle of 20° the EFS increases only to
$73 \, cm^2$, while with a top angle of 10° it was not possible to reduce the reflected
power[2] to an acceptable level (< 20%) and no SAR distribution could be measured
(see also table 1).

[2] For all other applicator configurations the reflected power could be reduced to < 10% by
adjusting the tuning rod located in the first part of the applicator.

Table 1. Effective field size of the conventional waveguide applicator and the Lucite waveguide applicator at 1 cm depth in a homogeneous muscle equivalent phantom: effect of field adapters. Waterbolus $18 \times 18 \times 1 \, cm^3$.

| Field adapter	Effective field size (cm^2)	
	Conventional waveguide applicator	Lucite waveguide applicator
None	32	67
Foam insert	37	106
PVC cone		
10°	39	
15°	38	99
20°	37	73

(a)
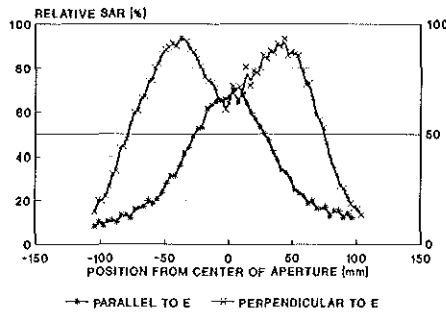
(b)

Figure 4. Lucite applicator with a foam wedge. (a) SAR distribution at 1 cm depth of a flat, homogeneous muscle equivalent phantom and a water bolus thickness of 1 cm; (b) Relative SAR along the central axes, parallel and perpendicular to the E-field. Each point of the curves represents a spatial mean of the SAR of four pixels (total width 1 cm).
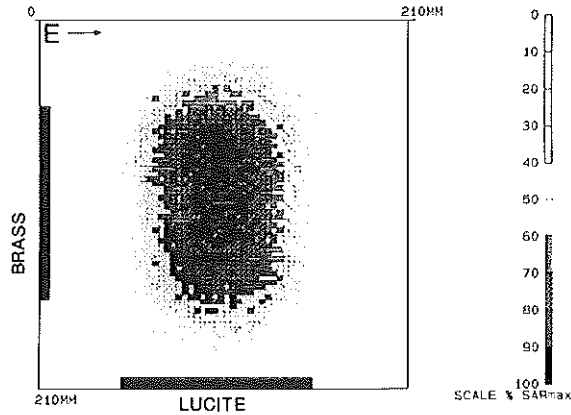
(a)
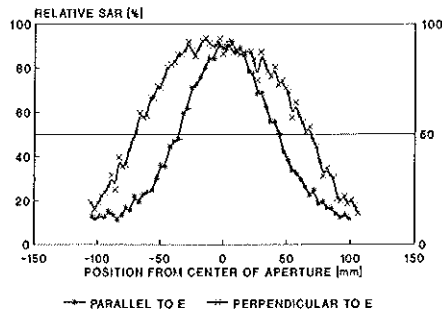
(b)

Figure 5.   Lucite applicator with a 15° PVC cone. (a) SAR distribution at 1 cm depth of a
flat, homogeneous muscle equivalent phantom and a water bolus thickness of 1 cm; (b)
Relative SAR along the central axes, parallel and perpendicular to the E-field. Each point
of the curves represents a spatial mean of the SAR of four pixels (total width 1 cm).

3.4. *Influence of waterbolus size and thickness, fat layer and tilted position on the*
SAR distribution of the Lucite Cone applicator

Table 2 shows the resulting EFS of the LCA as function of the waterbolus
thickness for two different waterbolus sizes. An EFS of $62\,cm^2$ is measured when
the LCA is placed directly on the phantom. For a waterbolus size of $18 \times 18\,cm^2$ the
EFS increases to $98\,cm^2$ for a waterbolus thickness of 0.5 cm and to $103\,cm^2$ for a
waterbolus thickness of 2.0 cm. For the larger waterbolus of $25 \times 30\,cm^2$ the EFS
measures 62 and $65\,cm^2$ for a waterbolus thickness of 1.0 and 2.0 cm respectively.

Table 3 provides an overview of normalized EFS's at different depths as meas-
ured for the LCA using a homogeneous and a fat-muscle layer phantom configura-
tion. Normalization has been performed to the EFS value measured at 1 cm depth in

Table 2. Average effective field size of the LCA at 1 cm depth in a homogeneous muscle
equivalent phantom for various thicknesses and sizes of the waterbolus between the
applicator and phantom.

Average effective field size (cm^2)	Waterbolus size (cm^2)	
Waterbolus thickness (cm)	18×18	25×30
0	62	62
0.5	98	
1.0	92	62
2.0	103	65
3.0		64

Table 3. Normalized[1] effective fieldsize of the LCA at different depth and for two phantom
configurations. Waterbolus $18 \times 18 \times 1$ cm^3.

Location	Muscle phantom	Fat-muscle phantom[2]
Surface fat layer		0
Surface muscle tissue	133	148
At 1 cm depth in the muscle phantom	100	118

[1]Normalization is performed to the EFS at 1 cm depth in the homogeneous muscle equivalent phantom.
[2]Fat-muscle phantom includes a 1 cm thick fat equivalent layer on the muscle phantom.

the homogeneous muscle equivalent phantom. It was found that a 1 cm thick layer of fatty tissue in front of the aperture resulted in a 20% increase of the EFS at 1 cm depth in muscle tissue.

Tilting the aperture of the applicator 20° parallel with the direction of the E-field results in a small effect on the SAR distribution. The SAR-profile along the axis parallel to the E-field is shifted by approximately 10–15 mm towards the direction of the lower end of the applicator aperture (figure 6). For the SAR-profile perpendicular to the E-field the width of the 50% iso-SAR is reduced by 18 mm (−70 to 69 mm in figure 5b versus −61 to 60 mm in figure 6). The effective field, however, still measures 98 cm^2. For a 20° tilt perpendicular to the direction of the E-field the EFS is reduced to 81 cm^2 and a shift of the effective field towards the elevated side of the applicator occurs (figure 7). For the SAR-profile along the axis perpendicular to the E-field this shift is from −70 and +69 mm to −81 and +60 mm. In this case the width of the SAR-profile parallel to the E-field above the 50% value is reduced by 9 mm (−35 to 43 mm in figure 5b versus −29 to 40 mm in figure 7). When this type of tilt would occur in an array of applicators the latter effect may cause a stronger coupling to the adjacent applicator.

3.5. *Efficiency*

From the calorimetric measurements performed it was found that the efficiency of the LCA is comparable to the efficiency of the conventional water filled waveguide applicator, $50 \pm 8\%$ ($n = 8$) and $56 \pm 76\%$ ($n = 6$) respectively (average ± 1 s.d.).
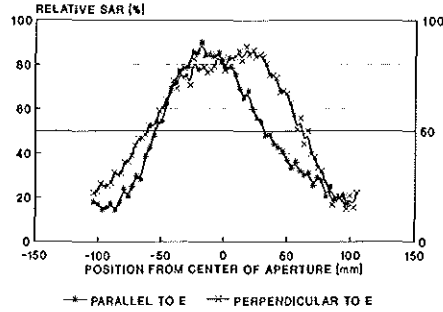
Figure 6. LCA with a 20° tilt of the aperture parallel with the direction of the E-field. Relative SAR along the central axes, parallel and perpendicular to the E-field. Each point of the curves represents a spatial mean of the SAR of four pixels (total width 1 cm).

Figure 7. LCA with a 20° tilt of the aperture perpendicular to the direction of the E-field. Relative SAR along the central axes, parallel and perpendicular to the E-field. Each point of the curves represents a spatial mean of the SAR of four pixels (total width 1 cm).
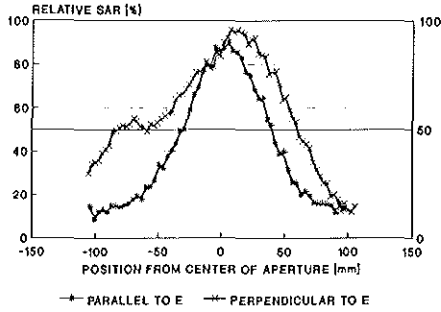
3.6. Stray radiation levels

Table 4 gives the stray radiation levels for both the conventional waveguide applicator and the LCA along the major axes at various distances to the applicator. As is shown in table 4 the stray radiation level of the LCA is higher than that of the conventional waveguide. For both applicators the maximum intensity of the stray radiation is measured along the axis parallel to the direction of the E-field.

4. Discussion

A limitation of all presently used electromagnetic, radiative applicators is their small EFS compared to the aperture size (Lee 1995). Especially in the hyperthermia treatment of chest wall recurrences, which generally extend over large areas, the small EFS is a serious disadvantage. A significant increase of the EFS for multi-applicator arrays compared to the EFS of a single applicator with the same dimensions has been demonstrated theoretically and experimentally by Hand (1989). Of course for practical clinical use a trade-off has to be made between a small aperture

Table 4. Stray radiation levels (mW/cm^2) measured for the conventional waveguide applicator and the LCA along the major axes. Values are normalized to an input power of 100 W.

Distance from applicator (cm)	Conventional waveguide applicator		LCA	
	'H'	'E'	'H'	'E'
50	—	—	—	0.02
25	0.01	0.03	0.03	0.16
10	0.07	0.39	0.10	0.6

'E': axis parallel to the direction of the E-field.
'H': axis perpendicular to the direction of the E-field.

size for spatial control of the energy distribution and a large aperture size for sufficient penetration depth (Cheever *et al.* 1987, Hand 1987). Interesting approaches for applicator arrays are the flexible microstrip applicator (Lee *et al.* 1992), the current sheet applicator (Gopal *et al.* 1992) and the Microtherm 1000 system (Diederich and Stauffer 1993). Alternatively to the array approach several groups have investigated the possibilities to improve the EFS of the applicator itself. The resulting EFS of these modified applicators, dual spiral applicator, EFS 55% of the aperture (Ryan *et al.* 1995) and dual-antenna waveguide applicator, EFS 47% of the aperture (Leybovich *et al.* 1991) cannot compete with the size and quality of the EFS obtained by the above mentioned array systems.

Other methods focused on optimization of the SAR distribution through scanning of the treatment area with a single applicator (Samulski *et al.* 1990, Tennant *et al.* 1990), or by the use of a selective absorption bolus (Sherar *et al.* 1993, 1994). For the latter method the maximum reported EFS covered up to 60% of the aperture area (Sherar *et al.* 1993). The disadvantage of this method is, however, that the power efficiency of the whole system (applicator plus absorbing bolus) is dramatically reduced and thus applicability of this method depends on the available power of the microwave generator.

Compared to the above described methods our approach to improve the SAR distribution of the applicator is different in the way that is based on older and more established techniques to modify the characteristics of conventional waveguides. The use of the nonzero E-field boundary in the Lucite applicator can be regarded as a way to increase the width of the H-plane within the aperture (Epis 1961). For a conventional, homogeneously loaded, square aperture waveguide the E- and H-plane radiation patten beamwidths usually are unequal with a radiation polar diagram that is elliptical in cross-section. Theoretically increasing the width of the H-plane is expected to result in a circular symmetrical polar diagram. This effect was indeed found for the Lucite applicator without field adapters and resulted in a doubling of the EFS to 67 cm^2 compared to 32 cm^2 for a conventional waveguide (table 1).

A well-known and simple method to improve the uniformity of the E-field distribution across the aperture of a rectangular waveguide applicator is to partially load it with high dielectric slabs (Kantor 1981, Tsandoulas and Fitzgerald 1972). The introduction of the heterogeneous permittivity in the waterfilled Lucite applicator shows some resemblance to this technique. As a result of the low permittivity insert,

foam insert or PVC-cone, at the centre of the aperture a dielectrically loaded horn applicator is mimicked with water as the dielectric slabs of high permittivity. Here again our experimental results, as reported in figures 4 and 5, agree with expectations. Although, the EFS of the Lucite applicator with a PVC cone (top angle 15°) is slightly smaller than that of the Lucite applicator with the foam insert, we consider the more uniform SAR-distribution of the Lucite applicator with PVC-cone better suitable for use in array applications.

Characteristic for the LCA is that the major axis of the elliptical SAR distribution is oriented perpendicular to the direction of the E-field (parallel for a conventional waveguide) and extends outside the aperture, which might be advantageous in array applications. The results obtained with the experiments using an inhomogeneous phantom are in agreement with those for the homogeneous phantom and showed an additional increase of the EFS by approximately 20% with a 1 cm thick fat layer in front of the muscle tissue.

The experiments performed with various shapes of the waterbolus indicate that size and shape of the waterbolus are affecting the resulting EFS. Dependence of the EFS of a microwave applicator on the waterbolus size is a known phenomenon and has been reported by others (Lee *et al.* 1992, Sherar *et al.* 1993, Ryan *et al.* 1995). However, the large difference in EFS as found here for the waterboli of $18 \times 18\,cm^2$ and $25 \times 30\,cm^2$ is unexpected and cannot be explained from the current experiments. A possible explanation might be the occurrence of resonance effects related to the precise dimensions of the waterbolus. This will be the subject of further experimental work and 3-D modelling.

For clinical applications it was encouraging that the EFS was only affected, a decrease by 15%, for a tilt position of the LCA perpendicular to the E-field direction. Additionally, the facts that the efficiency of the LCA is comparable to that of a conventional waveguide and that the stray radiation is negligible at a distance of 50 cm from the LCA, are of importance during the clinical use of this applicator.

Concerning weight and size microstrip applicators offer clear advantages over the bulky and rigid waveguide applicators. However, for treatment of tumours at the chest wall this problem is less important. Generally, there is enough room to place multiple applicators above the treatment field. By fixing the applicators to a well-designed mounting system as we have in use (hydraulic arms, movable and attached to the ceiling) most applicator set-ups can be made with minimal discomfort to the patient.

5. Conclusions

Under laboratory conditions and within a flat, layered, inhomogeneous muscle equivalent phantom the efficiacy of: (1) replacing two brass side walls in the horn of a waveguide applicator by two Lucite side walls; and (2) placing 'field adapters', like a foam insert or a PVC cone, in the aperture of the Lucite applicator as a means to significantly increase the relative effective field size has been demonstrated. This method provides a simple and inexpensive means to realize an increased effective field size for waveguide applicators. For the Lucite Cone applicator preferred by us for clinical treatment the effective field size was increased from $32\,cm^2$ to $91 \pm 6\,cm^2$ in an homogeneous muscle phantom. We expect that under clinical condition factors such as the dimensions of the waterbolus and the complex anatomy of the patient will influence the effective field size. The latter is subject of further experimental work.

References

CHEEVER, E., LEONARD, J. B., and FOSTER, K. R., 1987, Depth of penetration of fields from rectangular apertures in lossy media. *IEEE Transactions on Microwave Theory and Technics*, 35, 865–867.

DEURSEN, J. B. P. VAN, and RHOON, G. C. VAN, 1987, Microprocessor-controlled interface for an Aga thermograph. *Biomedical Measurement Informatics and Control*, 2, 10–13.

DIEDERICH, C. J., and STAUFFER, P. R., 1993, Pre-clinical evaluation of a microwave planar array applicator for superficial hyperthermia. *International Journal of Hyperthermia*, 9, 227–246.

EPIS, J. J., 1961, Compensated electromagnetic horns. *Microwave Journal*, 4, 84–89.

GOPAL, M. K., HAND, J. W., LUMORI, M. L. D., ALKAHAIRI, S., PAULSEN, K. D., and CETAS, T. C., 1992, Current sheet applicator arrays for superficial hyperthermia of chestwall lesions. *International Journal of Hyperthermia*, 8, 227–240.

GUY, A. W., 1971, Analysis of electromagnetic fields induced in biological tissues by thermographic studies on equivalent phantom models. *IEEE Transactions on Microwave Theory and Techniques*, 19, 205–214.

HAND, J. W., 1987, Electromagnetic applicators for non-invasive local hyperthermia. *Physics and technology of hyperthermia*, edited by S. B. Field and C. Franconi (Dordrecht, Boston, Lancaster: Martinus Nijhoff Publishers), pp. 189–210.

HAND, J. W., LAGENDIJK, J. J. W., ANDERSON, J. B., and BOLOMEY, J. C., 1989, Quality assurance guidelines for ESHO protocols. *International Journal of Hyperthermia*, 5, 421–428.

HAND, J. W., 1990, Biophysics and technology of electromagnetic hyperthermia. *Methods of external hyperthermia heating*, edited by M. Gautherie (Berlin, Heidelberg, New York: Springer Verlag), pp. 1–59.

INTERNATIONAL COLLABORATIVE HYPERTHERMIA GROUP: C. C. Vernon, J. W. Hand, S. B. Field, D. Machin, J. B. Whaley, J. van der Zee, W. L. J. van Putten, G. C. van Rhoon, J. D. P. van Dijk, D. González González, F. F. Liu, P. Goodman and M. Sherar, 1996, Radiotherapy with or without hyperthermia in the treatment of superficial localized breast cancer—results from five randomized controlled trials. *International Journal of Radiation Oncology, Biology and Physics*, 35, 731–744.

KANTOR, G., 1981, Evaluation and survey of microwave and radiofrequency applicators. *Journal of Microwave Power*, 16, 135–150.

LEE, E. R., WILSEY, T. R., TARCZY-HORNOCH, P., KAPP, D. S., FESSENDEN, P., LOHRBACH, A., and PRIONAS, S. D., 1992, Body conformable 915 MHz microstrip array applicators for large superficial area hyperthermia. *IEEE Transaction on Biomedical Engineering*, 39, 470–483.

LEE, E. R., 1995, Electromagnetic superficial heating technology. *Principles and practice of thermoradiotherapy and thermochemotherapy*, Vol. 1, *Biology, Physiology, Physics*, edited by M. H. Seegenschmiedt, P. Fessenden and C. C. Vernon (Berlin, Heidelberg, New York: Springer Verlag GmbH), pp. 193–217.

LEYBOVICH, L. B., EMAMI, B., MYERSON, R. J., STRAUBE, W. L., and SATHIASEELAN, V., 1991, Dual-antenna applicator for hyperthermia of tumours at intermediate depth. *International Journal of Hyperthermia*, 7, 455–464.

MYERSON, R. J., PEREZ, C. A., EMAMI, B., STRAUBE, W., KUSKE, R. R., LEYBOVICH, L., and VON GERICHTEN, D., 1990, Tumor control in long-term survivors following superficial hyperthermia. *International Journal of Radiation Oncology, Biology and Physics*, 18, 1121–1129.

OVERGAARD, J., GONZÁLEZ GONZÁLEZ, D., HULSHOF, M. C. C. M., ARCANGELI, G., DAHL, O., MELLA, O., and BENTZEN, S. M. for ESHO, 1995, Randomized trail of hyperther-

mia as adjuvant to radiotherapy for recurrent or metastatic malignant melanoma. *The Lancet*, **345**, 540–543.

PEREZ, C. A., GILLESPIE, B., PAJAK, T., HORNBACK, N. B., EMAMI, B., and RUBIN, P., 1989, Quality assurance problems in clinical hyperthermia and their impact on therapeutic outcome: a report by the Radiation Therapy Oncology Group. *International Journal of Radiation Oncology, Biology and Physics*, **16**, 551–558.

RYAN, T. P., BACKUS, V. L., and COUGHLIN, C. T., 1995, Large stationary microstrip arrays for superficial microwave hyperthermia at 433 MHz: SAR analysis and clinical data. *International Journal of Hyperthermia*, **11**, 187–209.

SAMULSKI, T. V., FESSENDEN, P., LEE, E. R., KAPP, D. S., TANABE, E., and MCEUEN, A., 1990, Spiral microstrip hyperthermia applicators: technical design and clinical performance. *International Journal of Radiation Oncology, Biology and Physics*, **18**, 233–242.

SHERAR, M. D., LIU, F. F., NEWCOMBE, D. J., COOPER, B., LEVIN, W., TAYLOR, W. B., and HUNT, J. W., 1993, Beam shaping for microwave hyperthermia applicators. *International Journal of Radiation Oncology, Biology and Physics*, **25**, 849–857.

SHERAR, M. D., CLARK, H., COOPER, J., KUMARADAS, J., and LIU, F. F., 1994, A variable microwave array attenuator for use with single-element waveguide applicators. *International Journal of Hyperthermia*, **10**, 723–731.

SHERAR, M. D., LIU, F. F., PINTILIE, M., LEVIN, W., HUNT, J. W., HILL, R., HAND, J. W., VERNON, C. C., VAN RHOON, G. C., VAN DER ZEE, J., GONZÁLEZ-GONZÁLEZ, D. G., VAN DIJK, J. D. P., WHALEY, J., and MACHIN, D., 1997, Relationship between thermal dose and outcome in thermoradiotherapy treatments for recurrences of breast cancer in a randomized phase III trial. International Journal of Radiation Oncology, Biology and Physics, **39**, 371–380.

TENNANT, A., CONWAY, J., and ANDERSON, A. P., 1990, A robot-controlled microwave antenna system for uniform hyperthermia treatment of superficial tumours with arbitrary shape. *International Journal of Hyperthermia*, **6**, 193–202.

TSANDOULAS, G. N., and FITZGERALD, W. D., 1972, Aperture efficiency enhancements in dielectrically loaded horns. *IEEE Transactions on Antennas and Propagation*, **21**, 69–74.

VAN DER ZEE, J., VAN RHOON, G. C., VERLOOP-VAN'T HOF, E. M., VAN DER PLOEG, S. K., RIETVELD, P. J. M., and VAN DEN BERG, A. P., 1992, The importance of adequate heating techniques for therapeutic outcome in *Hyperthermia Oncology, Volume 2*, edited by E. W. Gerner and T. C. Cetas (Arizona: Arizona Board of Regents), 349–352.

VAN DER ZEE, J., and VERNON, C. C., 1996, Thermoradiotherapy for advanced and recurrent breast tumours. *Principles and practice of thermoradiotherapy and thermochemotherapy*, Vol. 2, *Clinical Applications*, edited by M. H. Seegenschmiedt, P. Fessenden and C. C. Vernon (Berlin, Heidelberg, New York: Springer Verlag GmbH), pp. 35–48.

Chapter 5

Effectiveness of the Gaussian beam model in predicting

SAR distributions from the lucite cone applicator

PJM Rietveld, MLD Lumori, JW Hand, MV Prior, J van der Zee and GC van Rhoon

Effectiveness of the Gaussian beam model in predicting SAR distributions from the lucite cone applicator

P. J. M. RIETVELD†*, M. L. D. LUMORI‡, J. W. HAND§,
M. V. PRIOR¶, J. VAN DER ZEE† and G. C. VAN RHOON†

† University Hospital Rotterdam/Daniel den Hoed Cancer Center, Department
of Radiation Oncology, Section Hyperthermia, PO Box 5201,
NL-3008 AE Rotterdam, The Netherlands
‡ Vesalius College and Department of Electrical Engineering,
Vrije Universiteit Brussel, Pleinlaan 2, B-1050 Brussels, Belgium
§ Hammersmith Hospital, Department of Imaging, Radiological Sciences Unit,
Du Cane Road, London W12 OHS, UK
¶ Hammersmith Hospital, MRC Cyclotron Unit, Du Cane Road,
London W12 ONN, UK

The Gaussian beam model (GBM) has been shown to be a successful tool in the development of the current sheet applicator. As a result, the effectiveness of the GBM is investigated in single and dual array applications of the lucite cone applicator (LCA). The LCA is a modified water-filled waveguide applicator with an improved effective field size (EFS > 64 cm^2, aperture 10 cm × 10 cm). The GB-source parameters were calculated from the emanating E-field of a single LCA. The SAR distribution from a single LCA was measured by E-field scanning and thermographic (TG) imaging, and compared with the GB-predicted SAR distribution. Deviations in the principal planes were found to be less than 5%. TG-measured and GB-predicted SAR distributions from three different dual LCA configurations were compared and evaluated. When water was used as intermedium between LCAs and phantom, a maximum SAR difference of 27% was calculated. In the absence of water as intermedium, this difference increased to 44%. These large deviations were only found in areas where the measured SAR distribution was disturbed due to antenna interactions. The average SAR differences with and without water as intermedium were 7% respectively 11%, indicating that the GBM can provide good qualitative information about the SAR distribution of dual LCA-arrays.

Key words: Superficial hyperthermia, microwave antenna, Gaussian beam modelling, SAR distribution.

1. Introduction

In the last decade various theoretical models have been developed (Bach Andersen 1987, Paulsen 1990a, b, 1995) and are being used as an investigating tool for the development of microwave antennae. The models available differ in their degree of complexity, accuracy, computation time and computer requirements. Also the choice of the model to be applied depends on the necessity of modelling full three dimensional objects or whether a simpler approach is possible. In the general clinical application of superficial hyperthermia, most decisions on antenna choice

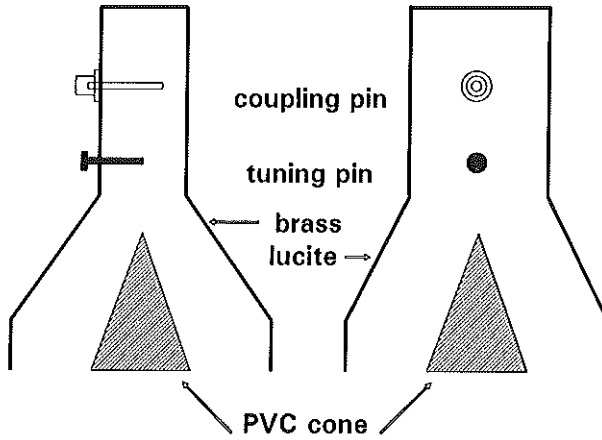* To whom correspondence should be addressed.

Figure 1. Schematic diagram of the lucite cone applicator. The left drawing shows the cross section in the principal E-field plane, the right drawing shows the H-field principal plane cross section. The aperture measures 10 cm × 10 cm.

and its configurations are based on knowledge of the specific absorption rate (SAR) distributions obtained in homogeneous muscle-equivalent phantoms. In such a situation the use of the Gaussian beam (GB) model as developed by Bach Andersen (1987), Lumori (1988) and Lumori *et al.* (1990a) might be a method of obtaining more knowledge of the behaviour of the SAR distribution from various antenna array configurations.

The GBM has been used extensively by other groups (Lumori *et al.* 1990b, Gopal *et al.* 1992, Prior *et al.* 1955) in the development of the current sheet applicator (CSA). They found the GBM to be a reliable tool in studying SAR distributions from CSA-array configurations in a multi-layered phantom. The advantage of the GBM is its simplicity with regard to the required source parameters and its low demand for computer power.

As the lucite cone applicator (LCA, figure 1) is a completely different type of antenna (E-field) compared to the CSA (H-field), it was felt necessary to make a separate verification of the effectiveness of the GBM for the LCA. The results of these investigations are reported here.

It was found that the differences between predicted and measured SAR distributions from LCA arrays are generally increased due to antenna interactions especially when water as intermedium was excluded.

2. Materials and methods

The investigation consisted of two parts. Firstly, the source parameters for the GBM were attained from measurements of amplitude and phase by a geometrical (approximate) method (Lumori 1988) and GB-predicted SAR distributions have been compared to TG-measured SAR distributions from a single antenna. Secondly, these primary tests were followed by dual-antenna set-ups for which, again, predicted and measured SAR distributions in homogeneous muscle-equiva-

lent tissue were compared to allow a more thorough testing of the GBM since the
LCAs are commonly used in array applications. In this study dual antenna set-ups
without and with a water layer/waterbolus as intermedium between antenna and
phantom were included. Measurements without waterbolus can be modelled exactly
while a *finite* water layer (i.e. a waterbolus) cannot be properly modelled in the GBM
and its effect on the predicted SAR distributions was investigated.

2.1. *Lucite cone applicator*

The lucite cone applicator (LCA), depicted in figure 1, is a modified water-filled
horn applicator operating in TE_{10} mode at 433 MHz and has been described earlier
by Van Rhoon *et al.* (1992, 1998). In summary, the LCA is obtained by replacing the
two diverging metal side walls parallel to the E-field of a conventional horn appli-
cator with lucite and adding a PVC cone in the centre of the aperture. By taking
these measures the effective field size (EFS) is increased by a factor of 2–4 (Rietveld
et al. 1990, Rietveld and Van Rhoon 1991, Van Rhoon *et al.* 1998). The radiating
aperture of the LCA is 10 cm × 10 cm (outer dimensions: 10.5 cm × 10.5 cm).

2.2. *Electric field probe*

The E-field distribution along the main axes of the antenna was measured using
two types of unbalanced dipole antennae. The dipole arm lengths were 5 mm and
10 mm (total lengths of the dipole were 10 and 20 mm, respectively). The dipole
antennae were constructed from an open-folded coaxial cable (outer diameters
1.0 mm and 2.0 mm, respectively).

The probes were connected to a HP8751A network analyser to measure the
transmission coefficients from antenna to probe. The positioning of the E-field
probe relative to the antenna was controlled by an xyz-steppermotor device
(Wellhöfer Kernphysik, Schwarzenbruck, Germany), with stepsize 5 mm and
0.5 mm precision. Measurements with the large E-field probe were performed manu-
ally. When using the smaller E-field probe, both the network analyser and the
Wellhöfer steppermotor device were IEEE-interfaced to a PC which coordinated
the position of the probe and measurement of amplitude and phase.

For these measurements a tank containing a liquid muscle-equivalent phantom,
consisting of water, alcohol and salt (Hand *et al.* 1989a) was used. The tank meas-
ured 40 cm × 32 cm × 14 cm (l × w × d) and the antenna was positioned centrally
under the tank, radiating upwards.

In general, E-field scans were done at 10, 20 and 30 cm depths relative to the
radiating aperture with the probe orientation parallel to the main E-field direction
(x) of the LCA. To minimize disturbance of the E-field, the coaxial leads of the
unbalanced E-field dipole antennae were led in the z-direction when E-field profiles
of the LCA were measured in the xy-plane. When measuring in the z-direction the
leads were orientated in the y-direction (perpendicular to the dominant E_x-field
direction).

Measurements were obtained with 5 mm spacing. No waterbolus was used
between antenna and phantom. To correct for the imbalance of the E-field probe,
the average of two oppositely orientated E-field scans was used to obtain the *final* E-
field profile of the antenna.

2.3. *Thermographic SAR measurements*

SAR distributions at 1 cm depth in muscle were obtained using a layered semi-solid muscle-equivalent phantom (48 cm × 48 cm × 10 cm) made of Super Stuff (Guy 1971). A thermographic camera (AGA Thermovision System 680/102B, Lidingö, Sweden) interfaced to a PC was used to measure the temperature distribution at the exposed surface.

In order to measure a proper SAR distribution in a dual-antenna set-up with the thermographic (TG) technique, the duration of the power pulse was set to 1.5 min. Although the ESHO Quality Assurance (QA) guidelines (Hand *et al.* 1989a) were violated with respect to the power pulse duration, heat conduction in the phantom was still in the order of millimetres (<5 mm) which was within the spatial resolution of the TG-camera. In other aspects the ESHO QA guidelines were followed.

After correction for background radiation and non-linearity of the camera, a relative SAR distribution was calculated. Net power input per antenna during the experiments was about 130 W. In the case of a dual-antenna set-up, the antenna were driven incoherently with equally set input power.

The E-field orientations for the dual array configurations were: both E-fields horizontally orientated (HH); both E-field orientations vertically orientated (VV); the left E-field horizontally and right E-field vertically orientated (HV).

When a waterbolus was used in a single LCA TG-measurement, the dimensions were 18 cm × 18 cm × 1 cm. In all dual-antenna TG-measurements, the waterbolus measured 28 cm × 20 cm × 1 cm. The waterbolus dimensions are chosen according to the clinical set-up of LCAs.

2.4. *Gaussian beam model*

The Gaussian beam (GB) model has been described extensively elsewhere (Bach Andersen 1987, Lumori 1988, Lumori *et al.* 1990a, b). The model describes the E-field distribution in lossy media by local Gaussian curves outside the near field region of the aperture. The source parameters for the model are the half-width (S) and the phase curvature of the wave front (R) both in the E- and H-principal planes. The source parameters for the GBM were calculated from the E-field measurements along the main axes of the antenna according to an algorithm described by Lumori (1988).

A dual-layered flat phantom configuration was used in the GB-predictions for incoherently driven LCA-configurations. The top layer represented water ($\varepsilon_r = 76$, $\sigma = 0.001$ S/m) and the second layer represented muscle-equivalent tissue. The properties of muscle tissue were set to $\varepsilon_r = 57$ and $\sigma = 1.2$ S/m.

In order to allow for a comparison between TG-measured and GB-predicted SAR distributions, it was necessary that the relative net-power outputs of the two antennae were comparable for both the measured and predicted SAR distributions. Therefore, the ratio of the net-power output of the two antennae, as estimated from the local maxima in the measured SAR distributions, were used as power parameters for the GB-modelling to predict the respective SAR distributions. By optimizing these power settings in order to decrease the difference between TG- and GB-SAR distributions, a compensation can be made (partially) for the interactions between two antennae in the GB predictions.

ESHO QA guidelines demand the use of a waterbolus (Hand *et al.* 1989a paragraph 6.2) if appropriate in a clinical set-up. For that reason, first antenna set-ups without water as an intermedium have been performed to check the reliability of the

GBM in (dual) array applications of the LCA, and secondly, the ESHO appropriate 'clinical' relevant set-up has been used to evaluate the technical usefulness of the GBM in array applications of the LCA.

Overall SAR distributions from array applications where mixed E-field orientations were used (i.e. the HV-configuration) could be predicted only by calculating separately the SAR distribution of the horizontal (H) and the vertical (V) E-field alignment. Locally-written software was used to combine these H and V antenna SAR distributions into the required array-application.

2.5. *SAR-range related differences*

In order to make a quantitative evaluation of the effectiveness of the GB-predicted SAR distributions in comparison to TG-measured SAR distributions, the area of the array aperture plus 5 cm around the dual-antenna set-up was evaluated on SAR differences (20 cm × 30 cm). The TG-measured SAR distribution was aligned with the GB-predicted SAR distribution and a regular grid (21 × 31 nodes) was created for both SAR distributions. The absolute SAR differences between both distributions $|SAR_{TG}-SAR_{GB}|$ were calculated for all grid nodes resulting in SAR-range related differences (SRDs). These SAR differences were sorted per range of 10%-SAR_{GB} level intervals (10, 20, ..., 100) and the average SAR difference per 10%-SAR_{GB} range was calculated as well as the standard error of the mean. Also the maximum difference per SAR-range was obtained.

3. Results

3.1. *Single LCA set-up*

3.1.1. *Electric field measurements and Gaussian beam source parameter selection.* In the single scan of E-field profiles, the location of the maximum power level was measured up to 20 mm off-centre. Averaging two oppositely orientated E-field scans corrected this imbalance and created symmetrical profiles which were suitable for calculating GB-source parameters. Table 1 gives a summary of the half-width (S) of the power-profiles and radii (R) of the phase profiles as a function of depth obtained with both the small and large E-field probe. The averaged parameters measured at 10 mm depth, $S_E = 3.9$ cm, $R_E = \infty$, $S_H = 5.0$ cm and $R_H = 35$ cm, were selected for further GB-calculations.

For additional E-field scans performed along the main axes, it was found that the contributions of $|E_y|^2$ and $|E_z|^2$ to the overall SAR distribution at 10 mm depth in muscle-equivalent tissue were less than 0.5% and 2% respectively. The maximum $|E_z|^2$ values were found under the brass rim of the aperture. The PVC cone did not increase the local near-field levels at 10 mm depth.

Table 1. Half-power half-width (S) and phase radius (R) of the LCA as function of depth.

Dipole	Depth (mm)	S_E (cm)	R_E (cm)	S_H (cm)	R_H (cm)
1	10	3.6/3.9	∞/∞	4.9/5.0	35/35
1	20	3.4/3.7	∞/∞	4.7/5.1	35/67
1	30	3.5	∞	4.6	35
2	10	4.2	∞	5.0	22
Average	10	3.9*	∞*	5.0*	31*

*Average value, calculated from all measurements at 10 mm depth.
Dipole 1: unbalanced, length 10 mm; dipole 2: unbalanced, length 20 mm.
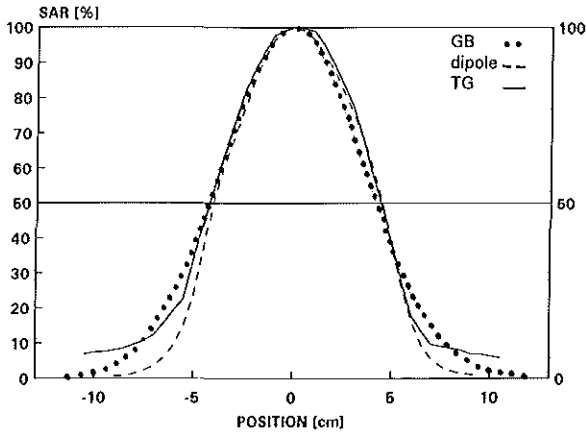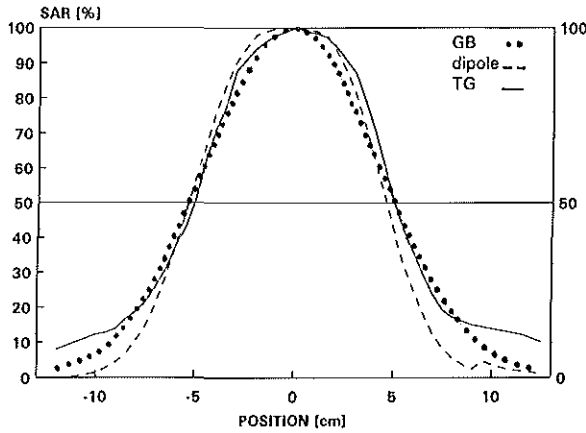
Figure 2.   Relative SAR distribution at 10 mm depth in muscle in the principal (a) E-field plane and (b) H-field plane of the LCA as measured with the thermographic- and the E-field scanning technique (20 mm wide unbalanced dipole antenna) or as predicted by the Gaussian beam model. The E-field amplitudes as measured with the dipole are converted to a parameter proportional to SAR (E × E). Half-power half-widths (a) TG: 4.3 cm; dipole: 4.2 cm; GB: 4.2 cm; (b) TG: 5.1 cm; dipole: 5.0 cm; GB: 5.2 cm.

3.1.2. *Comparison of GB-predicted and TG-measured SAR distributions.* The power-profiles in the principal planes were derived for a single LCA from a TG-measured SAR distribution. Use of a waterbolus was excluded to enable a direct comparison with the E-field measurements and the GB-predicted SAR distributions. Figure 2 shows the power-profiles in the principal planes derived from the

(a)

(b)

(c)
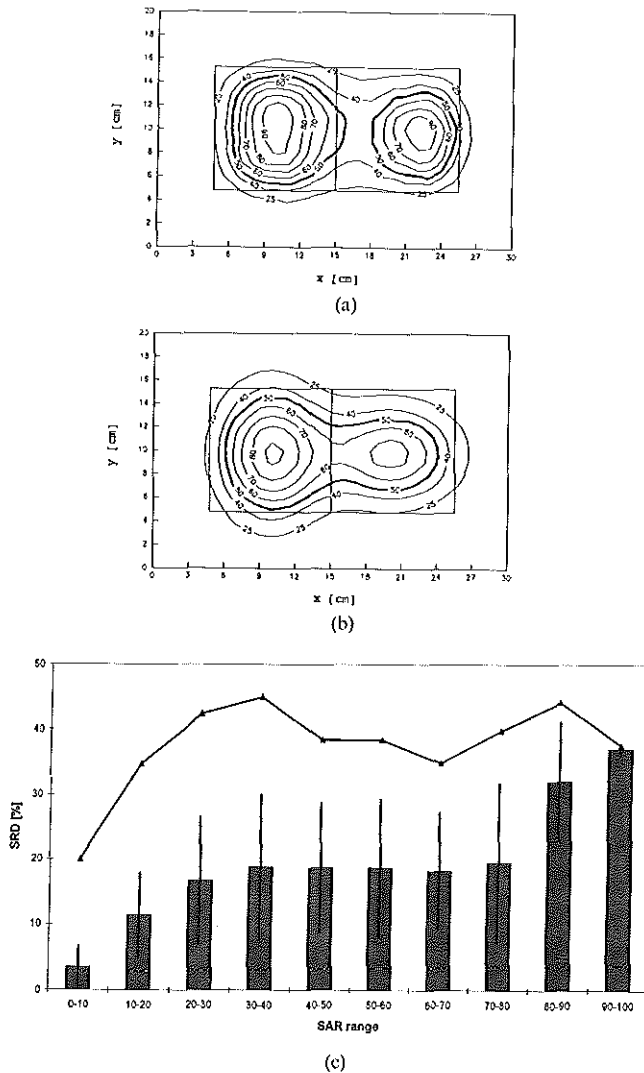
Figure 3. SAR at 10 mm depth in muscle-equivalent phantom from the HV-configuration. No water-bolus/layer was used as intermedium. The antennae are indicated by the squares. SAR range: 0–100. (a) thermographic-measured SAR distribution; (b) Gaussian beam-predicted SAR distribution; and (c) absolute SAR-differences (SRDs) between the GB-predicted and TG-measured SAR distributions. The SAR-differences were calculated per GB-related 10% SAR-intervals. The bars represent the mean value per interval, the error bars represent the corresponding standard error of the mean. The line indicates the maximum difference per GB-interval.

Table 2. Estimated power settings derived from TG-measured SAR distributions and corresponding optimized GB-power settings. The power settings are normalized to 1. Also TG-measured and GB-predicted effective field sizes (EFS) obtained at 1 cm depth in muscle-equivalent phantom from three different E-field orientated dual array applications of the LCA are presented for antenna set-ups without and with a water layer/bolus.

Antenna configuration	HH		VV		HV	
	TG	GB	TG	GB	TG	GB
no waterbolus/water layer as intermedium						
P_1, P_2	1, 0.9	0.9, 0.83	1, 0.9	0.9, 0.77	1, 0.9	0.9, 0.74
EFS [cm^2]	134	129	98	119	115	123
1 cm thick waterbolus/water layer as intermedium						
P_1, P_2	1, 0.93	0.93, 0.84	1, 1	0.84, 0.84	0.9, 0.95	0.89, 0.95
EFS [cm^2]	136	131	123	110	139	144

SAR measurement, the E-field scan with the large dipole E-field probe and the SAR distribution as predicted by the GBM. The full widths at half power as calculated from all three techniques are given in the legend of figure 2.

3.2. *Dual LCA set-up*

3.2.1. *Comparison of GB-predicted and TG-measured SAR distributions without water as intermedium.* Figure 3a shows the TG-measured SAR distributions from HV orientated LCA array and figure 3b shows its corresponding GB-predicted SAR distribution. (In all figures containing relative SAR distributions, the 50% SAR contour has an increased line thickness.)

Table 2 gives a summary of the measured (TG) and set (GB) power levels together with calculated and predicted EFSs of the HH, VV and HV E-field orientated dual-LCA configurations.

Figure 3c shows the calculated SRDs for the HV configuration. The average SRD as well as its standard deviation and the maximum of SRD per 10% SAR interval are indicated. The average SRD within the predicted EFS area, (SRD$_{EFS}$), equals 25%. The results from the HH and VV configuration showed less pronounced differences between TG-measured and GB-predicted SAR distributions, the SRD$_{EFS}$ equalled 8% (HH) and 11% (VV).

In order to understand the enhanced SAR differences in the HV set-up between TG- and GB-SAR distribution, an additional experiment was performed to quantify the antenna interaction. In this set-up only the 'V' antenna was powered and the 'H' antenna was connected to a 50 ohms dummy load. Figure 4a shows the TG-SAR distribution. A shift of the maximum SAR level of 3 cm in the outward direction of the array was measured.

3.2.2. *Comparison of GB-predicted and TG-measured SAR distributions with water as intermedium.* The antenna interaction in the HV-set-up was measured firstly, with the powered 'V' antenna and 'H' antenna connected to the dummy load. Figure 4b shows the TG-SAR distribution with water as intermedium. The antenna interaction showed up less prominently. The shift of the maximum levels
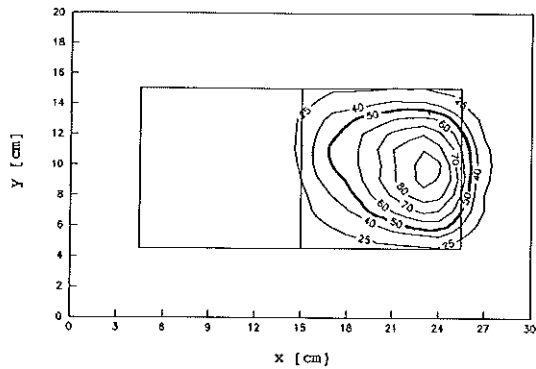
(a)
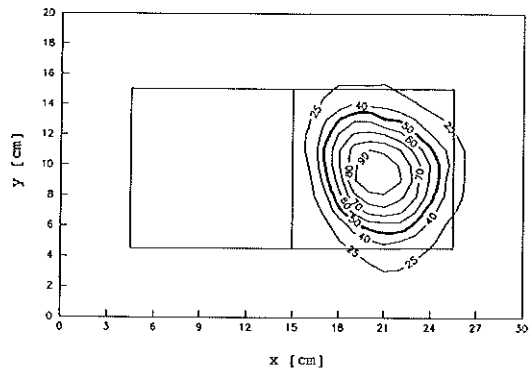
(b)

Figure 4. Thermographic-measured SAR distributions (range: 0–100) of the HV-orientated dual LCA-array configuration at 10 mm depth in muscle-equivalent phantom. The 'V' antenna was powered in order to show the effect of antenna interaction on the SAR distribution and the 'H' antenna was connected to a 50 ohm load. The antennae are indicated by the squares. (a) no water used as intermedium; and (b) waterbolus of 1 cm thick used as intermedium.

almost disappeared (<1 cm) but still a distortion of the symmetry in the TG-measured SAR distribution is shown.

Figures 5a and 6a show the TG-measured SAR distributions from two parallel orientated LCA arrays HH and VV respectively, whereas figure 7a shows the TG-measured SAR distribution of two LCAs with perpendicular orientated E-fields (HV). The corresponding GB-predicted SAR distributions are shown in figures 5b to 7b: HH, VV and HV. Table 2 gives a summary of the power ratios together with measured and predicted EFSs of the various dual antenna configurations.
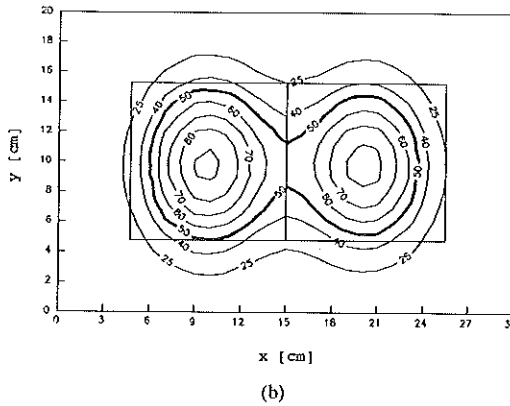
(a)

(b)

Figure 5. TG-measured (a) and GB-predicted (b) SAR distribution (range: 0–100) of the HH-orientated dual LCA-array configuration at 10 mm depth in muscle-equivalent phantom. Water-bolus/layer 1 cm thick. The antennae are indicated by the squares.

Figure 8 shows the calculated SRDs for the dual array applications of the LCA with water as intermedium. The SRD_{EFS} per E-field configuration equal 6% (HH), 8% (VV), and 12% (HV).

4. Discussion

Experimental assessment of the behaviour of the SAR distribution of an array of antennae can be regarded as a cumbersome procedure as it is difficult or impossible to distinguish between the effect of each relevant parameter on the resulting SAR distribution. In such cases, the aid of proper theoretical models can be of great value in dramatically reducing the period of time needed to develop a clinical applicator.

The reliability of a mathematical model is limited by the quality of the required source parameters. Measurement of the source parameters for the GBM is done by
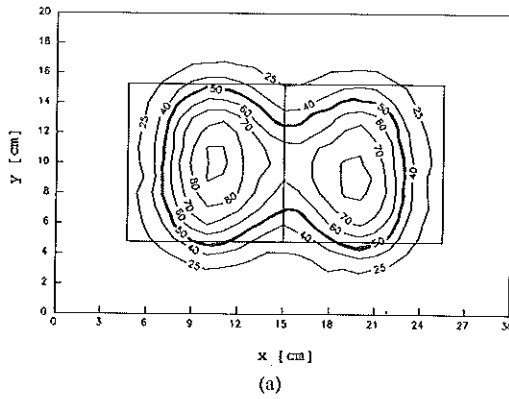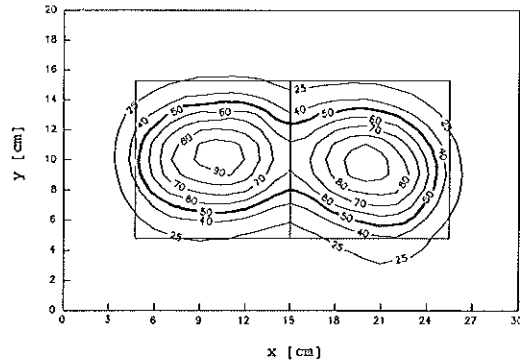
(a)
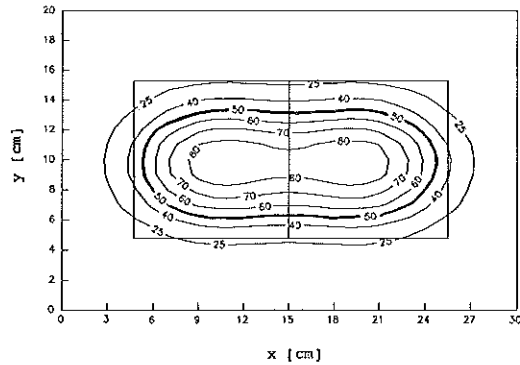
(b)

Figure 6. TG-measured (a) and GB-predicted (b) SAR distribution (range: 0–100) of the VV-orientated dual LCA-array configuration at 10 mm depth in muscle-equivalent phantom. Water-bolus/layer 1 cm thick. The antennae are indicated by the squares.

means of a miniature dipole antenna. Some research groups have developed miniature probes to measure the E-field amplitude and phase emanating from an antenna (Schneider *et al.* 1991, Meier *et al.* 1992, Gopal *et al.* 1995, Wust *et al.* 1995). These have dedicated designs which compensate for imbalance. Alternatively, as was demonstrated by Lumori *et al.* (1990a), it was possible to use unbalanced open-folded coaxial cable as dipole antennae in order to probe the E-field of the LCA. The imbalance of the E-field probes can be corrected by averaging two opposing E-field scans. Using this technique we found, in the case of the LCA, that the contribution to the SAR distribution of the near-field components, E_y and E_z, at 10 mm depth, was negligible (less than 2%) and that the E_x-field measurements at 10 mm depth formed a good representation of the E-field profiles.
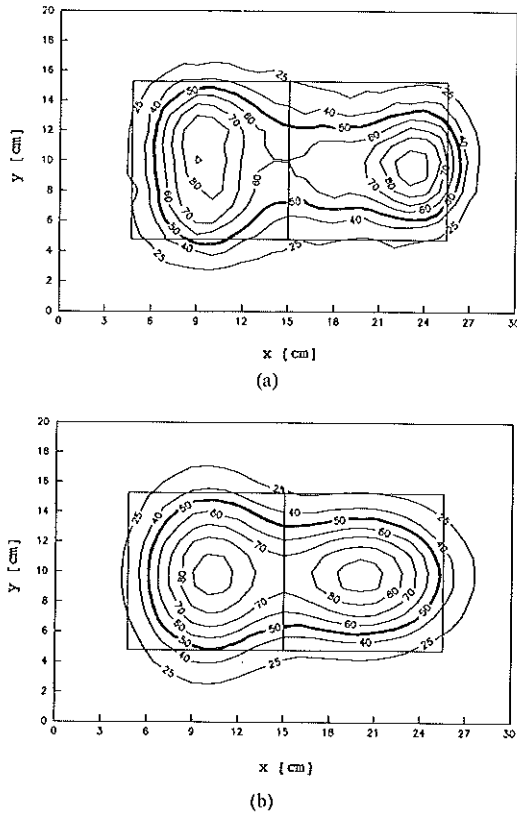
Figure 7. TG-measured (a) and GB-predicted (b) SAR distribution (range: 0–100) of the HV-orientated dual LCA-array configuration at 10 mm depth in muscle-equivalent phantom. Water-bolus/layer 1 cm thick. The antennae are indicated by the squares.

From the comparison of the SAR profiles in the principal planes at 10 mm depth in muscle for the three different techniques (E-field measurement, TG-measurement and GB-prediction, figure 2) it was concluded that the GBM can be used to predict SAR distribution from a single LCA. This was without the use of water as inter-medium and the error was less than 5%.

Other groups have already shown that the GBM can predict SAR distributions from array applications with good accuracy when antennae are placed directly on a muscle-equivalent phantom (Lumori *et al.* 1990b, Gopal *et al.* 1992). However, in LCA clinically relevant configurations a waterbolus is used as intermedium. In this case the finite dimensions of the 18 cm × 18 cm waterbolus influence the EFS of a single LCA by 30% (Van Rhoon *et al.* 1998). It is possible to adjust the GBM for these finite waterbolus effects on a single antenna by using the waterbolus when

(a)

(b)

(c)
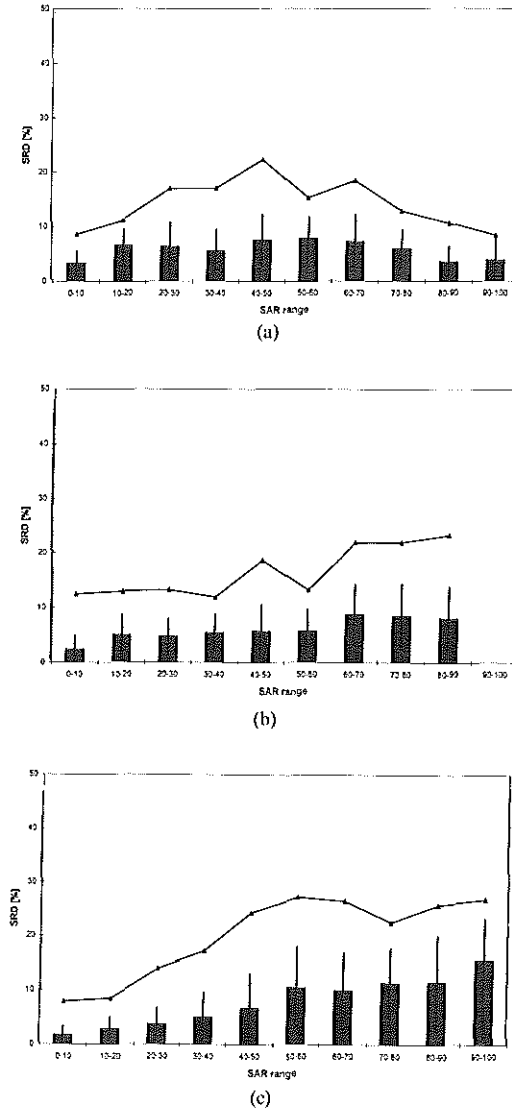
Figure 8.   Absolute SAR-differences (range: 0–100) between the GB-predicted and TG-meas-
ured SAR distributions from dual LCA arrays. 1 cm thick water layer/bolus used as
intermedium. The SAR-differences were averaged per GB-related 10% SAR-intervals.
Errorbars indicate the standard error of the mean and the line represents the maximum
SAR-difference per GB-interval. (a) HH-dual array configuration of LCAs; (b) VV-dual
array configuration of LCAs; and (c) HV-dual array configuration of LCAs.

measuring the E-field profiles. However, in predicting SAR distributions from array configurations the latter would require E-field measurements for each relevant antenna orientation in the array configuration as the total waterbolus is a variable and asymmetric load to each antenna. This is considered to be too time-consuming and contra-indicative for the usability of the GBM. On the other hand, if a relatively large waterbolus is used (25 cm × 30 cm × 1 cm) for single LCA experiments, TG-measured and GB-predicted SAR distributions correlate well (64 and 68 cm^2 respectively, Van Rhoon *et al.* 1998). For these reasons we used the GB-source parameters derived from a single LCA, measured without the use of a waterbolus, for GB-based predictions of SAR distributions from LCA arrays.

Dual array configurations *without* water as intermedium can be described exactly with the GBM. Although the GB-power settings were optimized to minimize SAR-distribution differences (table 2), large quantitative differences were found: a SRD maximum of 44% in the HV-configuration; maximum average over all 10% SAR ranges per dual array configuration: 19% (HV) and global average 12%, averaged over all three E-field configurations and all SAR ranges were calculated. Especially in the HV-configuration (figure 3), the 3 cm shift of the local 'V'-SAR maximum caused high values of the SRD. Additionally, in this set-up there was also a poor qualitative similarity (i.e. general shape of the SAR-contours) between TG- and GB-obtained SAR distribution. These deviations are considered unacceptable for model predictions. The large deviations were caused by antenna interactions which cannot be incorporated in the GBM. This effect was demonstrated clearly in the experiment of a single powered 'V' antenna in the HV-configuration, for which high SRDs were calculated in the plus 50% SAR range. The SAR distribution from the 'V' antenna is pushed aside by the adjacent 'H' antenna (figure 4a).

The quantitative SAR differences were generally smaller (figure 8) for the water layer/waterbolus set-up (SRD maximum: 27% (HV); maximum average over all 10% SAR ranges: 8% and global average 7%, averaged over all three E-field configurations and all SAR ranges). Again deviations between measured and predicted SAR distributions are caused by unmodelled antenna interactions (figures 5, 6 and 7). It is as yet unclear how the antenna interactions behave exactly and further investigation is necessary. However, the TG-measured SAR distribution from the single powered 'V' LCA in the HV-configuration (figure 4b) showed that these antenna interactions are less prominent when a waterbolus is used. The effect of a finite waterbolus on the SAR distribution is of less magnitude than the antenna interactions (and might even compensate partly for these interactions). The qualitative comparison between the GB-predicted and TG-measured SAR distributions, with respect to the general shape of the SAR-contours and to the 50% SAR-contour (=EFS) in particular, is of a greater resemblance which is reflected in a lower average SRD$_{EFS}$: 14.5% (no water) versus 8.4% (including a water layer/waterbolus).

In conclusion, for a single LCA, the GBM predicts the SAR distribution correctly if the source parameters for the GBM are obtained according to the experimental set-up. If single LCA source parameters are used to predict SAR distributions from dual arrays of LCAs with a waterbolus, the GBM is accurate enough for qualitative predictions. This is not the case without a waterbolus as intermedium.

As the configuration parameters (e.g. power input antenna or alignment) are better controlled in the GBM than in experimental set-ups and because only a single antenna is necessary to obtain source parameters for the clinically more interesting

array configurations, the GBM is found to be a useful tool for (a) guiding experimental verifications of LCA configurations and (b) performing qualitative studies of SAR distribution from clinically relevant LCA array configurations.

Acknowledgements

References

BACH ANDERSEN, J., 1987, Electromagnetic power deposition: inhomogeneous media, applicators and phased arrays. *Physics and Technology of Hyperthermia*, edited by S. B. Field and C. Franconi (Dordrecht: Martinus Nijhoff Publishers), 159–188.

GOPAL, M, K., CETAS, T. C., and ROSMAN, D., 1995, Miniature dipole E-field probes for characterizing both phase and amplitude of microwave radiators for hyperthermia. *International Journal of Hyperthermia*, **11**, 769–784.

GOPAL, M. K., HAND, J. W., LUMORI, M. L. D., ALKHAIRI, S., PAULSEN, K. D., and CETAS, C. T., 1992, Current sheet applicator arrays for superficial hyperthermia of chestwall lesions. *International Journal of Hyperthermia*, **8**, 227–240.

GUY, A. W., 1971, Analysis of electromagnetic fields induced in biological tissues by thermographic studies on equivalent phantom models. *IEEE Transactions of Microwave Theory and Techniques*, **19**, 205–214.

HAND, J. W., 1990, Biophysics and technology of electromagnetic hyperthermia. *Methods of external hyperthermic heating (Clinical thermology. Subseries thermography)*, edited by M. Gauthier (Berlin, Heidelberg: Springer-Verlag).

HAND, J. W., LAGENDIJK, J. J. W., BACH ANDERSEN, J., and BOLOMEY, J. C., 1989a, Quality assurance guidelines for ESHO protocols. *International Journal of Hyperthermia*, **5**, 421–428.

HAND, J. W., PAULSEN, K. D., LUMORI, M. L. D., GOPAL, M. K., CETAS, T. C., and ALKHAIRI, S., 1989b, Microwave array applicators for superficial hyperthermia. *Hyperthermic oncology 1988*, vol. 1, edited by T. Sugahara and M. Saito (London: Taylor and Francis), pp. 827–828.

LUMORI, M. L. D., 1988, Microwave power deposition in bounded and inhomogeneous lossy media, PhD dissertation, Department of Electrical and Computer Engineering, The University of Arizona.

LUMORI, M. L. D., BACH ANDERSEN, J., GOPAL, M. K., and CETAS, T. C., 1990a, Gaussian beam representation of aperture fields in layered, lossy media: simulation and experiment. *IEEE Transactions on microwave theory and techniques*, **38**, 1623–1630.

LUMORI, M. L. D., HAND, J. W., GOPAL, M. K., and CETAS, T. C., 1990b, Use of Gaussian beam model in predicting SAR distribution from current sheet applicators. *Physics in Medicine and Biology*, **35**, 387–397.

MEIER, TH., KOSTRZCEWA, K., SCHÜPPERT. B, and PETERMANN, K., 1992, Electro-optical E-field sensor with optimised electrode structure. *Electronics Letters*, **28**, 1327–1329.

PAULSEN, K. D., 1990a, Calculation of power deposition patterns in hyperthermia. *Thermal Dosimetry and treatment planning (Clinical thermology. Subseries thermotherapy)*, edited by M. Gautherie (Berlin, Heidelberg: Springer-Verlag).

PAULSEN, K. D., 1990b, Power deposition models for hyperthermia applicators. *An introduction to the practical aspects of clinical hyperthermia*, edited by S. B. Field and J. W. Hand (London: Taylor and Francis).

PAULSEN, K. D., 1995, Principles of power deposition models. *Thermoradiotherapy and Thermochemotherapy, Volume 1: Biology, Physiology, Physics*, edited by M. H. Seegenschmiedt, P. Fessenden and C. C. Vernon (Berlin, Heidelberg, New York: Springer-Verlag).

PRIOR, M. V., LUMORI, M. L. D., HAND, J. W., LAMAITRE, G., SCHNEIDER, CHR. J., and VAN DIJK, J. D. P., 1995, The use of a current sheet applicator array for superficial hyperthermia: incoherent versus coherent operation. *IEEE Transactions on biomedical engineering*, **42**, 694–698.

RIETVELD, P. J. M., and VAN RHOON, G. C., 1991, Preliminary results of the improved water filled waveguide applicator in an array application. *Strahlentherapie und Onkologie*, **167**, 335–336.

RIETVELD, P. J. M., VAN RHOON, G. C., and BROEKMEYER-REURINK, P. M., 1990, Improvement of SAR distribution of a 433 MHz water filled waveguide applicator. *Strahlentherapie und Onkologie*, **166**, 528–529.

SCHNEIDER, C. J., ENGELBERTS, N., and VAN DIJK, J. D. P., 1991, Characteristics of a passive RF field probe with fibre-optic link for measurements in liquid hyperthermia phantoms. *Physics, Medicine and Biology*, **36**, 461–474.

VAN RHOON, G. C., RIETVELD, P. J. M., BROEKMEYER-REURINK, M. P., and VAN DER ZEE, J., 1992, A 433 MHz Waveguide applicator system with an improved effective field size for hyperthermia treatment of superficial tumors at the chest wall. *Hyperthermic Oncology 1992 Volume 1, Proceedings of the 6th International Congress on Hyperthermic Oncology*, edited by E. W. Gerner, Tucson, Arizona.

VAN RHOON, G. C., RIETVELD, P. J. M., and VAN DER ZEE, J., 1997, A 433 MHz lucite cone waveguide applicator for superficial hyperthermia. *International Journal of Hyperthermia*, **14**, 13–27.

WUST, P., MEIER, T., SEEBASS, M., FÄHLING, H., PETERMANN, K., and FELIX, R., 1995, Noninvasive prediction of SAR distributions with an electro-optical E field sensor. *International Journal of Hyperthermia*, **11**, 295–310.

Quantitative evaluation of 2 × 2 arrays of Lucite cone applicators in flat layered phantoms using Gaussian-beam-predicted and thermographically measured SAR distributions

PJM Rietveld, MLD Lumori, J van der Zee and GC van Rhoon

Quantitative evaluation of 2 × 2 arrays of Lucite cone applicators in flat layered phantoms using Gaussian-beam-predicted and thermographically measured SAR distributions

P J M Rietveld†§, M L D Lumori‡, J van der Zee† and G C van Rhoon†

† University Hospital Rotterdam—Daniel den Hoed Cancer Center, Department of Radiation Oncology, Subdivision of Hyperthermia, Rotterdam, The Netherlands
‡ Vesalius College and Department of Electrical Engineering, Vrije Universiteit Brussel, Pleinlaan 2, B-1050 Brussels, Belgium

Abstract. SAR distributions from four different E-field-orientated 2 × 2 arrays of incoherently driven Lucite cone applicators (LCAs) were investigated. The LCAs operated at 433 MHz with an aperture of 10.5 cm × 10.5 cm each. Two techniques were used to obtain SAR distributions in flat layered phantoms: Gaussian beam (GB) predictions and thermographical (TG) imaging. The GB predictions showed that the effective field size of the different array configurations varied by up to 3%.

The TG-measured SAR distribution showed significant deviations from the GB-predicted SAR distributions (maximum 34.6%). The difference between GB-predicted and TG-measured SAR levels (averaged per 10% GB-predicted SAR intervals) equalled less than 11.3% for the parallel E-field orientated array and respectively 15.1% for the clockwise-orientated array. When antennae in the clockwise-orientated array were more widely spread (array aperture 23 cm × 23 cm) in order to diminish their mutual interactions, these differences decreased to 12.4%. However, the overall difference within the 50% SAR or higher range decreased from 14% to 9%. The results lead us to conclude that LCAs can be used clinically and their antenna interactions are not considered to be a problem under clinical conditions.

1. Introduction

In earlier publications (Rietveld *et al* 1990, 1991, 1998, Van Rhoon *et al* 1992, 1998) we have reported on the progress of the development of the Lucite cone applicator (LCA). In the same publications we have demonstrated the value of the Gaussian beam model (GBM) (Lumori *et al* 1990a) as an efficient and practical tool for investigating the specific absorption rate (SAR) distributions from single- and dual-element array configurations of the LCA. Although a disadvantage of the currently available GBM is that antenna interactions and other practical side effects can only partly be integrated by means of optimizing GB input parameters (Lumori *et al* 1990b), current available 3D models capable of dealing with tissue structures and antenna interactions are yet not feasible for applications presented here.

§ Reprint requests to: P J M Rietveld, Daniel den Hoed Cancer Center, Department of Radiation Oncology, Subdivision of Hyperthermia, PO Box 5201, NL-3008 AE Rotterdam, The Netherlands. E-mail address: rietveld@hyph.azr.nl

However, time-consuming thermographic (TG) measurements of SAR distributions in flat layered muscle equivalent phantoms demonstrate such interaction effects clearly.

In this paper we report on the *technical* performance of the four possible E-field-orientated 2 × 2 LCA array configurations and a comparison is made between the GB-predicted and TG-measured SAR distributions in a flat layered muscle equivalent phantom. The quality of the arrays will be evaluated based on the ESHO quality assurance guidelines for superficially used single antennae (Hand *et al* 1989).

Differences between GB-predicted and TG-measured SAR distributions of the four 2×2 LCA-array configurations will be discussed. These differences cannot be expressed only by the effective field size (EFS: area enclosed by 50% SAR contour at 1 cm depth in muscle tissue, Hand *et al* 1989) since location or shape of the effective field relative to the aperture is not incorporated in this parameter. Therefore, an additional SAR-derived variable, the SAR-related difference parameter (SRD), will be defined to quantify the TG-measured SAR deviations from the GB-predicted SAR distributions. It will be found that the relative E-field orientations in the 2 × 2 LCA array do not contribute to a significant difference in EFS and that the mean difference between GB-predicted SAR distributions and TG-measured SAR distributions is caused by antenna interactions and finite water bolus effects.

2. Materials and methods

In order to evaluate the technical performance of array applications of the LCA, firstly the SAR distributions at 1 cm depth in a homogeneous muscle-equivalent phantom from all four possible E-field configurations in a 2 × 2 array set-up are predicted with the GBM. Secondly, the SAR distributions from the parallel and clockwise orientated array set-ups of the 2 × 2 array are measured and compared to their corresponding GB-predicted SAR distributions.

2.1. Lucite cone applicator

The Lucite cone applicator (LCA) is a modified water-filled horn antenna operating in TE_{10} mode at 433 MHz and has been described in detail by Van Rhoon *et al* (1992, 1998). The outer dimensions measure 10.5 cm × 10.5 cm and thus a 2 × 2 LCA array creates a total aperture of 21 cm × 21 cm.

2.2. Antenna array configurations

Figure 1 shows the four relative E-field configurations in a 2 × 2 array of LCAs which were tested. In all experiments a non-perfused water bolus at room temperature was used which measured 28 cm × 25 cm × 1 cm.

Two series of experiments were performed. In the first series, the antennae were positioned adjacent to each other (compact array). The total aperture of the compact 2 × 2 array was 21 cm × 21 cm.

In the second series the antennae were separated from each other by creating a virtual antenna aperture of 11 cm × 12 cm (11 cm in the E-field direction and 12 cm in the H-field direction). In this series only the clockwise orientation was evaluated concerning properties of the SAR distribution. The total aperture of this inter-antenna-spaced 2 × 2 array was 23 cm × 23 cm.

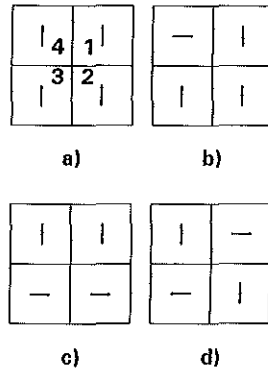**Figure 1.** Relative *E*-field orientations in a 2 × 2 array of LCAs. The *E*-field directions are indicated by arrows, the antennae by squares. (*a*) Parallel orientated, (*b*) Q-orientated, (*c*) U-orientated and (*d*) clockwise orientated.

2.3. Thermographic SAR measurements

SAR distributions at 1 cm depth in muscle were obtained using a layered semi-solid muscle-equivalent phantom (48 cm × 48 cm × 10 cm) made of Super Stuff (Guy 1971). A thermographic camera (AGA Thermovision System 680/102B) interfaced to a PC was used to measure the temperature distribution of the exposed surface.

Net power input per antenna during the experiments was about 130 W; the heating time was set to 1.5 minutes in order to obtain a significant temperature rise. The antennae were driven incoherently and powers were adjusted in order to obtain an equal net power output at the aperture of each antenna. If within the aperture of each antenna a local SAR maximum of 70% (relative to the absolute SAR maximum under the antenna array) was measured then this measurement was considered acceptable.

2.4. Gaussian beam model

The Gaussian beam (GB) model has been described extensively elsewhere (Bach Andersen 1987, Lumori 1988, Lumori *et al* 1990a,b). The LCA source parameters for the model, the half-power half-width (*S*) and the phase curvature of the wave front (*R*), in both the *E*- and *H*-principal planes were derived from *E*-field measurements: $S_E = 3.9$ cm, $R_E = \infty$, $S_H = 5.0$ cm and $R_H = 35$ cm (Rietveld *et al* 1998) and are based on single antenna measurements without use of water as an intermedium. The *E*-field measurements were derived from the dominant *E*-field component (E_x). E_y and E_z contributed less than 2% to the entire *E*-field distribution (Rietveld *et al* 1998).

A triple-layered flat phantom configuration was used in the GB predictions for incoherently driven LCA configurations. The top layer represented water ($\varepsilon_r = 76$, $\sigma = 0.001$ S m^{-1}), the second layer represented fat ($\varepsilon_r = 5.6$, $\sigma = 0.05$ S m^{-1}) and the third layer represented muscle-equivalent tissue ($\varepsilon_r = 57$ and $\sigma = 1.2$ S m^{-1}). Locally written software was used to calculate SAR distributions from the mixed *E*-field configurations and to calculate EFSs.

The antenna power settings in the GBM were set equally when investigating the effect on the EFS of the four possible E-field configurations. For comparison of TG-measured with the GB-predicted SAR distributions, the GB-set power level of each antenna was estimated from the TG-measured local maximum under the antenna. By trial and error these power settings were adjusted in order to minimize the difference between the TG-measured and its corresponding GB-predicted SAR distribution.

2.5. *Quantification of differences between TG-measured and GB-predicted SAR distributions from array applications of LCAs*

In order to compare SAR distributions from the GBM and TG measurements, the ESHO quality assurance (QA) guidelines provide the EFS, the surface enclosed by the 50% SAR contour(s). However, the EFS does not contain information about the location of the 50% SAR contour(s) related to the antenna apertures in the array. The SAR-related difference (SRD) represents an average SAR difference between GB-predicted and TG-measured SAR distributions based on ranges of 10% SAR values as predicted by the GB model. Since the GBM predicts Gaussian beams with its centre located in the middle of the aperture, the SRD also incorporates a location sensitivity. The SRD_i is defined by:

$$|SAR_{TG} - SAR_{GB}(i)|/n_i$$

n_i = number of data in GB-predicted SAR range i; $i = 1$: [0, 10), 2: [10, 20), ..., 10: [90, 100]% iso-SAR.

By averaging the SRD_is in the 50–100% SAR range, an EFS-derived parameter is defined, the SRD_{EFS}, which contains both information on position misfits and SAR differences for the enclosed GB-predicted 50% SAR contour(s). The SAR distributions were superposed on a 55 × 55 grid, resulting in a 0.5 cm × 0.5 cm resolution.

2.6. *Measurement of cross-coupling in 2 × 2 arrays*

Cross-coupling in the 2 × 2 arrays was measured on a muscle-equivalent phantom using the HP network analyser 8751A. Firstly, the reflection coefficient was minimized for all antennae, secondly the transmission between two antennae was measured both with and without the use of a water bolus. The other two antennae were terminated with 50 ohm loads. The accuracy of the measurements was ±3 dB.

3. Results

3.1. *First series: compact 2 × 2 LCA arrays*

Figures 2(*a*) to 2(*d*) show the GB-predicted SAR distributions at 1 cm depth in muscle of the four different E-field configurations of the compact 2 × 2 LCA array with equally set power levels. Figures 2(*e*) to 2(*h*) show the SAR distributions for the same configurations but now with an additional 1 cm thick fat layer. Table 1 gives a summary of the GB-predicted EFSs of all E-field configurations of a 2 × 2 LCA array both without and with the use of a 1 cm thick layer of fat on top of muscle tissue. The minimum SAR in the centre of the 2 × 2 array equalled 55% without and 65% with a 1 cm thick fat layer.

Figures 3(*a*) and 3(*b*) show the TG-measured and the corresponding GB-predicted SAR distribution of the *parallel* orientated 2 × 2 LCA array. The EFSs equalled 331 cm^2 and 261 cm^2 respectively. During the experiment with the LCAs in the parallel orientation, reflected power levels of 5–12 W (still below 10% of the forward power level) were
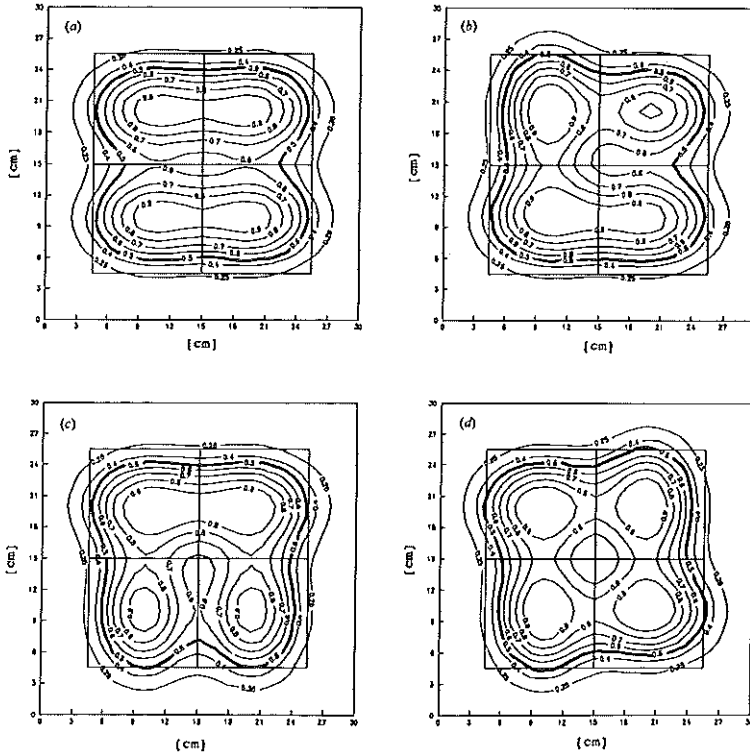
Figure 2. Gaussian-beam-predicted SAR distributions (SAR range 0–1) from 2×2 LCA arrays at 1 cm depth in muscle-equivalent tissue. The antennae (indicated by squares) are equally powered and the total aperture measured 21 cm $\times$ 21 cm. The E-fields are orientated according to figure 1. A 1 cm thick water layer was modelled as intermedium. The effective field is indicated by the bold line. The used configurations are: (a) parallel orientated, (b) Q-orientated, (c) U-orientated and (d) clockwise orientated.

measured. In the H-field direction (the 'Lucite' direction of the LCA) the width of the 50% iso-SAR contour measured 18.8 cm and 21.4 cm for the GB-predicted SAR distribution and the TG-measured SAR distribution respectively. In the E-field direction this width measured 17.1 cm and 17.3 cm.

Figures 4(a) and 4(b) show the TG-measured and its corresponding GB-predicted SAR distributions of the *clockwise*-orientated 2×2 LCA array. The EFSs equalled 303 cm^2 and 248 cm^2 respectively. The reflected power levels were in the range of 1–6 W. The local maxima under each antenna showed a significant shift in the H-field direction, towards the edge of the array.

Figures 3(c) and 4(c) show the calculated SRDs from the parallel and clockwise TG-measured and their corresponding GB-predicted SAR distributions. The SRD$_{EFS}$ equalled 9.4% and 14.0% for the parallel respectively the clockwise configuration.
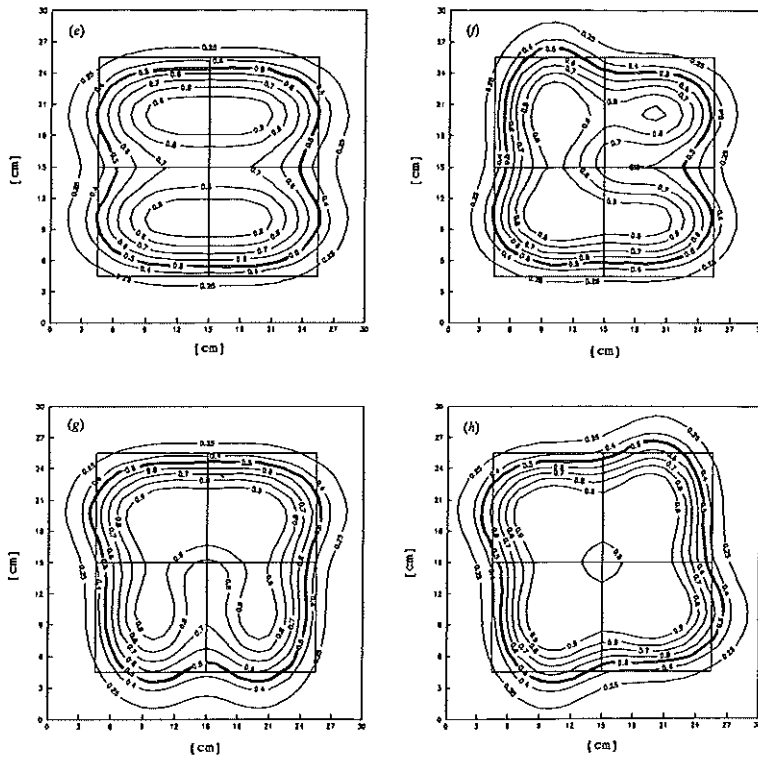
Figure 2. (*Continued*). (*e*) to (*h*) like (*a*) to (*d*) but now including a 1 cm fat layer on top of the muscle-equivalent tissue.

Table 1. Summary of the GB-predicted effective field sizes of four different 2 × 2 LCA array configurations. The antennae were equally powered and closely packed. A water layer of 1 cm thickness has been modelled. The total aperture covered 21 cm × 21 cm.

2 × 2 LCA array configuration	EFS [cm²] no fat	EFS [cm²] 1 cm fat layer added
parallel	341	358
Q	343	363
U	350	390
clockwise	359	419

    To quantify the shift of the local maxima, as shown in figure 4(*a*), a single antenna in the clockwise-orientated array was powered while the remaining antennae were terminated with a 50 ohm load. The resulting SAR distribution is shown in figure 5(*a*). The corresponding
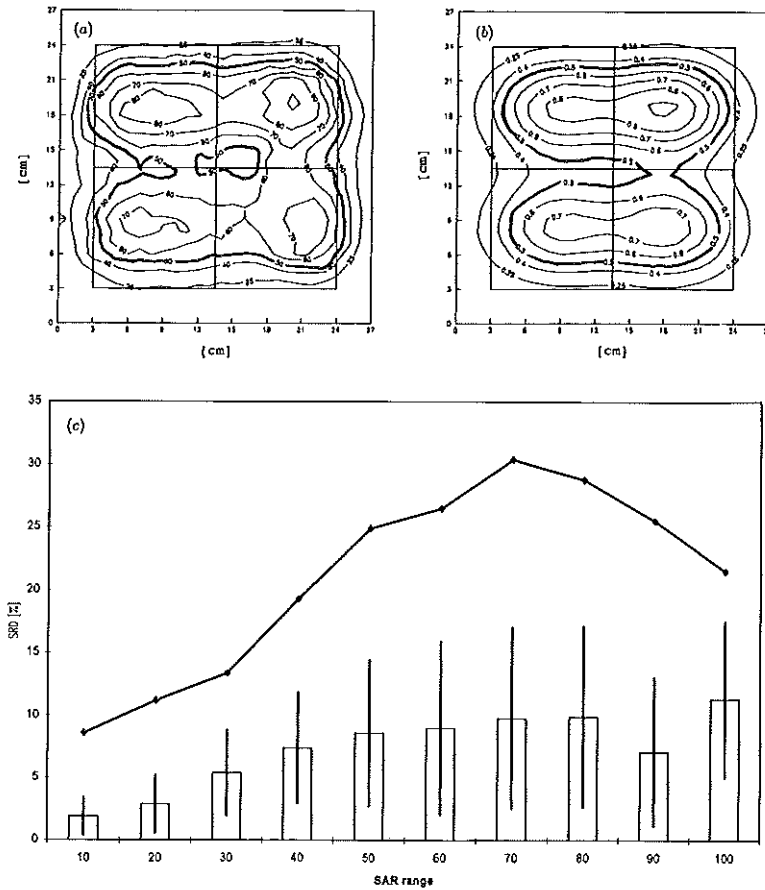
Figure 3. SAR distributions at 1 cm depth in muscle equivalent tissue obtained from a parallel E-field orientated 2 × 2 LCA array. A 1 cm thick water bolus (TG) or water layer (GB) was included as intermedium. The antennae are indicated by squares; the effective field (EF) is indicated by the bold line. (a) Thermographic (TG) measurement (SAR range: 0–100); (b) Gaussian beam (GB) predicted, with power settings optimized to fit the corresponding TG measurement (SAR range: 0–1); (c) absolute SAR differences (range: 0–100) between the GB-predicted and TG-measured SAR distributions calculated relative to 10% GB-predicted SAR ranges. Bars indicate the average per SAR range, errorbars indicate the standard error of the mean and the line represents the maximum difference per 10% GB-predicted SAR range.

EFS was 41 cm^2 and the shift of the local maximum in the H-field direction equalled 3 cm. No shift was observed in the E-field direction.

Table 2 summarizes the measured cross-coupling between antennae in the compact parallel- and clockwise-orientated arrays.
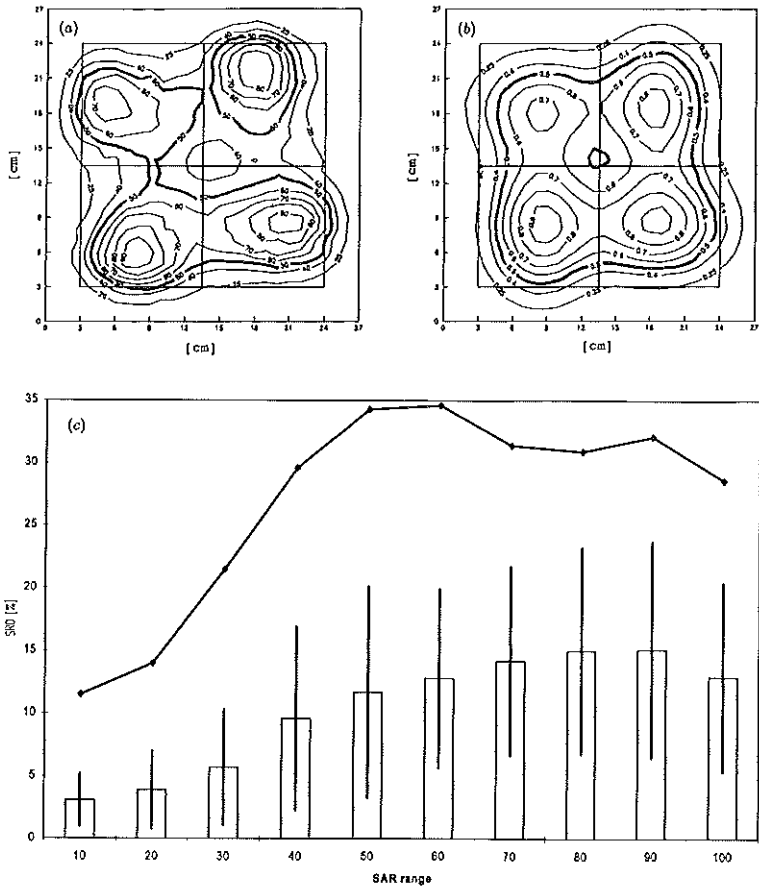
Figure 4. SAR distributions at 1 cm depth in muscle equivalent tissue obtained from a clockwise-*E*-field-orientated 2 × 2 LCA array. The *E*-fields are orientated according to figure 1(*d*). A 1 cm thick water bolus (TG) or water layer (GB) was included as intermedium. Antennae are indicated by squares; EF is indicated by the bold line. (*a*) Thermographic (TG) measurement (SAR range: 0–100); (*b*) Gaussian beam (GB) predicted, with power settings optimized to fit the corresponding TG measurement (SAR range: 0–1); (*c*) absolute SAR differences (range: 0–100) between the GB-predicted and TG-measured SAR distributions calculated relative to 10% GB-predicted SAR ranges. Bars indicate the average per SAR range, errorbars indicate the standard error of the mean and the line represents the maximum difference per 10% GB-predicted SAR range.

3.2. Second series: inter-element spaced clockwise-orientated 2 × 2 LCA array

Figure 5(*b*) shows the SAR distribution of a single-powered antenna in the inter-element spaced 2 × 2 LCA array setup, while the other antennae were terminated with 50 ohm
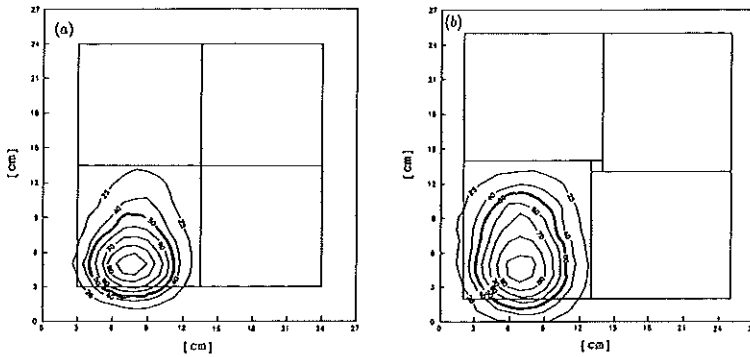
Figure 5. TG-measured SAR distribution (range: 0–100) from a single-powered LCA in a 2 × 2 clockwise-orientated LCA array. The *E*-fields are orientated according to figure 1(*d*). The total aperture measured: (*a*) 21 cm × 21 cm (closely packed array) and (*b*) 23 cm × 23 cm (inter-element spaced array).

Table 2. Summary of the cross-coupling between LCAs in a 2 × 2 array. The antenna configurations are chosen as in figure 1. In the compact configuration the array aperture measured 21 cm × 21 cm; in the inter-element spaced configuration the array aperture measured 23 cm × 23 cm. The water bolus measured 25 cm × 28 cm × 1 cm.

Antenna configuration	Couple	No bolus [dB]	With bolus [dB]
parallel, compact	'1' → '2'	−18	−18
parallel, compact	'1' → '3'	−26	−27
parallel, compact	'1' → '4'	−22	−24
clockwise, compact	'1' → '2'	−28	−33
clockwise, compact	'1' → '3'	−26	−32
parallel, spacious	'1' → '2'	−36	−33
parallel, spacious	'1' → '3'	−39	−33
parallel, spacious	'1' → '4'	−21	−21
clockwise, spacious	'1' → '2'	−32	−36
clockwise, spacious	'1' → '3'	−34	−35

loads. The shift in the *H*-direction of the SAR maximum still equalled 3 cm. However, the TG-measured EFS equalled 61 cm^2 which was an increase of 20 cm^2 compared to the equivalent compact setup. Figure 6 shows the SAR distribution of the inter-element spaced 2 × 2 LCA-array: (*a*) GB predicted, equally powered, (*b*) TG measured, (*c*) GB predicted with TG-derived and optimized power settings. Figure 6(*d*) shows the SRDs as calculated from the TG-measured and GB-predicted SAR distributions. The measured EFS (384 cm^2) and predicted EFS (equal antenna powers: 370 cm^2; power settings according to TG measurement: 330 cm^2) vary by 16%. When a 1 cm fat layer was incorporated in the GB model, the EFS equalled 444 cm^2. The SRDs ranged from 8.2% to 9.4% and the SRD$_{EFS}$ equalled 8.8%. The GB-predicted minimum SAR at the centre of an equally powered inter-element spaced 2 × 2 LCA array was 39% and 59% respectively without and with a 1 cm thick fat layer.
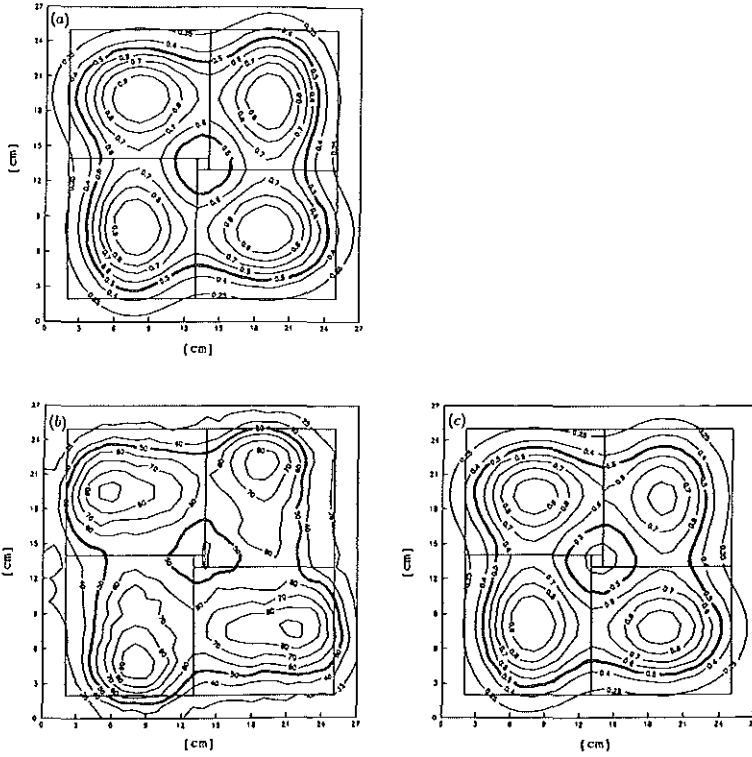
Figure 6. SAR distributions from the inter-element spaced 2 × 2 clockwise-orientated LCA array. The *E*-fields are orientated according to figure 1(*d*). Data are obtained from: (*a*) GB prediction with equally set power levels, (*b*) TG measurement and its (*c*) corresponding GB prediction.

Table 2 also summarizes the measured cross-coupling of the inter-element spaced clockwise-orientated configuration.

4. Discussion

4.1. Quantificaton of the quality of arrays of antennae

The total SAR distribution of an array of antennae is generally not a superposition of the SAR distributions of individual elements, since adjacent *E*-field distributions may overlap or antennae may interact. Although only incoherently driven LCA arrays are evaluated and constructive *E*-field interference between individual antennae can be excluded, the array must be evaluated as if it were a single antenna (Ibbott *et al* 1989), i.e. an evaluation is made of the total EFS, as defined by Hand *et al* (1989). The expected penetration depth
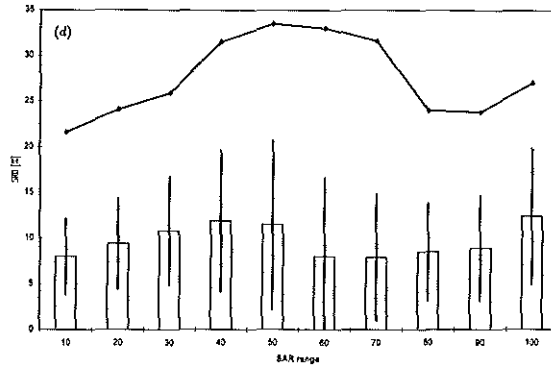
Figure 6. (*Continued*). (*d*) Absolute SAR differences (range: 0–100) between the GB-predicted and TG-measured SAR distributions calculated relative to 10% GB-predicted SAR ranges. Bars indicate the average per SAR range, errorbars indicate the standard error of the mean and the line represents the maximum difference per 10% GB-predicted SAR range.

of the incoherently driven array will be of the same order as of a single LCA (Hand *et al* 1992). Evaluation of the penetration depth of 2×2 LCA arrays is excluded from this report since deviations from the single-LCA penetration depth of up to 20% are not measurable with techniques available to us.

The EFS of an array of antennae quantifies the technical usefulness since it is a measure of the covered treatment area under the total aperture. However, whether the EFS (relative to the total aperture's physical dimensions) is the measure for ensuring clinical quality of an antenna array, is still debatable (Oleson 1989, Myerson *et al* 1990, Gelvich *et al* 1996). In fact, unambigious clinical quality requirements of a SAR distribution for any application of hyperthermia has not been defined as yet (Hand *et al* 1989, Ibbott *et al* 1989, Oleson 1995).

For arrays of antennae, the EFS is calculated from the total SAR distribution from the array. However, the location of the effective field (EF), relative to the total aperture, is not expressed in the EFS. This is not considered to be a problem when used for single antenna applications: the EF has its centre of gravity located near the centre of the aperture. For arrays of antennae, the EF has generally a more complex shape. In characterizing antenna arrays, the mutual interaction between antennae can cause changes in the SAR distribution which may not influence the EFS from that array significantly but which can change the shape of the EF significantly. In the GBM, effects of antenna interactions on SAR distributions can be discriminated into a superposition of (*a*) a change of GB power settings of each individual antenna and (*b*) a change of GB source parameters for each antenna. The latter will result in a different SAR print of each individual antenna depending on its place in the configuration of the array. This is only possible when the 2×2 antenna interactions are fully analysed. This is beyond our comprehension. For that reason we use the GB source parameters obtained from a single antenna operated without adjacent antennae.

The SAR-related difference (SRD) combines differences between TG-measured and GB-predicted SAR distributions and relates these differences to the location in the GB-predicted distribution which is a superposition of aperture-centred single-antenna SAR

distributions. The SRD therefore quantifies the SAR anomalies in an array which are caused by antenna interactions in the array.

4.2. Effects of E-field configurations or a fat layer on the SAR distributions from 2 × 2 arrays

When optimizing the temperature distribution during a hyperthermia treatment, one of the procedures is to rotate an antenna over 90°, thereby changing the E-field orientation and thus creating a different array configuration. From GB-predicted EFSs for the four different E-field-configured 2 × 2 LCA arrays as shown in figure 2 and as summarized in table 1, it can be concluded that the different configurations have little effect on the resulting EFS of a 2 × 2 array and have equal power deposition quality.

All four E-field configurations of the compact 2 × 2 LCA array have a GB-predicted minimum SAR level at the centre of the array of above 55% when calculated at 1 cm depth in a homogeneous muscle-equivalent phantom. Incorporating a 1 cm thick fat layer in the GBM increased the minimum SAR at the centre of the array to 65% and the average EFS of the four possible E-field configurations from 348 to 383 cm^2. Incorporating a fat layer increases the reflected power level by up to 56% (Johnson and Guy 1972) and thus reduces the effective heating of the underlying muscle tissue. Since the available power units could not produce an adequate temperature rise within 90 seconds when a fat layer was used, TG measurements involving a fat layer were excluded from the experiments.

Although the QA guidelines (Hand *et al* 1989) have no regulations on the shape of the EF, we find it appropriate for array applications to demand a contiguous EF under the array when obtained in a homogeneous muscle phantom. SAR values within the 50% SAR contour should therefore not drop below this 50% SAR level. Adding a fat layer in the GBM improved the quality of the EF in this respect.

4.3. Comparison of GB-predicted and TG-measured SAR distributions from 2 × 2 LCA arrays

The TG-measured and GB-predicted SAR distribution of the parallel 2×2 array configuration showed a good qualitative resemblance (figure 3(*a*) and figure 3(*b*) respectively). This was reflected in low average SRDs of around 10% (figure 3(*c*)) and SRD$_{EFS}$ (9.4%). The main difference in TG-measured and GB-predicted EFS of the parallel 2 × 2 array configuration (331 versus 261 cm^2), especially in the 'open' H-field direction, is caused by a finite water bolus effect (Van Rhoon *et al* 1998).

Low reflected power levels are observed in the clockwise orientation of the 2 × 2 array, which is to be expected because the adjacent E-fields are orientated orthogonally. Therefore, the *average* cross-coupling is significantly lower than in the parallel configuration (5 dB, no water bolus used; 9 dB, with water bolus; table 2). However, in the case of the clockwise-orientated array, a 3 cm shift outwards in the H-field direction of the local maxima under each antenna was measured (figure 4(*a*)). This shift of local SAR maxima in the clockwise-orientated configuration is inherent to the 'open' design of the LCA and was confirmed by the single-powered LCA in the clockwise-orientated 2 × 2 array (figure 5(*a*)). This phenomenon is caused by interaction of the RF field through the 'open' Lucite side wall with a metal side wall of an adjacent antenna. This was reflected in a high SRD$_{EFS}$ (14.0%) whereas the SRD$_{EFS}$ equalled 9.4% for the parallel configuration.

In the second series the LCAs were separated from each other by a gap of 2 cm, and through taking this measure, the cross-coupling between the antennae was substantially

decreased (averaged over all configurations: 8.4 dB, without water bolus; 4.8 dB, with water bolus, table 2). The resulting TG-measured SAR distribution of a single-powered LCA in this inter-element spaced 2×2 clockwise-orientated array confirmed these findings (figure 5(*b*)). The EFS of the single-powered antenna in the inter-element spaced 2×2 array was in the range of the EFS of a single LCA as measured with a large water bolus (Van Rhoon *et al* 1998). Still the same shift of the maximum SAR level was found as in the compact array but the odd shape of the single-antenna EF in the inter-element spaced 2×2 array was less prominent, reflecting less disturbance. This was confirmed by a smaller SRD_{EFS} (9.1% for the inter-element spaced array versus 14% for the compact array). Although the lower level SRDs for the inter-element spaced array configuration were higher than for the compact configuration (figure 6(*c*) respectively 4(*c*)), the overall average SRD from the inter-element spaced array configuration was lower (9.7%) than that from the compact array (10.4%). Cross-coupling can have a significant effect on the position of the local SAR maximum under each antenna (figure 5(*a*)) but it neither results in poor quality (i.e. discontiguity) of the SAR distribution from a 2×2 LCA array (figure 4(*a*)) nor leads to unacceptable levels of reflected power.

By creating the inter-element spaced array, the GB-predicted EFS increased by 11 cm^2 to 370 cm^2 but also became discontiguous. Comparison between the TG-measured and GB-predicted SAR distributions again showed that the TG EFS was enlarged by antenna interaction and water bolus effects. The discontiguity of the GB-predicted EFS disappeared when a 1 cm thick fat layer was modelled.

In summary: the GB-predicted EFSs from the 2×2 arrays of LCAs showed no significant sensitivity to selected E-field configurations. Differences in shape between GB-predicted and TG-measured SAR distributions have shown firstly that GB predictions alone are insufficient to describe full RF behaviour of the LCA in an array application and secondly that for antenna array applications quality assurance guidelines should be formulated concerning necessity of contiguity of the EFS. The relatively large EFS of the 2×2 arrays of LCAs provides a solid basis for clinical use of the LCA power settings and E-field configurations.

References

Bach Andersen J 1987 Electromagnetic power deposition: inhomogeneous media, applicators and phased arrays *Physics and Technology of Hyperthermia* ed S B Field and C Franconi (Dordrecht: Martinus Nijhoff) pp 159–88

Gelvich E A, Mazokhin V N and Troshin I I 1996 An attempt at quantitative specification of SAR distribution homogeneity *Int. J. Hyperth.* **12** 431–6

Guy A W 1971 Analyses of electromagnetic fields induced in biological tissues by thermographic studies on equivalent phantom models *IEEE Trans. Microw. Theory Tech.* **19** 205–14

Hand J W, Lagendijk J J W, Bach Anderson J and Bolomey J C 1989 Quality assurance guidelines for ESHO protocols *Int. J. Hyperth.* **5** 421–8

Hand J W, Prior M V, Lumori M L D and Forse G R 1992 Current sheet applicators for superficial hyperthermia *Hyperthermic Oncology 1992, Proc. 6th Int. Congress on Hyperthermic Oncology (Tucson, AZ)* ed E W Gerner

Ibbott G S, Brezovich I, Fessenden P, Pipman Y, Sandhu T, Sathiaseelan V, Galdi A and Saylor T 1989 Performance evaluation of hyperthermia equipment *American Association of Physicists in Medicine Report* **26**

Johnson C C and Guy A W 1972 Nonionizing electromagnetic wave effects in biological materials and systems *Proc. IEEE* **6** 692–718

Lumori M L D 1988 Microwave power deposition in bounded and inhomogeneous lossy media *PhD Thesis* Department of Electrical and Computer Engineering, The University of Arizona

Lumori M L D, Bach Andersen J, Gopal M K and Cetas T C 1990a Gaussian beam representation of aperture fields in layered, lossy media: simulation and experiment *IEEE Trans. Microwave Theory Technol.* **38** 1623–30

Lumori M L D, Hand J W, Gopal M K and Cetas T C 1990b Use of Gaussian beam model in predicting SAR distributions from current sheet applicators *Phys. Med. Biol.* **35** 387–97

Myerson R J, Perez C A, Emami B, Straube W, Kuske R R, Leybovich L and von Gerichten D 1990 Tumor control in long-term survivors following superficial hyperthermia *Int. J. Radiat. Oncol. Biol. Phys.* **18** 1123–9

Oleson J R 1989 If we can't define the quality, can we assure it? *Int. J. Radiat. Oncol. Biol. Phys.* **16** 879

——1995 Review. Eugene Robertson Special Lecture. Hyperthermia from the clinic to the laboratory: a hypothesis *Int. J. Hyperth.* **11** 315–22

Rietveld P J M, Lumori M L D, Hand J W, Prior M V, van der Zee J and Van Rhoon G C 1998 Effectiveness of the Gaussian beam model in predicting SAR distributions from Lucite cone applicators *Int. J. Hyperth.* **14** 293–308

Rietveld P J M and Van Rhoon G C 1991 Preliminary results of the improved water filled waveguide applicator in an array application *Strahlenther. Onkol.* **167** 335–6

Rietveld P J M, Van Rhoon G C and Broekmeyer-Reurink P M 1990 Improvement of SAR distribution of a 433 MHz water filled waveguide applicator *Strahlenther. Onkol.* **166** 528–9

Van Rhoon G C, Rietveld P J M, Broekmeyer-Reurink M P and Van der Zee J 1992 A 433 MHz waveguide applicator system with an improved effective field size for hyperthermia treatment of superficial tumors at the chest wall *Hyperthermic Oncology 1992, Proc. 6th Int. Congress on Hyperthermic Oncology (Tuscon, AZ)* vol 2, ed E W Gerner, pp 187–90

Van Rhoon G C, Rietveld P J M and van der Zee J 1998 A 433 MHz Lucite cone waveguide applicator for superficial hyperthermia *Int. J. Hyperth.* **14** 13–27

Theoretical comparison of the SAR distributions from arrays of modified Current Sheet Applicators with that of Lucite Cone Applicators using Gaussian beam modelling

PJM Rietveld, J Stakenborg, TC Cetas, MLD Lumori and GC van Rhoon

abstract

The technical comparison of Current Sheet Applicator (CSA) and Lucite Cone Applicator (LCA) arrays covering an area of approximately $20*20$ cm^2 is investigated based on Gaussian beam (GB) predicted SAR distributions. The comparison is made in muscle equivalent tissue at 1 cm depth (maximum SAR normalised to 100%) and over a volume of 3 cm depth under the aperture of the antennae. The planar SAR distribution is tested on field sizes (FS$_x$: area covering x% SAR), penetration depth (PD) and homogeneity coefficient (HC = FS$_{75}$/FS$_{25}$). From the SAR volume, a SAR-Volume histogram (= volume enclosing y% SAR/ total volume) is calculated as well as the volumetric HC.

Firstly, the prototype CSA (aperture $58*67$ mm^2, FS$_{50}$ = 21 cm^2) is technically modified to assure clinical safety and load independence. The modified CSA, the D-CSA, has an aperture of $66*75$ mm^2 with an FS$_{50}$ = 28 cm^2 and a PD of 10 mm, the LCA (aperture $105*105$ mm^2) has an FS$_{50}$ = 76 cm^2 and PD = 12 mm. The HC equals 0.21 (D-CSA) respectively 0.22 (LCA).

Secondly, a $3*3$ D-CSA array is compared with a $2*2$ LCA array. The FS$_{50}$s equal 72% (D-CSA) respectively 75% (LCA). The SAR-volume histograms, planar and volumetric HC show no significant difference, however the planar HCs for D-CSA and LCA increase from 0.2 to 0.3 indicating that incoherently powered arrays from these antennae build SAR distributions constructively.

1. Introduction

In the treatment of recurrent breast cancer with superficial hyperthermia, we have shown that a) improved technology results in better clinical outcome (Van der Zee *et al.* 1999) and b) an enlarged effective field size results in higher interstitial temperatures (Rietveld *et al.* 1999). The basis for both these studies was a clear technical improvement of equipment: a) a change from 2450 MHz to 433 MHz combined with higher quality applicators and b) further technically improved applicators (Van Rhoon *et al.* 1998). Other groups have also reported on technically improved antennae and/or their clinical relevance. The technical possibilities of micro strip antennae in array applications have been extensively reported on by, for instance, Samulski *et al.* 1990, Lee *et al.* 1992, Tharp and Roemer 1992, Zhou and Fessenden 1993, Diederich and Stauffer 1993, Ryan *et al.* 1995, Stauffer *et al.* 1998, Rosetto and Stauffer 1999 and they show that small antennae are capable of heating a large area adequately. Also, the clinical performance of small antennae has been reported to be satisfactory.

In more than 1900 treatments (over 260 patients) we generally used arrays of 2 to 5 waveguide antennae operating at 433 MHz- i.e. conventional water-filled waveguide applicators (WGA) or the improved waveguide antennae, the Lucite Cone Applicators (LCA) (Van Rhoon *et al.* 1998, Rietveld *et al.* 1998a) – both with an aperture of about $10*10$ cm^2. We treated the *entire* reirradiated area and, since we drove the antennae non-coherently, the power level of each antenna was the main control parameter. The treatment area was composed of a complex distribution of varying tissue types and a very inhomogeneously distributed blood flow. These inhomogeneities require adjustment of power levels to create an optimal SAR deposition. Although theoretically one can make finer volumetric SAR adjustments with small antennae, the complexity of treatment optimisation increases quickly with the number of antennae. Also, theoretical studies have demonstrated that a negative consequence of small aperture antennae is lesser penetration depth (Hand and Hind 1986, Heinzl *et al.* 1990) which may counteract the benefit of higher spatial control.

As yet, it is not clearly understood what impact the combination of penetration depth and spatial resolution has on the quality of the 3D-SAR distribution for antenna used in array applications. The *technical* SAR-evaluation parameters as described in the current available Quality Assurance guidelines (Hand *et al.* 1989, American Association of Physicists in Medicine (AAPM) report No. 26 'Performance Evaluation of Hyperthermia Equipment'), the Effective Field Size (EFS=FS$_{50}$) and penetration depth (PD), are based on the 50% SAR value

(relative to the max. SAR value at 1cm depth in muscle-like tissue). However, thus far, the only *clinically* substantiated prospective SAR-indicator is the 25% SAR area from an array of antennae (Myerson *et al.* 1990, Lee *et al.* 1998). On the other hand, Gelvich *et al.* (1996) have defined an additional evaluation parameter from a more technical point of view: the Homogeneity Coefficient (HC) which is defined as the ratio of the 75% SAR field size (FS_{75}) over the 25% SAR field size (FS_{25}) at 1 cm depth in muscle-equivalent tissue. Because of these variations in quality definitions, we require an extensive technical comparison of antennae before we begin a clinical comparison between different antenna types.

To answer the first question concerning the relevance of spatial control and penetration depth, we technically compared the SAR quantities of the LCA (aperture: 105*105 mm²) and the Current Sheet Applicator (CSA, aperture about 70*60 mm²) at 75%, 50% and 25% in 1 cm depth in muscle-equivalent tissue We also compared the 3D-SAR distributions over the entire treatment volume.

Bach Andersen *et al.* (1984) and Johnson *et al.* (1987, 1990) have developed the basic principle of the CSA. Lumori *et al.* (1990a,b) and Gopal *et al.* (1992) have developed the antenna into a clinical version, the first of two prototypes, the G-CSA. Several groups used G-CSAs and have reported technical and clinical results (Leigh *et al.* 1994, Prior *et al.* 1995).

A second clinical prototype CSA, the P-CSA, became available to other groups via a COMAC-BME programme[1]. In 1993, we obtained two examples of the P-CSA. It was reported to have some major drawbacks concerning load dependency, tuning frequency and cross-coupling (T. C. Cetas, personal communication).

In this report we present *technical* results of the P-CSA and a redesigned and improved low-cost Dutch CSA, the D-CSA. The D-CSA will prove to have a better technical performance than the P-CSA concerning tuning stability as function of tissue load and a lower cross-coupling. The D-CSA meets the European Society for Hyperthermic Oncology (ESHO) Quality Assurance (QA)-guidelines making it suitable for clinical applications. Also we will show that the GB-modelled SAR distribution of a 3*3 array application of D-CSAs meets the quality of that of a 2*2 LCA array.

---

[1] official denominatio: COMAC-BME Concerted Action in Biomedical Engineering, EC Medical and Health Research Programma 1987-1991, Target II.1 Medical Technology Development, Area II.1.2 Treatment and Rehabilitation, Title 'Optimization of Hyperthermia Technology and the Assessment of its Clinical Efficacy in the Treatment of Cancer'

Currently we are carrying out a clinical study to compare the performance of the D-CSA with that of the LCA. This will bring our investigation on the D-CSA to an end.

2. Material and Methods

2.1. *Antennae*

In this study two CSA type antennae were used, the version two-prototype CSA (P-CSA) and the redesigned Dutch CSA (D-CSA). The technical behaviour of the CSA has been described in detail by Bach Andersen *et al.* (1984), Johnson *et al.* (1987, 1990) and Gopal *et al.* (1992). The LCA with which we compare the D-CSA has been described in detail by Van Rhoon *et al.* (1998). The technical qualities of the LCA in array applications have been reported by Rietveld *et al.* (1998b).

2.1.1. *P-CSA* Two P-CSAs were obtained through the COMAC-BME programme. The outer dimensions of the antenna are $67*58$ mm^2 (l*w) and 23 mm (h). The inner parts are constructed of polytetrafluorethylene (PTFE) plate (0.85 mm and 3.2 mm)' and copper plate (0.8 mm). The P-CSA is built in stainless steel housing. The PTFE-plate at the radiating surface is held in place by two metal rims from the steel housing located at the short side of the aperture. Note that the steel housing is in close contact with the radiating part of the applicator and its load. The RF-design of this antenna is symmetrical but the feeding line, a coaxial cable, is asymmetric i.e. the outer conductor is connected to earth. Since the outer conductor of the coaxial cable and feeding point are also connected to the housing of the antenna, the housing becomes a part of the radiating structure of the antenna.

2.1.2. *D-CSA* The locally redesigned CSA (D-CSA) is made of sticky copper foil (0.05 mm) and polyethene (PE) (for the RF-circuit 1 and 3 mm PE plates and the copper foil were used, see figure 1a). The outer dimensions of the antenna are $75*65$ mm^2 (l*w) and 19 mm (h). The radiating aperture equals $55*49$ mm^2. The housing is constructed of copper foil glued onto a PE-box. A 1:4 1/2 wavelength balun was integrated in the housing of the antenna creating a balanced radiating structure. The balun is made of type RG 316 U coaxial cable, positioned in the PE box holding the radiating parts, and is kept in place by (black) polyurethane-cement (figure 1a). The construction is such that the radiating antenna parts, including housing, are placed in the watertight PE-container (figure 1a (left side) and b). The D-CSAs can easily be set up in an array with use of Velcro which is attached to the side walls of the watertight PE-

container (not shown in figure 1) and which acts as a semi-rigid connection to adjacent CSAs. A heatsink is glued on top of the copper housing to transport internal RF-losses (figure 1b).
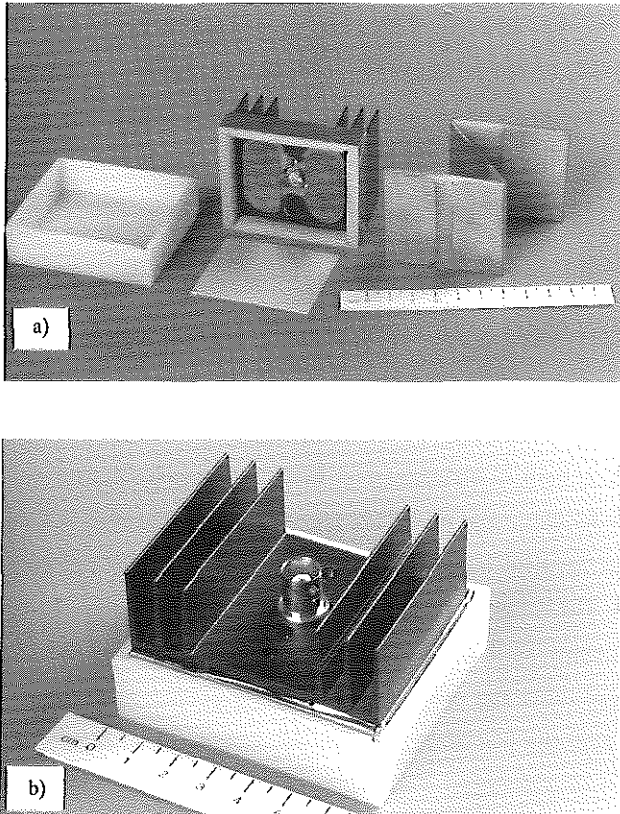
Figure 1. Photographs of the Dutch Current Sheet Applicator (D-CSA)
  a) shows the inner parts of which the D-CSA is constructed. At the left side the watertight PE container; in the middle the upper part of the radiator is shown, containing the coaxial feed plus the ¼ lambda balun which is held in position by black polyurethane-cement. The balun is connected to the two upper capacitor plates. In front of the upper part the 1 mm thick PE sheet, which is used as capacitor dielectric. At the right, the resonance circuit is shown which is constructed of copper foil glued on 3 mm and 1 mm (middle piece) thick PE plate. The front piece shows the capacitor parts, which face the upper part of the radiator.
  b) complete D-CSA with heat sink placed in the watertight PE-container.

2.2. *RF properties of antennae*

The measurements from a single CSA on resonance frequency, transmission and reflection (at 433 MHz) were obtained with a network analyzer (Hewlett Packard 8751A).

Efficiency of the antennae was measured via the transmission coefficient using two oppositely positioned antennae each connected to the network analyzer.

Load dependence of a single CSA was measured for four configurations: 1) CSA directly positioned on a flat semi-solid muscle-equivalent phantom $(48*48*(1+2+2+5)$ cm^3) made of Super Stuff (Guy 1971)), 2) 1cm-thick solid fat layer $(20*20$ cm^2, (Guy 1971) added on top of the muscle layer, 3) a 1cm-thick water bolus added, no fat and 4) both water bolus and fat layer added.

Stray radiation from one antenna positioned on muscle-equivalent tissue and powered at 50 W was measured with an isotropic Holaday-E-field probe (HI-3000) at 0.2 and 0.5 m distance in the aperture plane. No water bolus was used in these experiments.

Cross-coupling between two adjacent CSAs was measured on the flat muscle-equivalent phantom. Both $2*1$ array configurations i.e. long sides adjacent or short sides adjacent, were measured. In these experiments a water bolus $(20*12*1$ cm^3) was used as intermedium to the phantom. The accuracy of the measurements was $\pm$ 1dB.

2.3. *Thermographic SAR measurements*

SAR distributions at 1 cm depth in muscle were obtained using the layered semi-solid muscle-equivalent phantom with and without an additional 1 cm-thick fat layer on top of the muscle-equivalent tissue. The CSA was driven by a power pulse of approximately 75 W for 1 minute. A thermographic camera (AGA Thermovision System 680/102B) interfaced to a PC was used to measure the temperature distribution at the exposed surface.

The effective field size (EFS), defined by the ESHO QA-guidelines (Hand *et al.* 1989) was calculated from thermographically (TG)-measured SAR distributions.

2.4. *Gaussian beam modelling of SAR distributions from (arrays of) antennae*

Gaussian beam (GB) modelling is extensively used to predict SAR distributions from CSA arrays (Lumori *et al.* 1990a,b, Gopal *et al.* 1992, Prior *et al.* 1995). The GB-input parameters, half-power width (S) and phase radius (R) in both E- and H-field directions in the principal planes for the D-CSA, were obtained from measurements of the dominant E-field directions in

liquid muscle-equivalent tissue (Hand *et al.* 1989) using an unbalanced 1 cm wide dipole and measured: S_E= 2.1 cm, R_E= -50 cm, S_H= 3.7 cm and R_H= 23 cm. The unbalance of the dipole sensor was corrected for by averaging two opposite-orientated dipole scans.

The resolution of the GB-model was 0.6 cm in both x- and y-direction. This led to a P-CSA aperture of 75*66 mm^2 which was created by averaging the results from calculations with a 78*66 mm^2 and 72*66 mm^2 aperture. From the GB-predicted SAR distribution the EFS, FS_{25} and FS_{75} are calculated (FS_x: area covering x% or more SAR relative to the maximum at 1 cm depth in muscle-equivalent tissue). Also the homogeneity coefficient as defined by Gelvich *et al.* (1996) HC = FS_{75}/FS_{25} is calculated.

2.4.1. Spatial resolution and penetration depth from an array of antennae We compared a 3*3 CSA array with a clock-wise E-field orientated 2*2 LCA array (Rietveld *et al.* 1998b). Both LCA and D-CSA arrays covered about 20*20cm^2 of treatment area i.e. 21.0*21.0 cm^2 (LCA) and 22.5*19.8 cm^2 (D-CSA). By calculating a single D-CSA SAR footprint and adding a single footprint into a 3*3 CSA array pattern, a SAR distribution was obtained from an equally non-coherent powered 3*3 array of CSAs. From that SAR distribution, again the FS_{25}, EFS, FS_{75} and HC were obtained at 1 cm depth.

To incorporate the penetration depth into the quality evaluation of the antenna being tested, GB-predicted SAR distributions from the 2*2-LCA and 3*3-CSA array at different depths in muscle (delta z = 1 mm) were included to calculate a SAR-volume histogram. The SAR-volume histogram is defined by:

Volume of relative SAR [%] / total volume,

where the 100% SAR level is defined as the maximum SAR at 1 cm depth in muscle. The volumes are *restricted by the outer boundaries* of the antenna array times 3 cm depth into muscle tissue.

From the *total* SAR volume the ESHO defined PD was obtained as well as the volumetric field sizes (FSV) based on 25%, 50% and 75% SAR. The quotient FSV_{75}/FSV_{25} represents the volumetric HC (HCV).

3. Results

3.1. *Antenna properties*

For both the P-CSA and D-CSA an overview of the transmission at the resonance frequency and at 433 MHz as a function of (tissue) load is given in table 1. It clearly shows that the D-CSA was more stable in resonance frequency than the P-CSA as a function of the (tissue) load, δf=3 MHz versus 14 MHz. Also the reflected signal at resonance frequency was lower: (-9 .. –29 dB) for the D-CSA than for the P-CSA (–5 .. –21 dB) as a function of the tissue load.

The *efficiency* of the P-CSAs could not be measured accurately due to tuning problems. The efficiency of the D-CSA measured 60% (+/- 10%) and was comparable to that of the LCA, 50% (+/- 5%) (Van Rhoon *et al.* 1998).

Table 1. Overview of the resonance frequency f_{res} and reflected signal at 433 MHz $s_{21}(433)$ and at the resonance frequency $s_{11}(f_{res})$ of the prototype CSA (P-CSA) and the redesigned CSA (D-CSA) as a function of the antenna load.

Antenna:		P-CSA			D-CSA	
LOAD:	f_{res} [MHz]	$s_{21}(f_{res})$ [dB]	$s_{21}(433)$ [dB]	f_{res} [MHz]	$s_{21}(f_{res})$ [dB]	$s_{21}(433)$ [dB]
Muscle	442	-5	-5	436	-12	-11
1cm fat, muscle	456	-20	-2	436	-9	-8
1cm water bolus, muscle	445	-12	-6	433	-18	-18
1cm water bolus, 1cm fat, muscle	451	-21	-4	433	-29	-29

The TG-measured EFSs from the P-CSA and D-CSA equalled 21 cm² (standard deviation (sd): 1 cm², n = 4) respectively 28 cm² (sd: 3 cm², n = 5). A water bolus (20*20*1cm³) was used as intermedium. A complete overview of SAR-related parameters is given in table 2. For comparison, the G-CSA data (Gopal *et al.* 1992, Gelvich *et al.* 1996) and LCA data (Van Rhoon *et al.* 1998, Rietveld *et al.* 1998a) are included in table 2.

Table 2. Overview of basic SAR-related parameters from a single CSA or LCA.

	aperture [mm^2]	FS$_{25}$ [cm^2]	[%]	EFS (FS$_{50}$) [cm^2]	[%]	FS$_{75}$ [cm^2]	[%]	HC	PD [mm]
P-CSA (TG)	58*67	52	134	21	54	9	23	0.17	-
D-CSA (TG)	66*75	87	176	28	56	10	20	0.11	-
D-CSA (GB)	66*75	58	117	28	56	12	24	0.21	10
G-CSA (GB)	59*73	36	83	17	40	7	16	0.20[1] 0.27[2]	10
LCA (GB)	105*105	144	131	76	69	31	28	0.22	12

The 25%, 50% and 75% SAR related field sizes (respectively FS$_{25}$, EFS (=FS$_{50}$) and FS$_{75}$) from both thermographically (TG) measured and Gaussian beam (GB) predicted SAR distributions at 1 cm depth in muscle-equivalent tissue are calculated. Data are presented in both absolute measure and relative to the aperture size. Also the SAR homogeneity coefficient (HC = FS$_{25}$/FS$_{75}$) is given. The GB-predicted SAR distributions were obtained with an infinite water bolus of 1 cm thickness. Data from the G-CSA were obtained from Gopal *et al.* (1992), Gelvich *et al.* (1996) and additional Gaussian beam calculations (PD). Data from the LCA obtained from Van Rhoon *et al.* (1998) and Rietveld *et al.* (1998).
[1] according to our GB-predicted SAR distribution
[2] according to Gelvich *et al.* 1996

The *stray radiation* levels from the antennae fed with 50 W input and measured at 20 cm and 50 cm distance are given in table 3. For comparison, we also included data from the LCA in table 3. Although the LCA would appear to be of a design that permits more RF leakage, stray radiation levels are considerably lower than in the case of the D-CSA. The P-CSA generated the highest level of stray radiation, which was due to the unbalance in the antenna.

Table 3. Maximum stray radiation levels [mW/cm^2] of the P-CSA, D-CSA and LCA at 0.2 m and 0.5 m measured with a Holaday HI-3000 isotropic field strength meter. The power input equalled 50 W.

Antenna:	Stray radiation at 0.2 m	Stray radiation at 0.5 m
P-CSA	2.5	0.2
D-CSA	1.0	0.1
LCA	0.3	0.04

Table 4. Cross-coupling between two D-CSAs measured on a muscle-equivalent phantom with a water bolus of $25*18*1.5$ cm^3 as intermedium. The antennae were positioned centrally on the water bolus.

	cross-coupling (mean (sd)) between two D-CSAs with Velcro at side walls; [dB], n=5 (single antenna aperture $75*66$ mm^2)	cross-coupling (mean (sd)) between two D-CSAs without Velcro at side walls; [dB], n=3 (single antenna aperture $71*62$ mm^2)
long sides adjacent	-16 (0)	-16 (0)
short sides adjacent	-26 (2)	-29 (1)

An overview of the *cross-coupling* between two adjacent D-CSAs is given in table 4. This table also includes data from D-CSAs without Velcro strips.

3.2. *D-CSA- and LCA array-related parameters from GB-predicted SAR distributions*

The GB-predicted SAR distribution at 1 cm depth in muscle-equivalent tissue from an equally non-coherent powered close-packed $3*3$ array of D-CSAs is shown in figure 2a. The
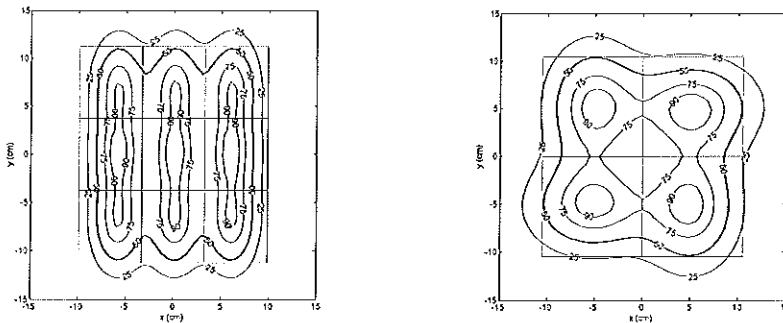
Figure 2. Gaussian beam predicted SAR distribution arrays of antennae. The SAR is calculated at 1 cm depth in muscle-equivalent tissue and the maximum normalised to 100%. The rectangles indicate the apertures.
a) $3*3$ D-CSA array (E-fields parallel)
b) $2*2$ LCA array (in a clock-wise E-field orientation)

corresponding EFS measured 320 cm^2 (72% of the $3*3$ array aperture). Figure 2a shows clearly that the GB-predicted EFS was contiguous over the $3*3$ array as was also the case for the $2*2$ LCA array (figure 2b, EFS=332 cm^2). The homogeneity coefficient HC equals 0.33

for the 3*3 CSA array and 0.34 for the 2*2 LCA array. The upper part of table 5 gives a complete overview of all 25, 50 and 75% SAR-based field sizes at 1 cm depth in muscle-equivalent tissue.

Table 5: SAR related parameters from GB-predicted SAR distributions of arrays of antennae.

	FS_{25}		FS_{50} (=EFS)		FS_{75}		HC
surface at 1 cm depth	[cm^2]	[%]	[cm^2]	[%]	[cm^2]	[%]	
3*3 D-CSA array	434	97	320	72	145	33	0.334
2*2 LCA array	495	112	332	75	170	39	0.344
	FSV_{25}		FSV_{50}		FSV_{75}		HCV
volume of 3 cm depth	[cm^3]	[%]	[cm^3]	[%]	[cm^3]	[%]	
3*3 D-CSA array	1094	82	554	41	261	20	0.239
2*2 LCA array	1250	94	622	47	290	22	0.232

The upper part gives values obtained from the SAR distribution at 1 cm depth in muscle. The lower part gives numbers based on the entire SAR volume, which covers 3 cm depth in muscle equivalent tissue.
The values in terms of percentage are related to the size of the aperture. The 3*3 array aperture of D-CSAs measures 19.8*22.5 cm^2, the 2*2 array aperture of LCAs measures 21*21 cm^2.

By calculating the SAR distribution from an array of antennae from 0 to 3 cm depth per 1 mm, a volumetric SAR distribution was obtained from which the SAR-volume histogram was derived. Figure 3 shows the GB-predicted SAR-volume histograms obtained from a 3*3 D-CSA array and a 2*2 array of LCAs. The GB-predicted 50% SAR volume of both antenna types was 41% for the D-CSA array and 46% for the LCA array relative to the covered volume. The array-PD of the D-CSA and LCA array: 11 and 12 mm respectively, we obtained using the volumetric SAR-data. A complete overview of the volumetric field sizes FSV_x (x=25, 50 and 75%), and volumetric homogeneity coefficient (HCV) is given in the second part of table 5.
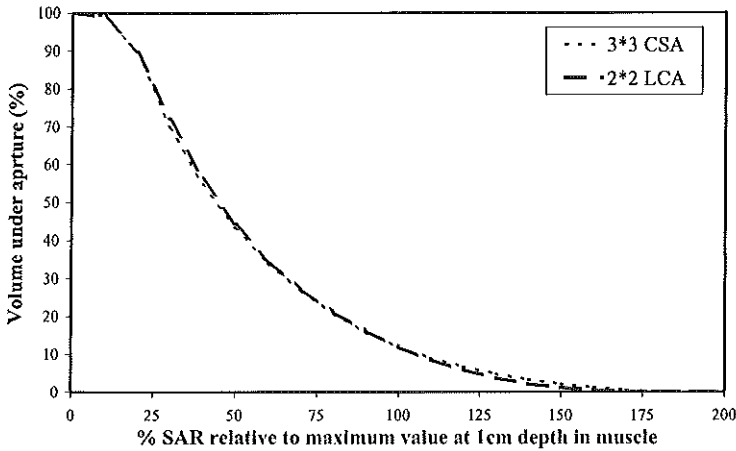
Figure 3. Relative SAR-volume histogram obtained from Gaussian beam predicted planar SAR distributions at 1 mm interval in depth. Normalisation is to the volume of 3 cm depth, which covers the entire aperture of the array under test. The 100% SAR is defined as the maximum SAR value at 1 cm depth.

4. Discussion

4.1. *Single CSA*

The predecessor of the P-CSA, the G-CSA, is used successfully under clinical conditions. It is a robust antenna, and gives no trouble. The P-CSA was an initial commercial prototype that was distributed to a few centres before satisfactory refinements were carried out. Due to several external causes, the final refinements were never made which left two main defects in the construction of the P-CSA.

The first defect was the metal housing. This became an active part of the radiating structure, as the outer conductor of the coaxial cable was both connected to the metal housing and also to one of the capacitor plates inside. The CSA is a RF symmetrically-designed radiator (Johnson *et al.* 1987, Bach Andersen *et al.* 1984) and since the metal housing of the P-CSA was in close contact with the load (less than 1 mm), the unbalanced P-CSA showed a RF-behaviour strongly dependent on the load (table 1). The second defect was the construction of the U-shaped bottom PTFE-plate in the P-CSA, which allowed water

contamination of the RF circuits and could lead to unsafe clinical situations. Due to these two serious drawbacks, we decided that a rigorous redesign of the construction was necessary.

4.1.1. RF-properties of a single antenna The unbalance in the feeding point of the P-CSA was neutralised by the implementation of a balun in the D-CSA. Also increasing the distance from the metal housing to the aperture from less than 1 mm (P-CSA) to 4.5 mm (D-CSA, including the PE-box) improved the stability of the resonance frequency as a function of tissue load (table 1).

Efficiency of the P-CSA was not measured. The opposed antenna set-up was not feasible because of a) direct coupling from one metal housing to the opposite metal housing which influenced the efficiency significantly and b) too large a discrepancy in resonance frequency between the two antennae. A caloric efficiency measurement on liquid muscle-equivalent tissue was not successful because the liquid penetrated the inner construction of the P-CSA. This caused power errors and the experiment had to be abandoned.

The efficiency of the D-CSA was equal in quality to that of the LCA.

Stray radiation from the P-CSA was largely due to standing waves at the outer conductor of the coaxial cable. By implementing a balun in the D-CSA the stray radiation levels dropped significantly to a level far below 1 mW/cm^2 at a distance larger than 0.5 m (table 3). Although the LCA has two open (i.e. Lucite) side walls, the stray radiation level was less even when operated at the average power level of 62 W (Rietveld *et al.* 1999).

The *cross-coupling* we measured for the D-CSA was the same level as measured by Gopal *et al.* (1992) for the G-CSA (-16 dB: long sides adjacent; -22 dB short sides adjacent) when an inter-element spacing of 10 mm was used. Since the D-CSA is contained in a PE-box, the inter-element spacing is intrinsically dealt with in its design. Furthermore, the PE-box automatically functions as insulation for the patient. We tested the D-CSA under clinical conditions and came to the conclusion that the Velcro-connections might not be suitable for larger arrays. Therefore, we did cross-coupling measurements without the Velcro attached to the PE-box. Although the inter-element spacing is reduced by 4 mm, the level of cross-coupling remained low (table 4).

4.1.2. SAR-related properties of a single antenna The FS_{25} and FS_{75} of the TG-measured SAR distributions from the P-CSA and D-CSA (table 2) were obtained from the most representative TG-images. We found the TG-obtained FS_{25} to be especially sensitive to heat

conduction during a 1 minute power pulse. This explains the discrepancy in the HC obtained from a TG-measured and a GB-predicted SAR distribution (table 2) and our preference to use GB-predicted SAR distributions to obtain quantitative parameters.

The EFS_{TG} of the P-CSA (54%) was larger than that of the G-CSA (37%, Gopal *et al.* 1992). The EFS_{TG} of the D-CSA compared with that of the P-CSA was larger on an absolute scale and (almost) equal if related to the sizes of the apertures. The GB-calculated EFS (EFS_{GB}) relative to the aperture for a single LCA was highest, followed by the D-CSA and G-CSA (table 2).

The PD obtained from GB-predicted SAR distributions showed that the D-CSA and G-CSA were of equal magnitude (10 mm, table 2) while the PD of the LCA was 2 mm larger, a significant difference on this scale.

Based on these EFS and PD findings, the quality (according to the ESHO guidelines) of the P-CSA and D-CSA are about equal. We incorporated the HC-parameter to further quantify the quality of the antennae. We used the *entire* SAR areas from an (array of) antenna(e) to define FS_{25}, EFS (and FS_{75}). We calculated the HC(G-CSA) to be 0.20 by weighing the areas covering 75% and 25% SAR cut out from an enlarged photocopy of figure 3b in Gopal *et al.* (1992). Using this method we obtained an EFS=17(.4) cm² (40%), as reported by Gopal *et al.* (1992). The corresponding values of the graphically obtained FS_{25} and FS_{75} (table 2) were used to calculate our HC-value. However, Gelvich *et al.* (1996) reported the HC(G-CSA) to be equal to 0.27 (table 2). Since we found an EFS(G-CSA) equal to that reported by Gopal *et al.* (1992), we concluded, using *our* data (table 2), that the GB-based HC of D-CSA, LCA and G-CSA were of comparable quality.

Use of the GB-predicted SAR distribution for obtaining a reliable FS_{25} and HC of the D-CSA in its comparison with the LCA was justified by the good similarity between the TG-measured and GB-predicted 50% and 75% SAR field sizes.

In conclusion, we found the construction of the D-CSA to be simple and cheap. It is a good quality antenna, suitable for use in the study of array applications and was a useful counterpart to the LCA in the comparisons made between the arrays of the two.

4.2. *SAR-related properties of antenna arrays*

The LCA array outperformed the D-CSA array by 3% in EFS (=FS_{50}). The FS_{25}, when calculated relative to the aperture, was 15% larger for the LCA than for the D-CSA. However, if the absolute 25% SAR area of both antenna arrays, are compared, as depicted in figure 2,

the difference is caused mainly by the LCAs 25% SAR areas outside the array-aperture. Since in our clinical practice the entire (RT-)treatment area is covered by antennae, this FS_{25}-difference between D-CSA and LCA does not play an important role.

In both arrays of antennae, the HC was increased significantly compared to the values of the single antennae (table 2 and table 5). This was due to a constructive inter-antenna SAR overlap. From the GB-predicted SAR distributions, we found that the SAR-volume histogram of the D-CSA array and LCA array differed by less than 3%.

Although it is not yet clear which parameter best describes the technical performance of an antenna array, we conclude, from the fact that their differences fall within acceptable limits, that the D-CSA and the LCA show comparable technical performance in array applications.

Up to now, the D-CSA worked without problems under clinical conditions (maximum array size 3*2). The reflected power remained within acceptable limits. However, in larger than 3*2 arrays, the Velcro inter-antennae connection was not sufficient to keep the antennae in position and additional rods have been placed on top of the heatsink to overcome this. These rods can be used to fix the CSA in a mounting device in order to maintain a stable position relative to the patient.

Technical adaptations in hard- and soft-ware are currently being made to be able to use up to 4*3 arrays of D-CSAs in the clinic and to extend the clinical evaluation.

4.3. Problems concerning the technical evaluation of antenna arrays

We lack one single parameter that reflects the quality in both spatial control and penetration depth of an array of superficial antennae (operating under clinical circumstances). In the presented study we compare a small aperture type of antenna with a large one. It is clear that a small antenna has better spatial control over a treatment area than a large antenna since the degrees of freedom to adapt to the SAR deposition requirements for that given treatment area are proportional to the number of antennae. On the other hand, it has been shown theoretically that an aperture of 8*8 cm^2 or smaller has less penetration depth than a 10*10 cm^2 aperture antenna (Hand and Hind, 1986). For that reason, a theoretical comparison between the LCA and D-CSA on their ability to adapt to clinical heterogeneous SAR requirements in a treatment volume will not help to determine the importance of the *combination* of spatial control and penetration depth. Therefore, we have decided to use a

basic approach to compare the SAR distributions from incoherently equally powered D-CSAs or LCAs in an array covering about the same treatment area.

The minimum quality requirements for an array can be tested by applying the ESHO guidelines (Hand *et al.* 1989) to a single applicator. These are based on 50 % SAR (EFS and PD) on an array of antennae. The AAPM Report No. 26 'Performance Evaluation of Hyperthermia Equipment' describes how an array can be evaluated, but it does not provide information on minimum required quality aspects. Since the performance of antennae in an array cannot generally be reflected by the superposition of a single antenna SAR distribution because of cross-coupling or other side effects (Gopal *et al.* 1992, Lumori *et al.* 1990b, Rietveld *et al.* 1998a) we believe that:

- the EFS from one antenna is not satisfactory as basic parameter in evaluating an array,
- the PD gives only very local information about an array i.e. *the* maximum depth of 50% SAR under 1 cm depth in muscle-equivalent tissue,
- the array must be evaluated as an intact unit (as suggested in the AAPM report No. 26 and the ESHO guidelines (Hand *et al.* 1989)) and
- insisting on 50 % SAR as an indicator of quality may be too strict a norm since Lee *et al.* (1998) and Myerson *et al.* (1990) have reported that the 25% SAR coverage is a prospective indicator which is correlated to clinical outcome.

Furthermore, Gelvich *et al.* (1996) have studied homogeneity of SAR distributions which were based on both 75% and 25% SAR levels. For these reasons, we have evaluated the SAR distributions from the arrays on 75%, 50% and 25% SAR levels with the restriction of equal powering of all antennae in the array.

We introduced the SAR-volume histogram, which takes the whole volume under the antenna array into account as a more global measure for the PD of an array of antennae. To enable comparison between the D-CSA array and LCA array SAR-volume histograms, the volumes are given as a percentage of the total volume. The 3 cm depth that we used was chosen rather arbitrarily but covers the maximum depth for which (incoherently driven) superficial antennae can be used.

Acknowledgements

References

Bach Andersen, J., Baum, A., Harmark, K., Heinzl, L., Raskmark P. and Overgaard, J., 1984, A hyperthermia system utilizing a new type of inductive applicator. *IEEE Transactions on Biomedical Engineering*, 31, 21-27

Diederich, C.J., and Strauffer, P.R., 1993, Pre-clinical evaluation of a microwave planar array applicator for superficial hyperthermia. *International Journal of Hyperthermia*, 9, 227-246

Gelvich, E.A., Mazokhin, V.N. and Troshin, I.I., 1996, An attempt at quantitative speculation of SAR distribution homogeneity. *International Journal of Hyperthermia*, 12, 431-436

Gopal, M.K., Hand, J.W., Lumori, M.L.D., Alkairi, S., Paulsen, K.D. and Cetas, T.C., 1992, Current sheet applicator arrays for superficial hyperthermia of chestwall lesions. *International Journal of Hyperthermia*, 8, 227-240

Guy, A.W., 1971, Analyses of electromagnetic fields induced in biological tissues by thermographic studies on equvalent phantom models. *IEEE Transactions on Microwave Theory and Techniques*, 19, 205-214

Hand, J.W. and Hind, A.J., 1986, A review of microwave and RF applicators for localized hyperthermia. *Physical Techniques in Clinical Hyperthermia*, edited by J.W. Hand and J.R. James, (New York and Chichister: Wiley), pp.98-148

Hand, J.W., Lagendijk, J.J.W., Bach Andersen, J. and Bolomey, J.C., 1989, Quality assurance guidelines for ESHO protocols. *International Journal of Hyperthermia*, 5, 421 – 428

Heinzl, L., Hornsleth, S.N., Raskmark, P. and Andersen, J.B. , 1990, Electromagnetic applicators, *An Introduction to the Practical Aspects of Clinical Hyperthermia*, edited by S.B. Field and J.W. Hand, (London, New York, Philadelphia: Taylor & Francis), pp.275-304

Johnson, R.H., Preece, A.W., Hand, J.W., James, J.R., 1987, A new type of lightweight low-frequency electromagnetic hyperthermia applicator. *IEEE Transactions on Microwave Theory and Techniques*, 35, 1317-1321

Johnson, R.H., Preece, A.W. and Green, J.L., 1990, Theoretical and experimental comparison of three types of electromagnetic hyperthermia applicator. *Physics in Medicine and Biology*, 35, 761-779

Lee, E.R., Wilsey, T.R., Tarczy-Hornoch, P., Kapp, D.S., Fessenden, P., Lohrbach, A. and Prionas, S.D., 1992, Body conformable 915 MHz microstrip array applicators for large surface area hyperthermia. *IEEE Transactions on Biomedical Engineering*, 39, 470-483

Lee, H.K., Antell, A.G., Perez, C.A., Straube, W.L., Ramachandran, G., Myerson, R.J., Emami, B., Molmenti, E.P., Bucker, A. and Lockett, M.A., 1998, Superficial hyperthermia and radiation for recurrent breast carcinoma of the chest wall: prognostic factors in 196 tumors. *International Journal of Radiation Oncology, Biology, Physics*, 40, 365-375

Leigh, B.R., Stea, B., Cassady, J.R., Kittelson, J. and Cetas, T.C., 1994, Clinical hyperthermia with a new device: the current sheet applicator. *International Journal of Radiation Oncology, Biology, Physics*, 4, 945-951

Lumori, M.L.D., Hand, J.W., Gopal, M.K., and Cetas, T.C., 1990a, Use of Gaussian beam model in predicting SAR distributions from current sheet applicators. *Physics in Medicine and Biology*, 35, 387-397

Lumori, M.L.D., Hand, J.W., Prior, M.V., Gopal, M.K., Cetas, T.C., 1990b, Gaussian beam optimization of bolus thickness and inter-element spacing of current sheet applicator arrays. *Strahlentherapie und Onkologie*, 8, 524.

Myerson, R.J., Perez, C.A., Emami, B. Straube, W., Kuske, R.R., Leybovich, L. and Von Gerichten D., 1990, Tumor control in long-term survivors following superficial hyperthermia. *International Journal of Radiation Oncology, Biology, Physics*, 18, 1123-1129

Prior, M.V., Lumori, M.L.D., Hand, J.W., Lamaitre, G. Schneider, J., and Van Dijk, J.D.P., 1995, The use of a Current Sheet Applicator Array for Superficial Hyperthermia: Incoherent Versus Coherent Operation. *IEEE Transactions on Biomedical Engineering*, 42, 694-698

Rietveld, P.J.M., Lumori, M.L.D., Hand, J.W., Prior, M.V., Van der Zee, J. and Van Rhoon, G.C., 1998a, Effectiveness of the Gaussian beam model in predicting SAR distributions from the lucite cone applicator. *International Journal of Hyperthermia*, 14, 293-308

Rietveld, P.J.M., Lumori, M.L.D., Van der Zee, J., and Van Rhoon G.C., 1998b, Quantitative evaluation of 2x2 arrays of Lucite cone applicators in flat layered phantoms using Gaussian-beam-predicted and thermographically measured SAR distributions. *Physics in Medicine and Biology*, 43, 2207-2220

Rietveld, P.J.M., Van Putten, W.L.J., Van der Zee, J. and Van Rhoon, G.C., 1999, Comparison of the clinical effectiveness of the 433 MHz lucite cone applicator with that of a conventional waveguide applicator in applications of superficial hyperthermia. *International Journal of Radiation Oncology, Biology and Physics*, 43, 681-687

Rossetto F, Stauffer, P.R., 1999, Effect of complex bolus-tissue load configurations on SAR distributions from dual concentric conductor applicators. *IEEE Transactions on Biomedical Engineering*, 46, 1310-1319

Ryan T.P., Backus, V.L. and Coughlin, C.T., 1995, Large stationary microstrip arrays fpr superficial microwave hyperthermia at 433 MHz: SAR analysis and clinical data. *International Journal of Hyperthermia*, 11, 187-209

Samulski, T.V., Fessenden, P., Lee, E.R., Kapp, D.S., Tanabe, E. and McEuen, A., 1990, Spiral microstrip hyperthermia applicators: technical design and clinical performance. *International Journal of Radiation Oncology, Biology and Physics*, 18, 233-242

Stauffer, P.R.,Rossetto, F., Leoncini, M., Biffi Gentilli, G., 1998, Radiation patterns of dual concentric conductor microstrip antennas for superficial hyperthermia. *IEEE Transactions on Biomedical Engineering*, 45, 605-613

Tharp, H.S. and Roemer, R.B., 1992, Optimal power deposition with finite-sized, planar hyperthermia applicator arrays. *IEEE Transactions on Biomedical Engineering*, 39, 569-579

Van der Zee, J., Van der Holt, B., Rietveld, P.J.M., Helle, P.A., Wijnmaalen, A.J., Van Putten, W.L.J. and Van Rhoon, G.C., 1999, Reirradiation combined with hyperthermia in recurrent breast cancer results in a worthwhile local palliation. *British Journal of Cancer*, 79, 483-490

Van Rhoon, G.C., Rietveld, P.J.M. and Van der Zee, J., 1998, A 433 Mhz Lucite Cone waveguide applicator for superficial hyperthermia. *International Journal of Hyperthermia*, 14, 13 - 28

Zhou, L. and Fessenden, P., 1993, Automation of temperature control for large-array microwave surface applicators, *International Journal of Hyperthermia*, 9, 479-490

Comparison of the clinical effectiveness of the 433 MHz Lucite Cone Applicator with that of a conventional waveguide applicator in applications of superficial hyperthermia

PJM Rietveld, WLJ van Putten, J van der Zee and GC van Rhoon

ELSEVIER

PII S0360-3016(98)00443-X

PHYSICS CONTRIBUTION

COMPARISON OF THE CLINICAL EFFECTIVENESS OF THE 433 MHz LUCITE CONE APPLICATOR WITH THAT OF A CONVENTIONAL WAVEGUIDE APPLICATOR IN APPLICATIONS OF SUPERFICIAL HYPERTHERMIA

PAUL J. M. RIETVELD, M.SC.,* WIM L. J. VAN PUTTEN, M.SC.,† JACOBA VAN DER ZEE, M.D., PH.D.,* AND GERARD C. VAN RHOON, PH.D.*

*Department of Radiation Oncology, Subdivision of Hyperthermia, and †Department of Statistics, University Hospital Rotterdam–Daniel den Hoed Cancer Center/Dijkzigt Hospital, Rotterdam, The Netherlands

Purpose: This report presents the final stage of our program to improve the quality of our superficial hyperthermia treatments. We have already demonstrated that the Lucite cone applicator (LCA), our technically improved water-filled, wave-guide applicator (WGA), is superior to the conventional WGA. The main objective of the present study was to investigate whether the technical improvements of a WGA were reflected in an improved clinical performance, e.g., a better temperature distribution.

Methods and Materials: Power and temperature analyses were performed retrospectively on 128 treatments of superficially located tumors (less than 4 cm depth). Twenty-three patients were treated alternately with a WGA setup and a LCA setup.

Results: The average power level per antenna in an array was 48 W and 62 W for the WGA and LCA respectively. The average invasively measured temperatures increased by $0.27°C$ when the LCAs were used. The temperature difference between the center and the periphery of an antenna, averaged over the complete array of antennae, was $0.43°C$ using WGAs and $-0.05°C$ using LCAs indicating a more uniform heating. The T_{90} of the invasively measured temperatures remained unchanged (WGA: $39.4°C$ versus LCA: $39.5°C$). .

Conclusion: The LCA is now our standard applicator for superficial hyperthermia treatments as it is technically and clinically proven to be superior to the WGA. © 1999 Elsevier Science Inc.

Superficial hyperthermia, Microwave antenna, Thermal dosimetry, Clinical study.

INTRODUCTION

Since 1985 we have used a conventional 433 MHz water-filled, wave-guide applicator (WGA) with aperture sizes of 5×5 cm², 5×10 cm², 7.5×10 cm², and 10×10 cm² for the clinical application of superficial hyperthermia (maximum depth 4 cm). The majority of our patients are treated with superficial hyperthermia in addition to reirradiation for recurrent breast cancer. The treatment surfaces of these patients vary from 64 cm² to 800 cm² with a mean of 316 cm². When hyperthermia is applied in combination with reirradiation, the department's strategy is to heat the entire radiation treatment field. This means that the majority of these patients are treated with an array of applicators, the number of applicators varying from 1 to 6. The combined treatment modality of reirradiation (8×4 Gy in 4 weeks)

and hyperthermia (following each fraction for a duration of 60 minutes) has resulted in good clinical results in this patient group. The overall probability of complete response (CR) is 74% which is higher than the results following 30–40 Gy of radiation alone (20–48% CR) (1). However, in larger tumors (maximum diameter > 3 cm) a significantly lower CR rate was observed (65%) compared to smaller tumors (maximum diameter < 3 cm: 87%) (2, 3). Although it is known that larger macroscopic tumor volumes are negatively correlated with treatment outcome (4, 5), we hypothesize that due to the intrinsic small effective field size[1] (EFS) of the WGA, the larger treatment fields have been treated with a lower hyperthermic quality (2, 6) and therefore we expect that the current clinical results can be improved by using a higher technical quality of specific absorption rate (SAR) distributions, i.e., Lucite cone applicator (LCA) arrays.

[1] The EFS is defined as the area enclosed by the 50% specific absorption rate (SAR) contour measured at a depth of 10 mm from the surface of a plane homogeneous phantom with the dielectric properties of muscle.
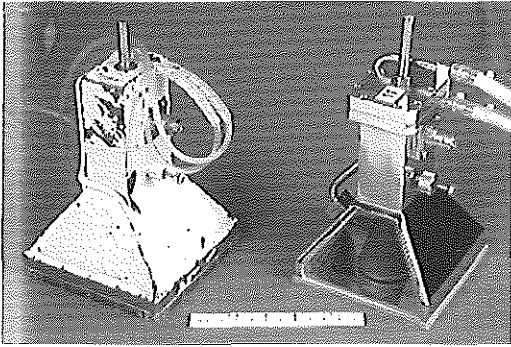
Fig. 1. Photograph of the conventional water-filled wave-guide applicator (left) and Lucite cone applicator (right). Both antennae have a radiating aperture of 10×10 cm².

In order to improve the technical quality of SAR distributions, we developed the LCA which is technically superior to the WGA and has an EFS of approximately 100 cm² (7–9) compared to 33 cm² for the WGA. In array configurations, the EFS is contiguous using LCAs as opposed to four local hot spots when using WGAs (6). Based upon this higher EFS value of the LCA, we expect that LCA arrays will heat the treatment area more homogeneously than WGA arrays and that the average temperature will increase. However, given the fact that a temperature distribution is greatly influenced by tissue irregularities and blood flow characteristics and given the good clinical results obtained with the WGA (10), we decided to quantitatively assess whether the LCA arrays would indeed perform better than WGA arrays under clinical conditions.

Therefore a clinical study was performed in which the same patient was treated alternately by WGA and LCA arrays. In this way a comparison could be made on power delivery and achieved temperatures between the two antenna types. Twenty-three patients with superficially located tumors were entered in this study.

It will be shown that the LCA is a better antenna than the WGA concerning invasively measured temperature (0.27°C) and that average temperature differences between the central area and periphery under the antennae decreased to zero when LCAs were used.

METHODS AND MATERIALS

Antennae

Both antennae, the conventional WGA and the LCA, operate in TE_{10} mode at 433 MHz and are water-filled. Both radiating apertures measure 10×10 cm². Figure 1 shows a photograph of both antennae.

The first part, that is the dipole, of the antennae are identical and measures 3.0 cm by 5.0 cm ($E \times H$). The second part of each antenna starts at approximately ½ lambda from the dipole. From this level, the wave-guide

cross-section diverges to the radiating aperture of 10×10 cm². The outer dimensions of the antennae are 11×11 cm² for the WGA and 10.5×10.5 cm² for the LCA. In case of the WGA the sidewalls are brass, as in the first part of the antenna. In case of the LCA, the two diverging sidewalls, which are parallel to the E-field, are replaced by Lucite. Further a polyvinyl chloride (PVC) cone (base diameter 3 cm, height 5 cm) is introduced into the center of the aperture.

Both modifications to the conventional WGA resulted in an EFS of 100 cm² (8×13 cm², $E \times H$ direction) for the LCA compared to an EFS of 33 cm² (8×5 cm², $E \times H$ direction) for the WGA. In any configuration of an LCA array, the EFS is a contiguous area whereas WGAs in an array configuration only produce local hot spots. The physical performance of both antenna types has been reported in detail elsewhere (6, 7, 9).

The efficiency of both antenna types is in the range of 45–55%.

Temperature recording

A 24-channel fiber optic thermometry system (Takaoka FT1210) was used to measure temperatures superficially or invasively. The temperature probes are immune to RF radiation and the probes are sequentially scanned. The average measuring time per channel is 3.3 seconds and an update of all 24 channels is given each 80 seconds. The technical performance under clinical conditions are (temperature range 30–45°C): resolution 0.1°C, accuracy 0.2°C. Multipoint probes have up to 4 measuring points with an interelement spacing of 10, 15, or 20 mm. Probes were placed invasively within a closed-tip catheter.

The average number of thermometry sites per treatment in this study was 21.0, of which 10.0 were invasive (5.1 sites in macroscopic tumor tissue and 4.9 in other tissue).

Power deliverance and recording

Each antenna is powered by a single RF generator (150 W max), therefore in an array application, the antennae are driven incoherently. After each optimization during treatment, the forward and reflected power level per antenna, as indicated by the generator, are manually recorded. In order to analyze power level data, the power levels as registered at each 5 minute-interval during steady state (i.e., more than 10 minutes treatment time), were copied into a unique patient- and treatment-related ASCII file.

Clinical procedures during hyperthermia treatments

Before the first hyperthermia (HT) treatment starts, the physician and physicist decide: (a) where invasive thermometry is possible and preferable and (b) the optimal antenna configuration for both WGA and LCA applications. Closed-tip catheters are positioned invasively and remain in place during the entire HT series (11). Information on thermometry sites concerning the location in the treatment field, tissue type, and depth, is documented (12). After each treatment the clinical team evaluates the treatment using the

available temperature data and dose parameters and if necessary, the clinical setup is adapted.

In the first half of the week WGAs were used and in the second half of the week LCAs were used during HT treatments. The start of a treatment series was dictated by the department's time schedule and can be considered as random. The first treatment is default started with 50 W forward power per antenna in order to learn the patient's characteristics, e.g., what temperature rise is obtained by the applied power level and how the patient reacts to the heat load. If possible the power level is increased gradually during the treatment. Since the two antenna types are used alternately and might behave differently, the second treatment in this study, which is performed with the other applicator type, is administered as if it were a first treatment. From the third treatment on, the power level settings at the beginning of each treatment are adjusted to the power levels used in the previous treatment of that antenna type.

During treatment, the hyperthermia technicians performed the normal procedures in order to optimize the treatment and to react to treatment-related information from patient and hardware. On indication of patient discomfort, pain and/or achieved temperatures, the E-field orientation of individual antennae, power distribution, antenna positioning and tilt, water bolus thickness, and water bolus temperature were changed according to the technician's experience. This was done regardless of the applicator type used and was permitted in order to achieve the highest quality of treatment. Changes in antenna setups (e.g., E-field orientation) during treatment were recorded but left out of the analyses.

Treatment characteristics

All patients received radiotherapy (RT) in combination with HT. The total RT dose (32 Gy) was administered as 8×4.0 Gy per treatment twice a week, Monday-Thursday or Tuesday-Friday. Each RT fraction was followed by a HT treatment with an average interval of 40 minutes. The combined treatment series started any of these 4 days. The HT treatments lasted 60 minutes.

Depending on the dimensions of the treatment area, the optimum number of antennae to be used during HT treatments was decided upon. The number of antennae in this study ranged from 1 to 5. When using WGAs, a 7.5×10 cm^2 aperture antenna also was available and was used to optimize the WGA treatment when necessary. In the LCA treatments only 10×10 cm^2 aperture sized antennae were available. In some cases a 2×2 array of WGAs was used whereas only a 2×1 array of LCAs was applied to have an optimal SAR coverage of the treatment area.

All patients were clearly informed about the nature of the clinical study and they gave informed consent to participate in this study.

Quantification of treatment parameters

Power level variables. Per treatment the net power per antenna was calculated during steady state. Per time recording (each 5 minutes), the standard deviation over the net

(A)   (B)   (C)
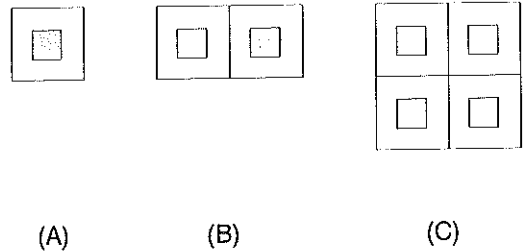
Fig. 2. Schematic diagram of a 1×1, 2×1, and 2×2 array of LCA indicating the areas "center" and "periphery". Each center area measures 6×6 cm^2 and is indicated by the shaded square.

powers was calculated. From these parameters, the average net power level over all antennae was calculated (P_{avg}) and the average standard deviation in time (P_{SD}) was calculated. P_{avg} expresses the deposited energy in the treatment volume and P_{SD} is a measure for the homogeneity in power levels over the entire treatment volume.

Temperature variables. Only invasively measured temperatures were included in the analyses since superficially measured temperatures are influenced by water bolus temperatures (13). In order to have the most useful temperature information during a treatment, the position of the temperature probes could change from treatment to treatment as a result of experience obtained during a former treatment and as a consequence, the number and/or position of invasively measured tissue temperatures per treatment series could vary. In all cases an optimized distribution of multipoint probes was used to have maximum invasive thermometry. Since the entire treatment area is considered at risk, no discrimination was made between temperature probe locations in invasive macroscopic tumor sites and other invasively measured locations.

For quantitatively technical comparison of the homogeneity of the temperature distributions obtained by WGA and LCA, the aperture of each antenna was divided in two regions. The *center* region measured 6×6 cm^2 and is located centrally under the aperture (approximately the dimensions of the EFS of the WGA); the remaining region of the aperture is named *periphery*. In this way an overall treatment area built with n antennae was divided into $n + 1$ regions (Fig. 2). Two corresponding temperature parameters were defined: the average invasive center located temperature (T_c) and the average invasive periphery located temperature (T_p) which were calculated during steady state of a HT treatment. The data were obtained by labeling the tissue-indicator of each invasive temperature site in the temperature files. The difference between these two parameters T_c and T_p expresses the homogeneity in the temperature distribution under the evaluated array.

For further clinically relevant evaluation of a HT treatment, the average temperature (T_{avg}) over all invasive temperature probes recorded during steady state and the T_{90}, i.e.

Table 1. Overview of number of patients, number of treatment series, and number of treatments as a function of treatment series

No. of treatment series *n*	No. of patients in *n* series *p*	Total no. of series *n×p*	Total no. of treatments
1	16	16	107
2	6	12	88
3	1	3	24
Total	23	31	219

the 10th centile of all invasive temperature recordings during steady state, were calculated.

Statistical setup and exclusion criteria. Twenty-three patients entered the study, of whom six patients received two series of treatments and one patient received three treatment series on separate areas (Table 1). In 10 series the number of HT treatments was less than 8 (range: 3–7 treatments; median 4.5). In total 31 series containing 219 treatments were entered in the study.

A series of exclusion criteria had to be met to enter the analyses of the study (Table provides an overview). From all 219 treatments evaluated (i.e., 219 records), 90 were performed with the WGAs, 118 were performed with the LCAs, and 11 treatments were performed with a mix of WGAs and LCAs. The mixed-antenna treatments were excluded from the analyses (208 records left). The average input power and invasive temperature showed a significant correlation ($p = 0.025$, by analysis of variance [ANOVA]) with the treatment number. All statistical analyses were performed with Stata 5.0 (Stata Corporation, College Station, TX). After excluding the first two treatments from the analysis, this trend disappeared ($p = 0.3$) and 151 records were left. Four treatments (in the range of 3rd–8th treatment) were excluded from analyses due to a lack of invasive thermometry (147 records left).

Table 2. Overview of effect of exclusion criteria* on number of evaluable treatments and series[†]

No.	Exclusion criterion	No. excl. trtments	No. excl. series
1	Mixed LCA-WGA antenna treatments	11	0
2	Treatment number 1 and 2	57	0
3	No invasive thermometry	4	1
4	Lack of WGA and LCA treatments in a series of 3rd to 8th treatment	19	8
Total		91	9

* The number of excluded treatments and series as given in the table are taken from the (sub)set of still included treatments and series. For example exclusion of treatment 1 and 2 in originally 31 series results in only 57 excluded treatments because the first applied exclusion criterion excluded already 5 treatments 1 or 2.
[†] Originally 31 series containing 219 treatments were entered into the study.

In order to be able to analyze differences between the two antenna types using a patient as his or her own reference, each patient had to be treated at least four times including two WGA and two LCA treatments since the first two treatments were excluded from the analyses. This criterion excluded 8 series with a total of 19 treatments from the analysis resulting in 128 evaluable records. From the total set of 219 treatments in 31 series, 128 treatments (59 WGA and 69 LCA treatments) in 22 series passed the exclusion criteria. The 22 series were obtained from 16 patients.

From this final set of 128 treatments, four treatments (2 LCA and 2 WGA treatments) were stopped after less than 60 minutes treatment time. Reasons for this premature stop were: general discomfort and pain of the patient (2) and technical problems (2). From the final data set, several parameters were calculated. Per treatment series and per antenna type (x), with x equal to LCA or WGA, the $P_{avg}(x)$, $P_{SD}(x)$, $T_{avg}(x)$, $T_c(x)$, $T_p(x)$, and $T_{90}(x)$ were calculated as the average of the corresponding parameter per treatment series as previously defined under "Power level variables" and "Temperature variables." Nine treatments did not have "center" thermometry sites and one treatment did not have a "periphery" thermometry site. This resulted in an average temperature difference dT_{cp} ($= T_c - T_p$) calculated over 118 records.

The average number of antennae used was 4.02 (SD: 1.03) for the WGA and 3.79 (SD: 1.27) for the LCA.

Statistical analysis consisted of the calculation of means and standard deviations over patients of the parameters per antenna type and their paired differences. Analysis of variance was applied to test for differences between the two antenna types in the distribution of the parameters per treatment. In this analysis treatment parameters, for example the T_{avg} of the treatment, were used as dependent variables, while patient and antenna type were included as categorical covariates.

RESULTS

The power and thermal dose parameters averaged over all treatment series per antenna type are shown in Table 3. The corresponding parameter differences per antenna type are also shown in Table 3 as well as their statistical *p*-values obtained from ANOVA.

The average power output of the LCA was statistically significantly higher than the output of the WGA. No difference was observed in the variation in an array of the output power. The average invasive temperature, using the LCA, was 0.28°C higher than under the WGA ($p = 0.004$), which was primarily due to higher peripheral temperatures T_p. No difference in centrally located invasive temperatures (T_c) was observed.

DISCUSSION AND CONCLUSION

The relationship between SAR and any thermal dose parameter is still a complicated matter and subject of dis-

Table 3. Overview of calculated power and temperature related dose parameters*

	WGA		LCA		Difference LCA-WGA		
	Mean	SD	Mean	SD	Mean	SD	p-Value
P_{avg} (W)	48	12	62	15	14	9	<0.0001
P_{SD} (W)	14.4	5.7	16.4	8.7	4	14	0.18
T_{avg} (°C)	40.90	0.69	41.17[†]	0.55	0.28	0.4	0.004
T_c (°C)	41.26	0.64	41.20	0.59	−0.03	0.6	0.8
T_p (°C)	40.77	0.81	41.20	0.70	0.43	0.5	0.0006
dT_{cp} (°C)	+0.43	0.92	−0.05	0.96	−0.49	0.7	0.005
T_{90} (°C)	39.44	0.77	39.54	0.73	0.10	0.6	0.46

* The average values were calculated over the treatment series per antenna type.
[†] The average invasively measured temperature for LCA treatments (T_{avg} 41.17 °C) is 0.03 °C lower than both corresponding T_c and T_p. This artefact is caused by lack of either T_c or T_p sites in 10 treatments.

cussion (14–17). In fact, literature concerning clinical evaluation of the dose–effect relations of hyperthermia provides a broad field of treatment-related parameters which all correlate more or less with CR or other defined endpoints (4, 14, 16–24). Hyperthermic quality expressed in terms of dose parameters is not defined yet (25).

The question whether the technical superior LCA will result in better clinical outcomes of the HT treatment series can only be conclusively demonstrated in a randomized prospective study. Since the CR rate is already in the range of 70–90% (2, 3) for combined reirradiation plus HT, it is statistically not likely that such a study with the current patient accrual (40–50/yr) can be finished successfully in an appropriate time scale (< 5 years).

In this study we are not primarily interested in a correlation between clinical outcome and antenna type used, therefore we concentrate only on basic treatment parameters as a function of antenna type used to quantitatively evaluate the effect of an increased EFS of the LCA under clinical conditions. Firstly the power-related parameters P_{avg} and P_{SD} are discussed and secondly the temperature-related parameters are discussed.

Evaluation of power-related parameters

Average power (P_{avg}). Although net power (P_{avg}) as a hyperthermic parameter does not contain any biological or clinical input except for patient tolerance, it is a simple variable to relate to SAR distributions (or EFS). If the EFS is small, the antennae will effectively heat only a small volume under the aperture. An increased EFS results in a smaller derivative of the SAR as a function of position x in the horizontal plane (dSAR/dx). Furthermore, the absolute maximum SAR level is dictated only by a small volume element under the antenna where either a maximum tolerable temperature is measured or the patient feels a pain sensation. Both antenna types have centrally located maximum SAR, therefore we think that the absolute maximum

SAR level is more patient/treatment-area-dependent than antenna-dependent. So, in a particular treatment area the 100% SAR in the relative SAR distributions from WGA and LCA will have about equal magnitude.

A positive correlation between P_{avg} and a SAR distribution (or EFS) is probable, because the LCA has a smaller dSAR/dx, and thus an overall higher energy deposition (as indicated by P_{avg}) can be delivered to the target volume under the antenna aperture. This effect is counteracted by the following factors: (1) local tissue properties: an increased energy deposition in areas where the WGA does not heat adequately can also lead to additional hot spots when the LCA is used and may cause additional limiting power depositions in those cases where LCAs are used, which are not present for WGAs; and (2) preheating of peripheral incoming blood can create an additional temperature rise in the center region of the aperture (26, 27). Although the EFS of the LCA is roughly threefold the EFS of the WGA, the combination of above-mentioned negative side effects resulted only in a significant 14 W power increase for LCA arrays (30%), 62 W versus 48 W for the WGA applications.

Homogeneity in power settings (P_{SD}). The homogeneity in power levels in an array application, as expressed by the standard deviation of power levels in an array, P_{SD}, did not change significantly as a function of antenna type (14.4 W versus 16.4 W for WGA and LCA treatments respectively). We expected that by using the LCAs the chance of creating hot spots would be diminished because the range of percentage SAR in the treatment area is smaller. This assumption was based on Gaussian beam predictions of SAR distributions from arrays of WGAs and LCAs (6). Although in an array of LCAs a contiguous EFS is feasible (by applying an equal power over the antennae) (6), local power steering remained a necessity in order to optimize the hyperthermia treatment. Anticipation on (dynamic) local tissue characteristics (e.g., blood flow and electromagnetic properties) had a strong impact on power settings independent of the antenna type used.

Evaluation of invasively measured temperature-related parameters

Tissue characteristics make the influence between a SAR and its corresponding temperature distribution a dynamic process which is still unpredictable in its development (28, 29). However, it is unlikely that an increased tissue temperature will result in a decreased hyperthermic effect (19), therefore we assume that improvement of the technical quality of a HT treatment (when using technically improved antennae) can also be tested by analyzing temperature-related variables.

Average temperature (T_{avg}). The average invasive temperature increased from 40.9°C for the WGA to 41.2°C when the LCA was used. Although this improvement may seem small from a clinical point of view, in the restricted setup of this study where the technical improvements were investigated clinically, it is statistically significant. More

detailed analyses (not presented in this paper) did not reveal any additional understanding of this minor increase in invasive temperature in relation to the major increase in EFS.

Temperature difference between center (T_c) and periphery (T_p) of the aperture. The small EFS of the WGA results in a hot spot located in the center region of the antenna. If the WGA is used in an array application, there are no significant overlapping SAR levels at the periphery of each aperture including the aperture periphery located in the center of the 2 × 2 array (6). A difference in dT_{cp} is expected for the WGA and LCA because the EFS of the LCA in an array application covered almost the entire outside contour of the 2 × 2 array and has a local SAR dip of 50–80% SAR at the center of the 2 × 2 array (6). For that reason, the periphery region located in the center of an array is not treated as a separate region.

In the clinical application of the LCA, the difference between temperatures (dT_{cp}) measured over the center region and periphery region of an array of antenna (Fig. 2) is about zero for the LCA, whereas in case of the WGA the center regions under the antennae reach a 0.43°C higher temperature than the periphery (Table 3). The average temperature in the center region of the aperture, the region of highest SAR levels for both antenna types, remained unchanged as a function of antenna type used (-0.03°C, $p = 0.8$) and therefore, with the increase of average peripheral temperatures in case the LCAs were used, the unchanged T_{90} (39.44°C [WGA] and 39.54°C [LCA]) can only be explained by a minimum peripheral temperature during treatment measured at a peripheral local volume element that could not be heated properly with either WGA or LCA. Since the T_{90} is more dependent on the location of the thermometry site, we think it is a less relevant thermal parameter in investigating a technical improvement than the invasive temperature.

The results obtained from these analyses have led us to the conclusion that use of the LCA in treatments of breast cancer with superficial hyperthermia does give a slightly better invasive temperature in the treatment area without any negative side effects. For that reason the LCA is now used as our standard antenna in the treatment of superficial hyperthermia.

REFERENCES

1. Van der Zee J, Vernon CC. Thermotherapy for advanced and recurrent breast tumors. In: Seegenschmiedt MH, Fessenden P, Vernon CC, editors. Thermoradiotherapy and thermochemotherapy. Volume 2: Clinical applications. Berlin: Springer-Verlag; 1995. p. 35–48.
2. Van der Zee J, Van Rhoon GC, Verloop-van 't Hof EM, Van der Ploeg SK, Rietveld PJM, van den Berg AP. The importance of adequate heating techniques for therapeutic outcome. In: Gerner EW, Cetas TC, editors. Proceedings Hyperthermic Oncology 1992, Volume 2. Tucson, Arizona; 1992. Arizona Board of Regents. p. 349–352
3. Van der Zee J, Van der Holt B, Rietveld PJM, Helle PA, Wijnmaalen AJ, Van Putten WLJ, Van Rhoon GC. Reirradiation combined with hyperthermia in recurrent breast cancer results in a worthwhile local palliation. Br J Cancer. In press.
4. Hand JW, Machin D, Vernon CC, Whaley JB. Analysis of thermal parameters obtained during Phase III trials of hyperthermia as an adjunct to radiotherapy in the treatment of breast carcinoma. Int J Hyperther 1997;13:343–364.
5. Vernon CC, Hand JW, Field SB, Machin D, Whaley JB, Van der Zee J, Van Putten WLJ, Van Rhoon GC, Van Dijk JDP, González D, Liu F-F, Goodman P, Sherar M. Radiotherapy with or without hyperthermia in the treatment of superficial localized breast cancer: Results from five randomized controlled trials. Int J Radiat Oncol Biol Phys 1996;35:731–744.
6. Rietveld PJM, Lumori MLD, Van der Zee J, Van Rhoon GC. Quantitative evaluation of 2 × 2 arrays of Lucite cone applicators in flat layered phantoms using Gaussian beam predicted and thermographically measured SAR distributions. Phys Med Biol 1998;43:2207–2220.
7. Rietveld PJM, Lumori MLD, Hand JW, Prior MV Van der Zee J, Van Rhoon GC. Effectiveness of the Gaussian beam model in predicting SAR distributions from the Lucite Cone Applicator. Int J Hyperther 1998;14:293–308.
8. Van Rhoon GC, Rietveld PJM, Broekmeyer-Reurink MP, Van der Zee J. 1992, A 433 MHz waveguide applicator system with an improved effective field size for hyperthermia treatment of superficial tumors at the chest wall. In: Gerner EW, Cetas TC, editors. Proceedings Hyperthermic Oncology 1992, Volume 2. Tucson, Arizona; Arizona Board of Regents 1992. p. 187–190.
9. Van Rhoon GC, Rietveld PJM, van der Zee J. A 433 MHz Lucite cone waveguide applicator for superficial hyperthermia. Int J Hyperther 1998;14:13–27.
10. Van der Zee J, Treurniet-Donker AD, The SK, Helle PA, Seldenrath JJ, Meerwaldt JH, Wijnmaalen AJ, Van den Berg AP, Van Rhoon GC, Broekmeyer-Reurink MP, Reinhold HS. Low dose reirradiation in combination with hyperthermia: A palliative treatment for patients with breast cancer recurring in previously irradiated areas. Int J Radiat Oncol Biol Phys 1988;15:1407–1413.
11. Van der Zee J, Van Rhoon GC, Broekmeijer-Reurink MP. Reinhold HS. The use of implanted closed-tip catheters for the introduction of thermometry probes during local hyperthermia treatment series. Int J Hyperther 1987;3:337–345.
12. Broekmeyer-Reurink MP, Rietveld PJM, Van Rhoon GC, Van der Zee J. Some practical notes on documentation of superficial hyperthermia treatment. Int J Hyperther 1992;8:401–406.
13. Lee ER, Kapp DS, Lohrbach AW, Sokol JL. Influence of water bolus temperature on measured skin surface and intradermal temperatures. Int J Hyperther 1994;10:59–72.
14. Leopold KA, Dewhirst MW, Samulski TV, Dodge RK, George SL, Blivin JL, Prosnitz LR, Oleson JR. Cumulative minutes with T_{90} greater than temp$_{index}$ is predictive of response of superficial malignancies to hyperthermia and radiation. Int J Radiat Oncol Biol Phys 1993;25:841–847.
15. Myerson RJ, Perez CA, Emami B, Straube W, Kuske RR, Leybovich L, von Gerichten D. Tumor control in long-term survivors following superficial hyperthermia. Int J Radiat Oncol Biol Phys 1990;18:1123–1129.
16. Oleson JR, Dewhirst MW, Harrelson JM, Leopold KA, Samulski TV, Tso CY. Tumor temperature distributions predict hyperthermia effect. Int J Radiat Oncol Biol Phys 1989;16:559–570.
17. Oleson JR, Samulski TV, Leopold KA, Clegg ST, Dewhirst MW, Dodge RK, George SL. Sensitivity of hyperthermia trial outcomes to temperature and time: Implications for thermal goals of treatment. Int J Radiat Oncol Biol Phys 1993;25:289–297.
18. Engin K, Leeper DB, Tupchong L, Waterman FM. Thermoradiotherapy in the management of superficial malignant tumors. Clin Cancer Res 1995;1:139–145.

19. Field SB, Morris CC. The relationship between heating time and temperature: Its relevance to clinical hyperthermia. *Radiother Onc* 1983;1:179–186.

20. Kapp DS, Cox RS. Thermal treatment parameters are most predictive of outcome in patients with single tumor nodules per treatment field in recurrent adenocarcinoma of the breast. *Int J Radiat Oncol Biol Phys* 1995;33:887–899.

21. Lindholm CE, Kjellen E, Nilsson P, Weber L, Hill S. Prognostic factors for tumour response and skin damage to combined radiotherapy and hyperthermia in superficial recurrent breast carcinomas. *Int J Hyperther* 1995;11:337–355.

22. Nishimura Y, Hiraoka M, Mitsumori M, Okuno Y, Li YP, Masunaga S, Koishi M, Akuta K, Abe M. Thermoradiotherapy of superficial and subsurface tumours: Analysis of thermal parameters and tumour response. *Int J Hyperther* 1995;11:603–613.

23. Visser AG, Van Rhoon GC. Technical and clinical quality assurance. In: Seegenschmiedt MH, Fessenden P, Vernon CC, editors. Thermoradiotherapy and thermochemotherapy. Volume 1. Berlin: Springer-Verlag; 1995. p. 453–472.

24. Wust P, Stahl H, Dieckmann K, Scheller S, Loffel J, Riess H, Bier J, Jahnke V, Felix R. Local hyperthermia of N2/N3 cervical lymph node metastases: Correlation of technical/thermal parameters and response. *Int J Radiat Oncol Biol Phys* 1996;34:635–646.

25. Oleson JR. If we can't define the quality, can we assure it? *Int J Radiat Oncol Biol Phys* 1989;16:879–879.

26. Crezee J, Lagendijk JJW. Temperature uniformity during hyperthermia: The impact of large vessels. *Phys Med Biol* 1992;37:1321–1337.

27. Lagendijk JJW. The influence of blood flow in large vessels on the temperature distribution in hyperthermia. *Phys Med Biol* 1982;27:17–23.

28. Akyürekli D, Gerig LH, Raaphorst GP. Changes in blood flow distribution during hyperthermia. *Int J Hyperther* 1997;13:481–496.

29. Waterman FM, Nerlinger RE, Moylan III DJ, Leeper DB. Response of human tumor blood flow to local hyperthermia. *Int J Radiat Oncol Biol Phys* 1987;13:75–82.

Effectiveness of FDTD in predicting SAR distributions

from the lucite cone applicator

T Samaras, *Member IEEE*, PJM Rietveld and GC van Rhoon, *Member IEEE*

Abstract

The benefits of using superficial hyperthermia together with radiotherapy has long been proven for recurrent breast carcinomas. The lucite cone applicator (LCA) has been introduced by some hospital hyperthermia units for superficial treatments. It is characterized by a large effective field size (EFS). The modeling techniques used in the past for the study of this as well as other applicators used for superficial hyperthermia have failed to address the significance in clinical practice of some treatment parameters, like the dimensions of the waterbolus. In this work the Finite-Difference Time-Domain (FDTD) method is used for modeling the applicators. The numerical results are compared with thermographic measurements. The agreement between predicted and measured SAR distributions is very good. The use of the FDTD method is expected to promote the study of treatment specific factors and help improve future treatment quality.

I. INTRODUCTION

The International Collaborative Hyperthermia Group has clearly demonstrated the benefits of combining radiotherapy with hyperthermia against radiotherapy alone in the treatment of superficial breast cancer [1]. Since the publication of the results superficial hyperthermia has become a standard treatment modality in several institutes, especially for the treatment of chest wall recurrences of breast cancer. Although it was found that clinical outcome is related to thermal dose [2], it still remains unclear which of the physical parameters of the treatment can improve its quality and, therefore, its efficacy.

The main requirements which are put forward in the development of new systems for superficial hyperthermia are the achievement of a large effective field size (EFS[1]), sufficient penetration depth[2] and good spatial control. It is usually necessary to employ an array of applicators to fulfill the above requirements.

The lucite cone applicator (LCA) is a superficial hyperthermia applicator which offers a large EFS and can be used in an array configuration. Its efficiency has been confirmed both in technical [4] and in clinical [5] terms. The theoretical modeling of the applicator with the Gaussian beam model (GBM) has given very good agreement with the experimental results for some configurations [6], [7]. However, there are some drawbacks of this modeling technique in the case of the LCA: The GBM cannot take into account the finite size of the waterbolus which is placed between the applicator and the patient in order to couple the electromagnetic energy into the body and to control the skin temperature. Yet, the waterbolus seems to have a direct effect on the SAR (specific absorption rate) distribution [4] and, hence, the ability to model it is important. Another disadvantage of the GBM is that it cannot predict correctly the coupling between the applicators, when they are used in an array configuration [6], [7]. The above problems of GBM can be overcome, if electric field measurements are performed before modeling for every treatment configuration, but this is a cumbersome task. Finally, the GBM cannot deal with tissue inhomogeneities, which are present in the clinical situation.

In this work it will be shown that it is feasible to study theoretically both the LCA and the older applicators used for superficial hyperthermia with the finite-difference time-domain

---

[1] The effective field size is defined as the area which is enclosed within the 50% iso-SAR curve at 1cm depth inside the flat homogeneous phantom [3].

[2] The penetration depth is defined as the depth in the phantom at which the SAR becomes $1/e^2$ of its value at the surface of the phantom.

(FDTD) technique. This numerical method allows the use of a more realistic model, but is more expensive in computational resources compared to the GBM. The major advantage of the FDTD method is that it allows a 3-D analysis of the applicator configurations, without the need for time-consuming measurements. Quantities like the penetration depth and the EFS can directly be deduced from the calculated results. From the 3-D analysis we expect to gain a good insight in the significant parameters of the treatment leading to treatments of better quality.

II. MATERIALS AND METHODS

A. Lucite cone applicator (LCA)

The conventional applicator which has been used in the past for superficial hyperthermia consists of a water-filled rectangular waveguide which ends to a horn antenna. The waveguide is made of brass and operates at TE_{10} mode at 433MHz. The waveguide dimensions are 3cm × 5cm and the aperture size of the radiating antenna is 10cm × 10cm. The LCA is a modification of the conventional applicator: The two diverging metal walls of the horn antenna which are parallel to the electric field are replaced by lucite walls. Additionally, a PVC cone with a height of 5.5cm is inserted in the applicator at the center of the aperture.
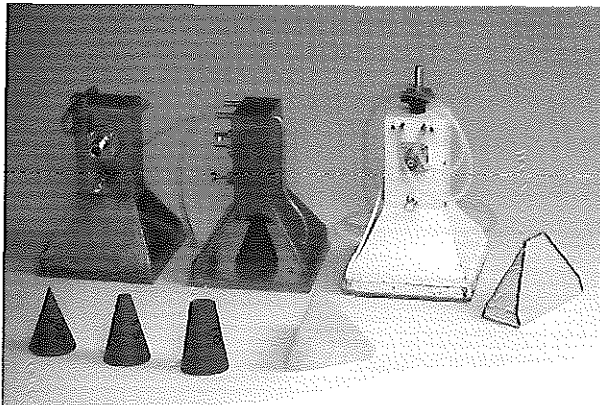

Fig. 1   Photograph of the various applicators: (left) the lucite applicator (LA) with the two
diverging walls of the horn antenna parallel to the electric field made of lucite;
(center) the lucite cone applicator (LCA) similar to the lucite applicator with a PVC
cone inserted in the center of the antenna; (right) the conventional applicator (CA)
made totally of metal.

Different cone angles have been tested and it was found that the angle of 15° gave the best results. The LCA is described extensively in [4]. The various applicators are shown in Fig. 1.

B. Electromagnetic modeling

The FDTD technique is used for modeling the LCA. The technique is well established in the field of biomedical applications of electromagnetic radiation [8], although most of the work performed with it in the area of hyperthermia concerns deep regional treatments.

The developed numerical model attempts to simulate the experimental set-up as closely as possible. The assumed electrical properties of the materials are shown in Table 1. The applicators are placed on top of a flat muscle-equivalent phantom constructed according to [9].

The size of the phantom used in the experimental measurements was $50 \times 50 \times 10cm^3$. However, the simulated phantom dimensions were chosen to be $38 \times 30 \times 14cm^3$, in order to reduce the computer memory requirements. The choice for these dimensions was based on the results presented in [6]. In this study it was shown that in a liquid muscle-equivalent phantom of almost the same size ($40 \times 32 \times 14cm^3$) the distribution measured with a scanning electric dipole under the aperture and at 1cm depth agrees with the measurements performed for the semi-solid phantom with the thermographic camera.

Table 1. Electrical properties of the materials used in the numerical calculations.

Material	ε_r	σ (S/m)
De-ionized water	76	0.001
Lucite	2.59	0.003
PVC	2.2	0.004
Muscle phantom	57	1.2

A uniform rectilinear mesh was used with a cell size of 0.2cm. The total size of the computational domain (including the applicator) was $190 \times 150 \times 225$ cells. The domain was terminated with Mur's second-order absorbing boundary conditions [10]. The applicators radiate mainly into the direction of the tissue-equivalent phantom which is made of a lossy material. The dimensions of the simulated phantom are large enough with respect to the

wavelength of the radiation in it to ensure that the largest part of the power reflected on the truncation planes will be dissipated on its way to the radiating aperture. Hence, the above boundary conditions are expected to be adequate in this case (see [11], [12]).

The metallic walls of the applicator were treated as perfect electric conductors (PEC's), so that the "diagonal split cell model" [8] could be used in a straightforward manner for the diverging metallic walls of the applicator which are oblique to the rectilinear mesh. This contour-path model is derived directly from Faraday's law and is simple to implement compared to the conformal modeling which had been used in other works for horn antennas [13]. The simulations have shown that even this simple modification for the metallic walls gave better numerical results than the "staircasing" approach, which was, however, retained for the lucite walls and the PVC cone.

The excitation was modeled by a group of co-linear electric field components which connect the lower metal wall of the waveguide with the end of the feeding pin. A sinusoidal signal at 433MHz with a linear time-ramp was used for the excitation.The total simulation time was twenty periods of the source signal. The CPU time for a simulation on a compatible PC with a Pentium II® microprocessor at 450MHz and 512MB of RAM memory was about 10 hours.

C. Thermographic SAR measurements

The SAR distributions were measured experimentally with an infrared camera (AGA Thermovision System 680/102B, Lidingö, Sweden) interfaced to a PC. The applicators were placed on top of a semi-solid muscle equivalent phantom ($50 \times 50 \times 10 cm^3$) [9]. Between the applicator and the phantom a waterbolus (a plastic bag filled with de-ionized water) was positioned. The phantom consists of 1 and 2cm layers for the first 5cm to allow the measurement of the SAR distribution at different depths from the phantom surface. The layers are made of the material enclosed in a 0.005cm thick PVC mylar which has no influence on the deposited electromagnetic energy. Because of the low sensitivity of the camera the phantom had to be heated for a maximum time of 1.5 minutes for the temperature to rise between 3-6°C. This time is slightly larger than the one specified in the ESHO quality assurance guidelines [3]. However, in [6] it is shown that the relative SAR distributions at 1cm depth as measured with the thermographic camera for the semi-solid phantom and with the scanning dipole technique agree very well, especially under the center of the aperture. The applicator, the waterbolus and the required phantom layers were removed after the power had

been turned off. The temperature distribution on the top surface of the remaining phantom was measured within 15s. The measured distribution of temperature rise corresponds essentially to the SAR distribution. The method is explained in detail in [4]. The time which is necessary for the experimental assessment of a single SAR distribution is roughly 1 hour. After each measurement a period of 2-4 hours is necessary for the phantom to reach again thermal equilibrium. Therefore, it is less convenient to acquire by means of measurement the 3-D information on the SAR distribution, which is provided with a single computer simulation.

III. RESULTS AND DISCUSSION

Numerical calculations have been carried out for all three types of applicators of Fig. 1, i.e., the conventional applicator (CA), the lucite applicator (LA) and the lucite cone applicator (LCA). The discretized model which was used for the simulations is shown in Fig. 2. A finite-size waterbolus of $18 \times 18 \times 1 \text{cm}^3$ similar to the one used during measurements was included in the model.

(a)   (b)
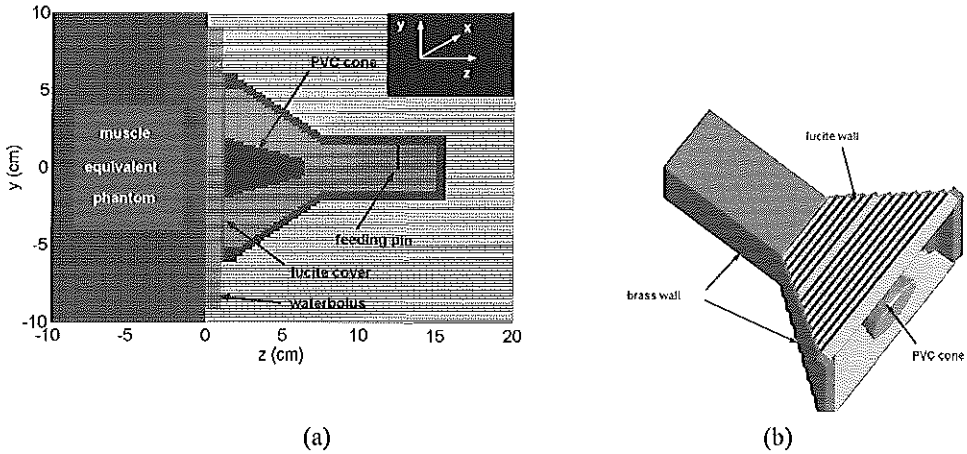
Fig. 2 Representation of the numerical model in (a) 2-D and (b) 3-D. In both models the "staircasing" effect is apparent. This requires that a contour-path approximation be employed for a more correct modeling.

(a)   (b)
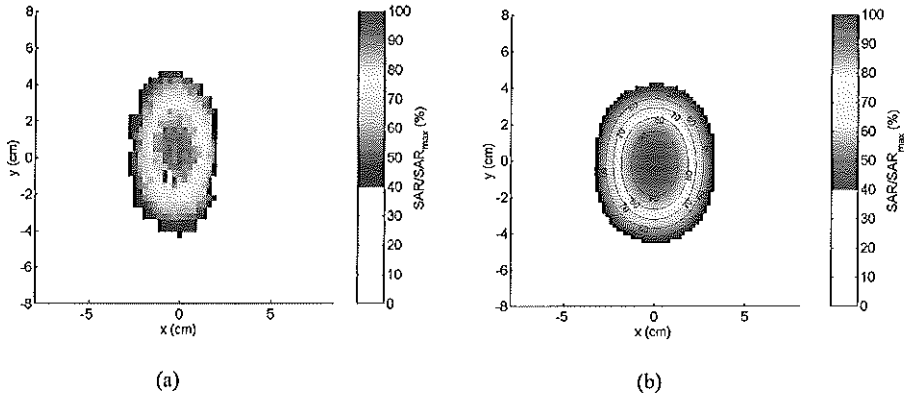
Fig. 3   SAR distributions (normalized to their maximum value) on the transversal cross-section of a flat homogeneous muscle-equivalent phantom at a depth of 1cm for a conventional applicator and a waterbolus of 1cm thickness.
(a) Measured distribution. (b) Predicted distribution.

(a)   (b)
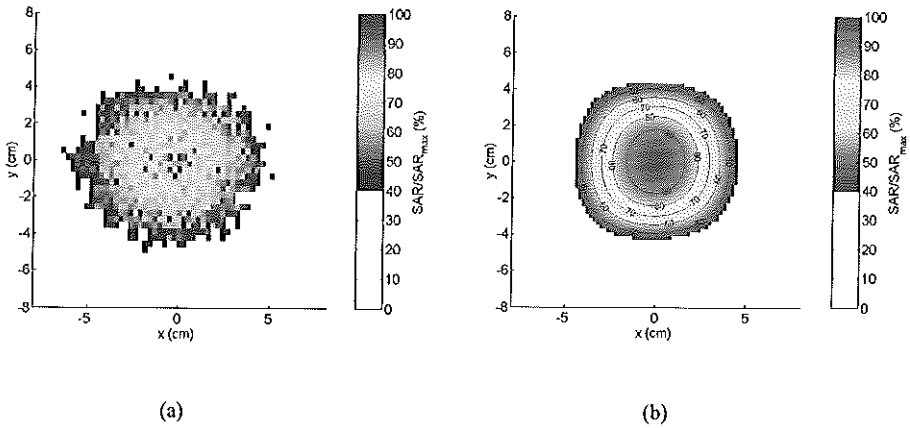
Fig. 4   SAR distributions (normalized to their maximum value) on the transversal cross-section of a flat homogeneous muscle-equivalent phantom at a depth of 1cm for a lucite applicator and a waterbolus of 1cm thickness.
(a) Measured distribution. (b) Predicted distribution.

(a)   (b)
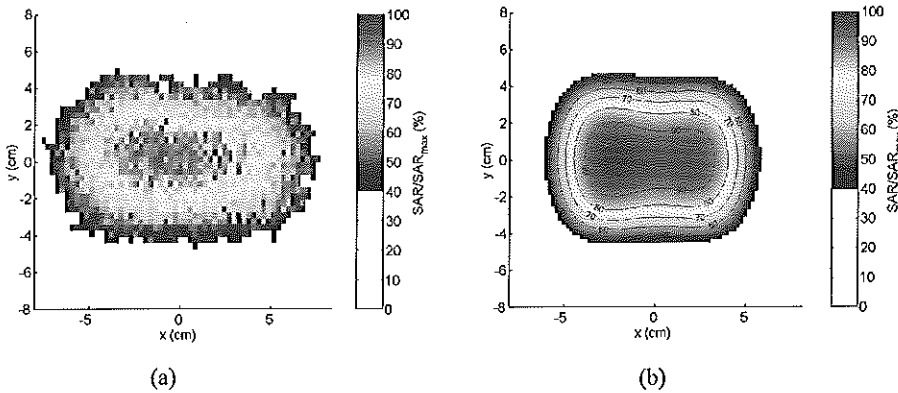
Fig. 5 SAR distributions (normalized to their maximum value) on the transversal cross-section of a flat homogeneous muscle-equivalent phantom at a depth of 1cm for a lucite cone applicator and a waterbolus of 1cm thickness.
(a) Measured distribution. (b) Predicted distribution.

On the cross-section of the muscle-equivalent phantom normal to the propagation direction the SAR distributions are compared at a depth of 1cm. Figs. 3-5 show the predicted and the measured distributions for all three types of applicators. The values are normalized to the maximum value of each distribution. For clarity only iso-SAR values above 40% are plotted. It should be pointed out that Fig. 4a which depicts the measured SAR distribution of the lucite applicator is of poor quality, due to the poor matching between the feeding line and the applicator. The reflected power for the measured lucite applicator was about 20%, whereas for the other two applicators the reflected power was about 3%. Consequently, the net output power from the lucite applicator was low and the maximum temperature rise achieved in the phantom was only 3°C. This resulted in a noisy measurement compared with the other two applicators for which the maximum temperature rise was 6°C.

Additionally, a comparison of the predicted and measured SAR profiles along the main axes of the aperture for all three applicator types is presented in Figs. 6a-c for the axis parallel to the E-field direction and in Figs. 6d-f for the axis perpendicular to the E-field direction. The SAR distributions of Fig. 6 are normalized to the maximum along each axis.

It can be seen from Figs. 3-6 that there is a very good agreement between the predicted and measured distributions for all applicators. As was mentioned above, these results were obtained with a cell size of 0.2cm. Initially a coarser mesh with a cell size of 0.5cm was tested

for which the lucite cover was modeled in one case and was omitted in another. The electromagnetic field distributions inside the phantom were significantly different in the two cases. Therefore, the cell size had to be reduced to 0.2cm to allow the correct modeling of the lucite cover in front of the radiating aperture. Work is currently under way to implement a "thin sheet" approximation for this dielectric cover in order to examine the use of a coarser mesh in the numerical calculations.
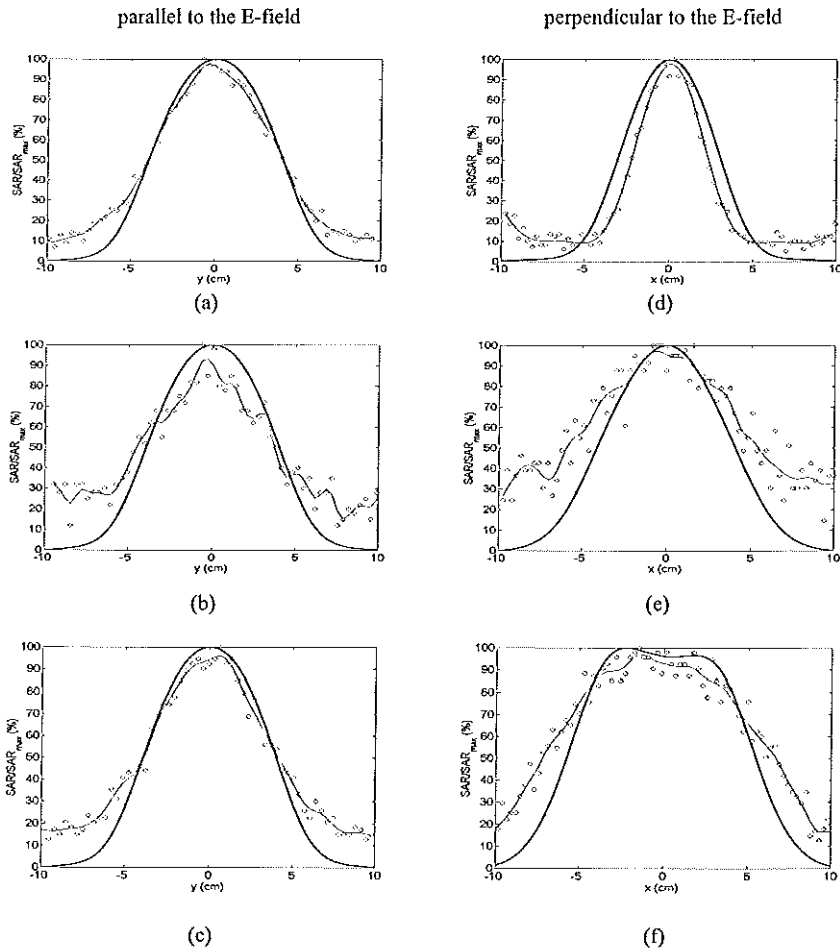
Fig. 6   The SAR distribution along the aperture axis of the applicators which is parallel (a-c) and perpendicular (d-f) to the electric field. The predicted (thick line), the measured (circle points) and the spline fit for the measured (thin line) distributions are given for the conventional (a,d), the lucite (b,e) and the lucite cone (c,f) applicators.

An important quantity for the characterization of superficial hyperthermia applicators is their effective field size (EFS). Table 2 summarizes the results with respect to the EFS. Beside the measured and predicted values at 1cm depth, predicted values are given around this point to show the steepness with which the EFS decays.

Table 2. Measured and predicted EFS for the three applicators.

	Measured at a depth of 1cm	Predicted at a depth of		
		0.8cm	1cm	1.2cm
Conventional applicator	$32cm^2$	$40.92cm^2$	$40.16cm^2$	$39.64cm^2$
Lucite applicator	$67cm^2$	$54.64cm^2$	$54.32cm^2$	$54.08cm^2$
Lucite cone applicator[a]	$91cm^2$	$85.92cm^2$	$84.88cm^2$	$83.40cm^2$

[a]The average measured value for six LCA's was $91 \pm 6cm^2$ (one standard deviation).

The difference between predicted and measured results can be attributed to errors of both the numerical and the experimental methods. It must be noted that the resolution of the infrared camera is poor with a pixel size of roughly 4mm × 3 mm. Furthermore, heat diffusion during measurements can alter significantly the measured distributions [14]. The determination of the effect which heat conduction has on the measured distribution is under investigation.

The results verify that the lucite cone applicator has an increased EFS compared to the other applicator types. This is achieved in the two steps which were considered for the development of the LCA:

(1) It was shown in [15] that the width of the H-plane within the applicator aperture can be increased by replacing the metal walls which are parallel to the electric field with lucite walls.

(2) It is known that the partial loading of a rectangular applicator with slabs of high permittivity leads to a better uniformity of the electric field across its aperture [16], [17]. The PVC cone which is inserted at the center of the aperture has a low permittivity compared to

de-ionized water. Thus, the water which surrounds it acts like a high permittivity slab, improving the uniformity of the electric field.

Along the direction of propagation it was not possible to measure the SAR distribution. The calculated SAR distributions on the H-field and the E-field planes show that there is little difference among the three applicator types for the energy deposition patterns inside the phantom as a function of depth. Nevertheless, the lucite cone applicator is still slightly superior to the other two applicator types in terms of the penetration depth. Its penetration depth - calculated with an exponential fit of the numerical results - was found to be 3.6cm compared to 3.2cm for the conventional applicator and 3.1cm of the lucite applicator. The penetration depth for plane wave exposure at this frequency is reported to be 3.56 cm [3],[9].

The efficiency of the applicators has also been calculated from the ratio of the power absorbed in the muscle phantom to the power input to the applicator. It was found that the efficiency of all three applicators was about 48%. Table 3 contains information about the calculated maximum SAR which is achieved at the surface of the muscle phantom and at 1cm depth in it per W of input power. It is assumed that the muscle-equivalent phantom has a density of $=1000kg/m^3$ [18]. The maximum temperature rise per W of input power for a heating period of 1min can be estimated from the maximum SAR values[3], assuming that the specific heat of the phantom is 3600J/kg/°C [18].

Table 3. Capability of applicators to deliver power to the phantom.

	SAR_{max} (W/kg/W_{in}) at surface	T (°C/min/W_{in}) at surface	SAR_{max} (W/kg/W_{in}) at 1cm	T (°C/min/W_{in}) at 1cm
Conventional applicator	5.25	0.0875	2.93	0.0488
Lucite applicator	4.15	0.0692	2.15	0.0358
Lucite cone applicator	2.81	0.0468	1.55	0.0258

---

[3] Using the equation $\Delta T = \dfrac{SAR \cdot \Delta t}{c}$, where Δt is the heating time and c is the specific heat.

IV. CONCLUSIONS

A three-dimensional model based on the Finite-Difference Time-Domain (FDTD) method was developed for the study of superficial applicators. With this model it is feasible to further investigate the three applicator types considered. The results have verified that the lucite cone applicator (LCA) has a better performance than the other two applicator types in terms of EFS. The relevant numerical results agreed with the experimental ones. They both confirmed the expectations of the two-step design process of the LCA as described in the above section. Moreover, the numerical results presented in this work have shown that the penetration depth of the LCA is higher than for the other two applicators. This adds another advantage to the LCA.

The approaches that had previously been attempted in modeling the applicators could offer limited information on the resulting SAR distributions. Furthermore, they did not carry the potential for examining clinically significant factors, like the dimensions of the waterbolus and the complex patient anatomy. On the contrary, the developed numerical model allows a direct 3-D analysis of the treatment set-up. This will certainly facilitate the determination of clinically significant treatment factors and help improve treatment quality. Although the model is based on a very fine mesh which is probably prohibitive for the simulation of 2×2 applicator arrays work is already being carried out for the use of coarser models.

REFERENCES

[1]   International Collaborative Hyperthermia Group: C.C. Vernon, J.W. Hand, S.B. Field, D. Machin, J.B. Whaley, J. van der Zee, W.L.J. van Putten, G.C. van Rhoon, J.D.P. van Dijk, D. González-González, F.F. Liu, P. Goodman, and M. Sherar, "Radiotherapy with or without hyperthermia in the treatment of superficial localized breast cancer – results from five randomized controlled trials", *Int. J. Radiation Oncology Biol. Phys.*, vol. 35, pp. 731-744, 1996.

[2]   M.D. Sherar, F.F. Liu, M. Pintilie, W. Levin, J.W. Hunt, R. Hill, J.W. Hand, C.C. Vernon, G.C. van Rhoon, J. van der Zee, D.G. González-González, J.D.P. van Dijk, J. Whaley, and D. Machin, "Relationship between thermal dose and outcome in thermoradiotherapy treatments for recurrences of breast cancer in a randomized phase III trial", *Int. J. Radiation Oncology Biol. Phys.*, vol. 39, pp. 371-380, 1997.

[3]   J.W. Hand, J.J.W. Lagendijk, J. Bach Andersen, and J.C. Bolomey, "Quality assurance guidelines for ESHO protocols", *Int. J. Hyperthermia*, vol. 5, pp. 421-428, 1989.

[4]   G.C. van Rhoon, P.J.M. Rietveld, and J. van der Zee, "A 433MHz Lucite Cone waveguide applicator for superficial hyperthermia", *Int. J. Hyperthermia*, vol. 14, pp. 13-27, 1998.

[5]   P.J.M. Rietveld, W.L.J. van Putten, J. van der Zee, and G.C. van Rhoon, "Comparison of the clinical effectiveness of the 433MHz lucite cone applicator with that of a conventional waveguide applicator in applications of superficial hyperthermia", *Int. J. Radiation Oncology Biol. Phys.*, vol. 43, pp. 681-687, 1999

[6]   P.J.M. Rietveld, M.L.D. Lumori, J.W. Hand, M.V. Prior, J. van der Zee, and G.C. van Rhoon, "Effectiveness of the Gaussian beam model in predicting SAR distributions from the lucite cone applicator", *Int. J. Hyperthermia*, vol. 14, pp. 293-308, 1998.

[7]   P.J.M. Rietveld, M.L.D. Lumori, J. van der Zee, and G.C. van Rhoon, "Quantitative evaluation of 2×2 arrays of lucite cone applicators in flat layered phantoms using Gaussian-beam-predicted and thermographically measured SAR distributions", *Phys. Med. Biol.*, vol. 43, pp. 2207-2220, 1998.

[8]   A. Taflove, *Computational Electrodynamics: The Finite-Difference Time-Domain Method*, Artech House, 1995.

[9]   A.W. Guy, "Analysis of electromagnetic fields induced in biological tissues by thermographic studies on equivalent phantom models", *IEEE Trans. Microwave Theory Tech.*, vol. 19, pp. 205-214, 1971.

[10]   G. Mur, "Absorbing boundary conditions for the finite-difference approximation of the time-domain electromagnetic field equations", *IEEE Trans. Electromagn. Compat.*, vol. 23, pp. 377-382, 1981.

[11]   P.-Y. Cresson, C. Michel, L. Dubois, M. Chive, and J. Pribetich, "Complete three-dimensional modeling of new microstrip-microslot applicators for microwave hyperthermia using the FDTD method", *IEEE Trans. Microwave Theory Tech.*, vol. 42, pp. 2657-2666, 1994.

[12]   L.-K. Wu and W.K. Nieh, "FDTD analysis of the radiometric temperature measurement of a bilayered biological tissue using a body-contacting waveguide probe", *IEEE Trans. Microwave Theory Tech.*, vol. 43, pp. 1576-1583, 1995.

[13]   D.S. Katz, M.J. Piket-May, A. Taflove, and K.R. Umashankar, "FD-TD analysis of electromagnetic wave radiation from systems containing horn antennas", *IEEE Trans. Antennas Propagat.*, vol. 39, pp. 1203-1212, 1991.

[14]   E.G. Moros and W.F. Pickard, "On the assumption of negligible heat diffusion during the thermal measurement of a nonuniform Specific Absorption Rate", *Radiation Res.*, vol. 152, pp. 312-320, 1999.

[15]   J.J. Epis, "Compensated electromagnetic horns", *Microwave Journal*, vol. 4, pp. 84-89, 1961.

[16]   G.N. Tsandoulas and W.D. Fitzgerald, "Aperture efficiency enhancements in dielectrically loaded horns", *IEEE Trans. Antennas Propagat.*, vol. 21, pp. 69-74, 1972.

[17]   G. Kantor, "Evaluation and survey of microwave and radiofrequency applicators", *J. Microwave Power*, vol. 16, pp. 135-150, 1981.

[18]   J.B. Leonard, K.R. Foster, and T.W. Athey, "Thermal properties of tissue equivalent phantom materials", *IEEE Trans. Biomed. Eng.*, vol. 31, pp. 533-536, 1984.

General discussion

In the last two decades, progress has been made in hyperthermia in the fields of biology (Kong and Dewhirst, (1999)), tumour physiology (Kanamori *et al.* (1999)), clinical applications and heating techniques (Dewhirst *et al.* (1997); Dahl *et al.* (1999)). Especially in interstitial hyperthermia and deep regional hyperthermia have 3D-adjustable heating techniques, 3D patient-orientated treatment planning and their clinically related data have been made accessible through several studies. Different groups have contributed to these results through their specialised know-how, based on either theoretical, technical or clinical research (Lagendijk, (1990); Sullivan *et al.* (1993); Sneed *et al.* (1998); Turner, (1998); Wust *et al.* (1999); Paulsen *et al.* (1999); Van der Zee *et al.* (2000)).

A combination of these more recent results has led to the overall mechanisms of hyperthermia being better understood. Although at present several clinical applications of hyperthermia are either under investigation or are (already) considered as part of a standard treatment modality, no consensus appears to exist in treatment schemes[1]. There are also large differences of opinion as to what is considered to be the main issue that should be investigated in hyperthermia.

In our group, the emphasis in the research done, was generally on the more practical sides of the clinical application of hyperthermia. We presented the clinical results of the treatment of recurrent breast cancer which formed the basis for this thesis (see chapter 2). It was clearly shown that the used techniques can have a great impact on the clinical outcome as was reported earlier

---

[1] In this discussion, the progress within the Asian hyperthermia community is not included for reasons of clarity. Research and development in Caucasian-related and Asian-related hyperthermia therapies have other technical and clinical accents. This has an impact on certain hyperthermic treatment aspects, which would complicate the discussion more than desirable. Asian hyperthermic research as an entity has, however, contributed significantly to the progress of hyperthermia.

by Perez *et al.* and Emami *et al.* (Perez *et al.* (1989); Perez *et al.* (1991); Emami *et al.* (1996)) and that hyperthermia can work providing a minimum quality is guaranteed.

Quality of hyperthermia can be measured on different levels. One ideally should compare quality relative to the standard treatment scheme through CR rates, local control or survival rate. However, this set up is sometimes not feasible due to a limited influx of patients or the expectation of relatively small differences in clinical outcome between the two treatment schemes. Alternatively, the hyperthermic quality can be expressed based on measured temperatures. However, in clinical practice, invasive thermometry has its limitations (chapter 3) in providing data for thermal dose analyses. Also, accurate non-invasive measurement techniques are not yet available on a routine basis. More merits and demerits of the use of measured temperatures will be discussed further on in this chapter.

The technical parameter of hyperthermic quality is SAR and its use is defined in the Quality Assurance (QA) guidelines of ESHO and RTOG (Hand *et al.* (1989); Dewhirst *et al.* (1990)). However, the SAR requirements for hyperthermic quality are not unequivocal when transferred from QA guidelines into clinical practice. Whether the QA guidelines-based 50% SAR coverage is the ultimate goal for clinical applications or the 25% SAR coverage that was found as prognostic factor for response (Myerson *et al.* (1990b); Lee *et al.* (1998)) or the homogeneity coefficient as defined by Gelvich *et al.* (1996) is as yet unclear. A validation of the 25% SAR correlation with CR in combination with the use of different types of antennae will make clear whether this parameter, which can be measured or calculated relatively accurately, will hold its prognostic capabilities and thus its clinical relevance.

For the remainder of this chapter, the discussion will be restricted to different aspects of thermal dosimetry in relation to the ultimate question, as described in the General Introduction: *'Does technical improvement in a hyperthermic application actually result in a quantifiable improvement in the clinical hyperthermia treatment?*

The following items will be addressed:

- Problems of confounding factors in thermal dosimetry
- The use of the T_{90}, T_{50}, $T_{20/10}$ or average temperature (T_{av}) and measure for deviation.
- The question of whether thermal dose-response studies should take place prior to the commencement of phase III studies.

The chapter concludes with future research possibilities for our Hyperthermia section of the Radiotherapy department of UHR-Daniel based on currently presented results.

10.1   Problems of confounding factors in thermal dosimetry

In vitro experiments have shown that higher temperatures generate more cell kill (Harisiadis *et al.* (1975); Dewey *et al.* (1977); Bhuyan, (1979)) i.e. there exists a thermal dose-response relationship. One of the important lines in hyperthermic research is the translation from *in vitro* thermal dosimetry into *in vivo* thermal dosimetry (Alfieri and Hahn, (1978); Perez and Sapareto, (1984)). However, *in vivo*, the thermal dos-response correlations are influenced by confounding factors like the dynamic micro environment of the (tumour) cells i.e. tumour characteristics like oxygenation, nutrition and pH, thermo-tolerance or -resistance. Not only the biological cell mechanisms have to be taken into account but also the (varying) dose of the other treatment modality (i.e. radiotherapy or chemotherapy) plus pre-treatment (chemo, radiation therapy). Also, the function of temperature in time acts as a complicating factor. The total effect of the response to the combined treatments is a function of all variables including thermal dose. To distinguish the contribution of hyperthermia to the clinical response via a thermal dose parameter from this complex of variables is difficult but not impossible. First results on the possibility of delivering a prescribed thermal dose have been reported (Thrall *et al.*(1999)).

When all variables with the exception of time-temperature are kept constant, a thermal *measure* for hyperthermic quality, not thermal *dose*, of the hyperthermia treatment can be obtained. The intra-patient comparison of LCA- and WGA-related invasive temperatures (chapter 8) is an example of such use of a thermal measure. In this comparison, it is not the absolute value of the average temperature per treatment (as a thermal dose parameter) which is important, but the difference between the two applied clinical set-ups. This parameter provides a measure for the evaluation of technical quality under clinical conditions based on a basic thermal dose parameter.

The development of thermal dose-response relationship is seen as critical for progress in hyperthermia by the major North American hyperthermia researchers (Dewhirst *et al.* (1997)). For this reason several definitions of thermal dose parameters have been tested (Oleson *et al.* (1993); Leopold *et al.* (1993); Kapp and Cox, (1995); Nishimura *et al.* (1995); Sherar *et al.*

(1997); Hand *et al.* (1997)). Many groups have reported on retrospective thermal dose parameter studies and in particular reported on minimum temperature based parameters, which showed correlation with treatment outcome (Oleson *et al.* (1984); Cox and Kapp, (1992); Kapp and Cox, (1995); Hand *et al.* (1997); Overgaard *et al.* (1996)).

From these clinical findings and the biological support in literature, it is evident that a strong association exists between a time-temperature parameter and clinical response. However, due to the above-mentioned confounding factors, it is impossible to say that an unequivocal causal connection exists. I will illustrate this by two examples.

Example I: Van der Zee *et al.* (1992) found that the series average maximum tumour temperature at the coldest spot correlated with the number of intra tumour measurement sites (figure 10.1) and that the number of temperature measurements correlated with tumour size (personal communication).

Also, Corry *et al.*, Perez and Emami and Overgaard *et al.* (Corry *et al.* (1988); Perez and Emami, (1989); Overgaard *et al.* (1996)) reported on a correlation between number of temperature sites and a thermal dose parameter. Their findings were based on either a minimum temperature (Overgaard *et al.*), an average temperature (Corry *et al.*) or the number of probes reaching a maximum temperature above an index temperature (Perez and Emami). Overgaard *et al.* and Perez and Emami also found that the response was smaller for large tumours than for small tumours and since a large tumour can accommodate more temperature sites (on average), the correlation between thermal dose and response actually may be a non-hyperthermic correlation between tumour size and response. Furthermore, the value of a thermal parameter may also be influenced by the temperature measurement technique (Overgaard *et al.* (1996)). Hand *et al.* (1997) reported *no* correlation between number of temperature sites and minimum- or average-based thermal parameters. They argued that their number of thermometry sensors (median 10) was considerably greater than those used by Corry *et al.* and Overgaard *et al.* (up to 8 respectively median 4). Also, a correlation between the position of thermometry catheters and the radiation characteristics of the used antennae can have an impact on the interdependence of temperature and number of sites. In short: the influences of tumour size and the quality of thermometry on the thermal dose concept are yet unclear.

43
42 ◆ 8
◆ 2450 MHz
▣ 433 MHz
degrees C
41 11
16
11 ◆
20
5
40
8
1 ◆
8
2 ◆
2
1
39
3 ◆
2
38
1   3   5   7   9   11   13   15   17   19
number of invasive tumour measurements
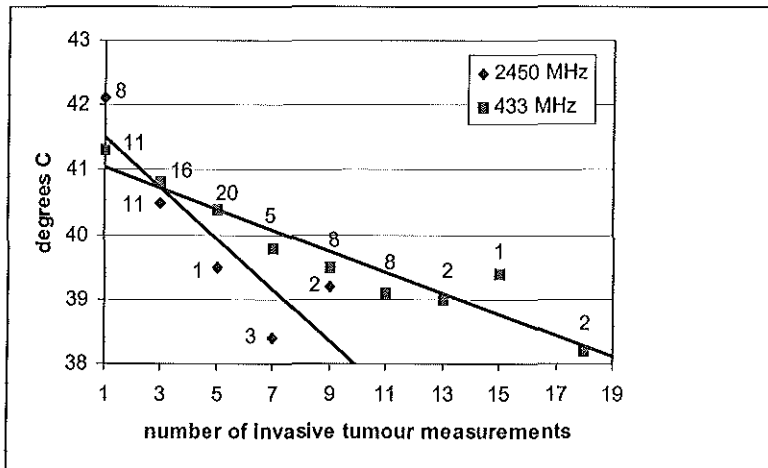
figure 10.1: The treatment series average of the maximum temperature at the coldest spot as a function of invasive tumour sites. The numbers of sites are grouped; the numbers of observations are indicated as the data points.

Example II: It has been shown in the treatment of cervix cancer with radiotherapy that vascularity of the tumour is a prognostic factor (Schlenger *et al.* (1995); Cooper *et al.* (1999)): cervix tumours with higher vascularity have less local control and survival probability. Suppose that:

1. this patient group was treated with radiotherapy plus hyperthermia,
2. the grade of vascularity was unknown and
3. vascularity is proportional to blood flow,

then most probably the patient group with (unknown) high vascularity and thus high blood flow will have a lower T_{90} and also an insufficient response to hyperthermia. However, as this group has already a lower chance on local control because of its vascularity-dependant effect of radiotherapy, this non-thermal tumour-related parameter would then influence the (retrospectively) obtained thermal dose-response correlation.

In conclusion, with the current available temperature data, results from retrospective thermal dose and thermal dose-response studies may be confounded by several partly unknown variables. Therefore, data from retrospective studies cannot be used to define optimal hyperthermic treatment strategies. Defining quantitative measures for hyperthermia treatments (in combination with other treatment modalities) can only be done through prospective thermal dose studies.

Should we concentrate first on defining clinically reliable thermal dose parameters that correlate with response by addressing the problem of confounding factors in a controllable experimental set-up or temporarily settle for limited quantitative temperature-based analyses?

10.2 The use of the T_{90}, T_{50} $T_{20/10}$ or average temperature (T_{av}) and measure for deviation

Good correlations between minimum temperature-related parameters and clinical response regarding the effect of hyperthermia have been reported (Engin *et al.* (1995); Kapp and Cox, (1995); Hand *et al.* (1997); Sherar *et al.* (1997); Lee *et al.* (1998)). Oleson (1990) introduced the T_{90} (i.e. 10th percentile) as an alternative to the minimum temperature in order to reduce statistical noise. Likewise, the T_{10} and T_{20} were introduced as representatives of the maximum temperature in thermal dose analyses.

A thermal dose parameter should:

- Handle the temperature and time independently. In this way, thermotolerance by step-up and thermosensitivity by step-down heating can be incorporated in the thermal dose model. Also the duration of the treatment or fractionation of the hyperthermia treatment series is then incorporated.

- Function in optimisation routines during treatments and in between successive treatments.

- Correlate well with response and with local control.

The clinically derived thermal dose parameter should ideally be independent of other patient/tissue-related properties such as treatment volume, perfusion and treatment history (e.g. former radiotherapy/chemotherapy/surgery). These requirements of independence are difficult if not impossible to meet.

The temperature data obtained from the clinical hyperthermic applications gives a limited reflection of the actual overall temperature distribution. With the currently available level of clinical thermometry we are confronted with clinical limitations:

- The number of invasively located catheters in the treatment volume is limited due to patient-related constraints.
- The number of invasive temperature sites per catheter is limited.
- The spatial distribution of invasive thermometry is always a sum of local linear maps (multi-point temperature measurements in mainly straight catheters).

With the assumption of $1cm^3$ tissue temperature information per invasive site, the order of coverage of the treatment volume is 1%. These limitations can have an effect on the accuracy of the thermal dose parameters and influence correlation relationships. Some efforts have been made to overcome the first two limitations: e.g. the clinical use of non-invasive temperature techniques (Bertsch *et al.* (1998); Delannoy *et al.* (1991)) and corrections in temperature distributions (Edelstein-Keshet *et al.* (1989)) in spherically shaped tumours. However, these solutions are only applicable in specific cases. Therefore, the use of currently available clinical thermometry in thermal dose calculations is of limited value and the search for the ultimate thermal dose parameter with the strongest association with response cannot be successful with the current quality of thermometry since the outcome of such analyses is still strongly data-dependent and dependent on the random fluctuations in the noise of each parameter.

To investigate the usefulness of the more *basic* 'thermal dose' parameters like T_{90}, T_{50} and T_{10-20}, calculations were performed using Stata[2] on temperature data from a selection of patients treated with superficial hyperthermia in our section. Each treatment lasted 60 minutes. The data set contained temperature measurements from:

- 176 patients;
- 1137 treatments,
- 6.5 treatments per treatment series (std: 2.1);
- an average of 20.2 temperature sites, (range 9 – 24), std: 3.3 of which

- 10.9 invasively (4.8 in tumour) located sites and
- an average of 53 readings per site per treatment (std: 22).

In the calculations presented hereafter, the first 10 minutes of the treatments are excluded from the analyses to eliminate side effects from the warming-up period.

Since the T_{90} and $T_{10/20}$ are estimates of the minimum respectively maximum temperature, it is important to have an understanding of the shape of the temperature distribution. It is often the case that biological data follow the Normal distribution (Campbell and Machin, (1993)). The temperature data set is therefore analysed on its resemblance to the Normal distribution. To implement this, the quantile-Normal plot, which emphasizes the tails of the Normal distribution, was used. The straight line in this plot represents the Normal distribution. Figure 10.2 shows quantile-Normal plots of the *average* temperature per invasive temperature site per treatment from nine randomly selected patient treatment series.

The quantile-Normal plots of patient numbers 208, 338, 477 and 604 show significant deviations from the Normal distribution. In patient 723 the quality of invasive thermometry is very poor. For five out of nine temperature distributions, the minimum or maximum temperature falls outside the Normal distribution. However, the T_{90} and $T_{10/20}$ in these distributions fall within the Normal distribution, but since these parameters do not represent the ultimate thermal dose parameters, it is conceivable that other temperature based parameters like the T_{50} or T_{av} can be used instead.

The interdependence of the T_{90}, T_{50}, average temperature T_{av} and $T_{20/10}$ is given in a matrix plot (figure 10.3). This plot clearly shows that the T_{50} and T_{av} are strongly correlated which makes their use interchangeable in a comparison of different temperature analyses. This is also the case for the T_{10} and T_{20}. However, the qualitative correlation between the T_{50} and T_{90} is of more importance. The T_{50} (based on the average temperature per invasive site) follows the Normal distribution relatively well (figure 10.2). If we take into account the T_{90}- and $T_{20/10}$-dependence on statistically based fluctuations (e.g. the number of temperature sites), the T_{50} plus a measure for deviation are favoured from a statistical point of view and inform us equally well.

---

[2] Stata Corporation, 702 University Drive East, College station, TX 77840, USA

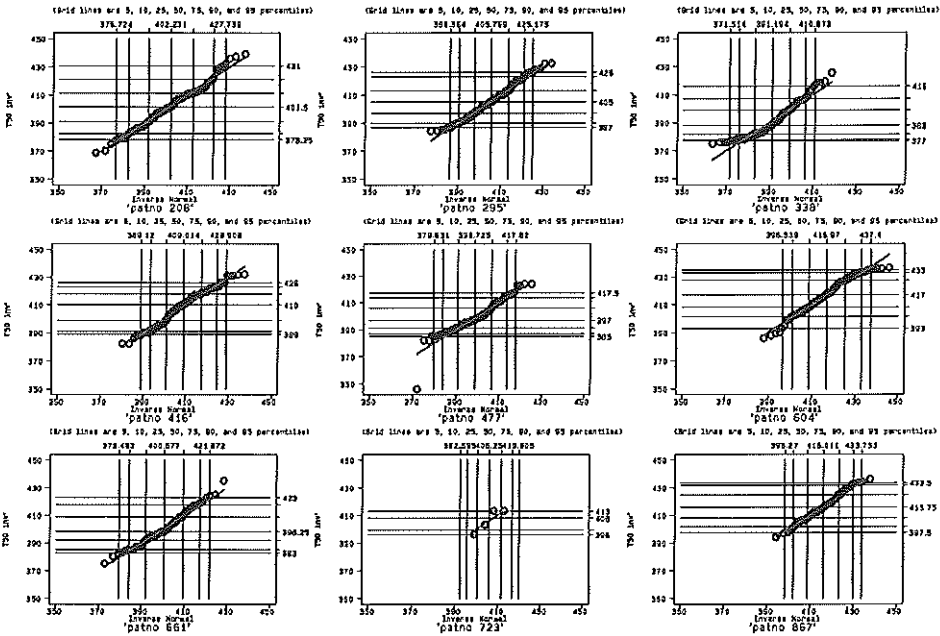figure 10.2: Quantile-Normal plots of the T_{50} per site per treatment over all invasive sites. Nine randomly selected patient treatment series are plotted.
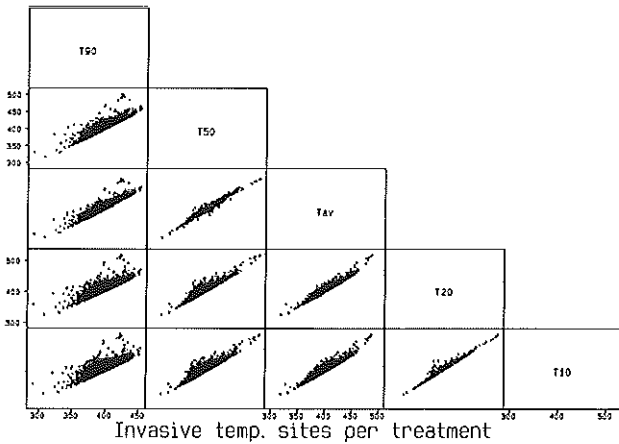The temperatures are handled in ten-fold to reduce PC memory usage.

figure 10.3: Interdependence matrix plot. Each dot represents a thermal dose parameter calculated per temperature site per treatment. The parameters are T_{90}, T_{50}, T_{av}, T_{20} and T_{10}.

Although a correlation between T_{90} and the number of intra-tumour temperature sites has been reported, this could not be confirmed in our current data set. A plausible reason for this could be the larger number of invasive temperature sites used. This amount was similar to that as reported by Hand *et al.* (1997) who did not find a correlation between T_{90} and the number of sites. In the current data set, WGA, LCA and CSA antennae have been used. The radiation characteristics of the LCA and CSA differ significantly from that of the WGA, this may have contributed to this non-reproducible result.

Closing remarks With the current available quality of invasive thermometry, it has been possible to make basic clinical verification of technical improvements (chapter 8). However, with the current level of treatment volumetric coverage it will be difficult to clinically confirm small technical differences as we showed in the technical comparison of SAR from the LCA and CSA (chapter 7).

With the current treatment planning tools it will be possible in the future to map modelled fine-meshed temperature distributions onto coarse clinically measured temperature data. When this technique becomes available, higher quality thermal dosimetry can be made available. Also, the possibility of non-invasive thermometry by MRI will boost know-how on the concept of thermal dose (Carter *et al.* (1998)) and last but not least the functionality of hyperthermia in general.

Concerning the dependence of the thermal dose parameters with variables other than time and temperature, it is essential that further biological research, with clinical backup, should be done. Only then can more know-how be obtained on the influence of non-hyperthermia treatment-related parameters on cell kill, which plays a significant role in clinical thermal dosimetry.

10.3   *The consideration of whether thermal dose-response studies should take place prior to the commencement of phase III studies*

The rationale to quantify the effect of hyperthermia is beyond discussion. Biological *in vitro* studies have clearly shown that hyperthermia is effective in cell kill. *In vivo* studies on hyperthermia alone and radiation with or without hyperthermia have demonstrated a thermal dose-response relationship (Dahl, (1982); Dewhirst *et al.* (1982); Denman *et al.* (1991);

McChesney Gillette *et al.* (1992); Frew *et al.* (1995); Meijnders, (1998); Stubbs and Griffiths, (1999)). However, these *in vivo* studies are based on non-human data and are somewhat limited as to direct human clinical relevance. We have already discussed that in clinical (human) hyperthermia the question of quality is as yet impossible to define due to clinically limiting or confounding factors. However, if technical or clinical progress in hyperthermia is to be monitored, we need a hyperthermic parameter that is capable of dealing with known confounding factors. Human-based clinical prospective phase I/II hyperthermia studies may help in that respect *if* the confounding factors from clinical (invasive) thermometry can be dealt with.

The importance of thermal dose-response studies In the Unites States of America, phase I/II studies on thermal dose-response prevail over the utilisation of the currently available new hyperthermic technologies for phase III studies (Emami *et al.* (1991); Dewhirst *et al.* (1997)). In general, clinicians are reluctant to start phase III studies. The main reason was the outcome of two American phase III trials (running from 1981 – 1987 respectively 1986 - 1992) that compared radiation alone to the combination of radiation plus hyperthermia (Perez *et al.* (1989); Perez *et al.* (1991); Emami *et al.* (1996)) and which failed to show a benefit from the addition of hyperthermia. In their analyses, it was shown that the temperature targets were not met in the majority of the hyperthermia treatments. The equipment used apparently was not capable of producing adequate heat in the treatment volumes and they concluded that this failure was the main reason hyperthermia appeared not to be beneficial. If a sound concept for thermal dose can be defined, this parameter will automatically reflect the technical quality of the hyperthermic treatments. One of the main problems is that if a thermal dose parameter has to be tested under clinical circumstances in phase I/II studies, one has to prescribe a (yet unknown) hyperthermic underdose to a subgroup of the cancer patients under study in order to correlate it with response over the whole clinical hyperthermic dose range. From an ethical point of view this could be considered not to be a viable option.

The justification of running phase III studies A different approach to estimate hyperthermic quality is by comparing patient- and treatment-related characteristics in different patient groups. If for a certain tumour type the addition of hyperthermia to the primary treatment results in an

improved CR rate and another tumour type has comparable initial CR rates after the primary treatment, one can anticipate the same improved CR rate through the addition of hyperthermia if at least the same technical quality for this type of hyperthermic application is available.

In the period 1980 – 1990, either new equipment became available or its limitations were better understood (Lagendijk, (1983); Turner, (1984)). Also promising results from superficial and interstitial hyperthermia studies were reported (Aristizabal and Oleson, (1984); Van der Zee *et al.* (1988); Van der Zee *et al.* (1992)). This resulted in new phase III studies carried out using the efficacy of the new 'second generation' techniques in the treatment of specific tumour groups. The rationale to start the Dutch Phase III study on treatment of inoperable pelvic tumours by radiotherapy (**RT**) with or without deep regional hyperthermia was:

1. For patients with inoperable pelvic tumours, RT alone gives relative low CR rates.

2. Our basic temperature analyses of superficial hyperthermia treatments of recurrent breast cancer show relatively low values (mean invasive temperature 40.9 °C). The CR rates for radiation alone are relatively low. The combined treatment of RT plus hyperthermia appears to be highly beneficial (Vernon *et al.* (1996)).

3. With radiative 'second generation' hyperthermia equipment Myerson *et al.* (Myerson *et al.* (1990a); Myerson *et al.* (1996)) measured temperatures comparable to our superficial hyperthermia treatment temperatures.

4. Even if an adequate hyperthermia treatment can be given to only a part of a patient group, improvement in CR can be expected for the whole group as we have seen in our study on treatment of recurrent breast cancer with RT plus HT (chapter 2, this thesis).

5. Solid proof was needed to establish a generally approved position in regular health care.

This study, and other recent phase III studies, using current state-of-the-art equipment, has shown a positive effect of hyperthermia in a combined treatment modality for both palliative and curative hyperthermia treatment set ups (Overgaard *et al.* (1995); Sneed *et al.* (1998); Van der Zee *et al.* (1999)). In these second series of phase III studies, a critical attitude towards technical (im)possibilities was credit to their clinical success. Application of the Quality Assurance

guidelines from the European Society of Hyperthermic Oncology (ESHO) (Hand *et al.* (1989)) and RTOG (Dewhirst *et al.* (1990)) made certain that a minimal technical quality was guaranteed.

Pros and cons of phase I/II and phase III studies The disappointing results from the first series of phase III studies have led to believe that the potential of hyperthermia can only be fully exploited if one can assure a certain minimal thermal dose, i.e. thermal quality. Some (American) groups believe that a second series of phase III studies with a negative result for the addition of hyperthermia will result in a total halt of hyperthermia research and they recommend that phase III studies are initiated only *after* methods are developed that allow for optimal treatment (Dewhirst, (1996)). Whilst from 1993 onwards the first positive results from the Dutch deep hyperthermia Phase III study were made public (during the 13th Meeting of the North American Hyperthermic Society in Nashville 1994 and by (De Wit *et al.*(1994a,b); Van der Zee and González González, (1995); Van der Zee *et al.*(1996)), still in 1996 a negative attitude continued to exist towards the application of deep regional hyperthermia because of the apparently insufficient technical quality (Gibbs, Jr. (1996)) and the uncertainty in providing an optimal treatment (Seegenschmiedt and Feldmann, (1996)).

If a clear proposal with well-founded (technical and clinical) boundary conditions for the application of hyperthermia is made, progress can be made in the treatment of cancer with hyperthermia, even in the cases whereby a beneficial contribution from hyperthermia is not found. The development of QA guidelines (Hand *et al.* (1989); Dewhirst *et al.* (1990)) were an indirect result of former (unsuccessful) experiences in applications of hyperthermia. If one can *assure* a minimal quality of a treatment modality by means of QA guidelines, the chance of a phase III failure is substantially diminished. On the one hand, the consequence of conducting a phase III study on specific cancer types, guided by yet insufficiently defined QA guidelines which could result in the conclusion that hyperthermia is not beneficial, is far-reaching and could effect the applications of hyperthermia in other fields (due to mechanisms of non-scientific nature). On the other hand, if no phase III study is initiated at all, the scientific (and financial) support for hyperthermia could soon significantly diminish.

The question of a) whether the more theoretically based (American) approach of assurance of a minimum thermal dose before applying hyperthermia clinically or b) the more pragmatic attitude

in the (European) approach in heating up to the maximum tolerance will result in a long term acceptance of hyperthermia in the treatment of well-defined cases of cancer is still to be answered in the current decade.

10.4   Future research possibilities based on current presented results

This thesis describes a series of studies involving the development of superficial hyperthermia antennae. These studies were performed as a result of funding by the Dutch Cancer Society project entitled 'Clinical verification and optimisation of the quality of hyperthermic treatment of large superficial tumours of the chest wall' (grant DDHK 93-603).

We encountered two recurring problems relating to the different studies: a) the lack of appropriate technical QA guidelines for evaluating arrays of antennae for superficial hyperthermia and b) how to perform simple and adequate clinical studies to evaluate technical improvements.

Recently, technical QA guidelines for deep regional hyperthermia have been formulated. However, the specific demands for deep regional hyperthermia cannot be transferred into the field of superficial hyperthermia. The current available superficial hyperthermia QA guidelines do not cover the (RF-radiating) multi-element non-coherent antenna array techniques. Reports on these systems show a wide variety of ideas in addressing the possibilities and restrictions (Auger *et al.* (1993); Diederich and Stauffer, (1993); Ryan *et al.* (1995); Rietveld *et al.* (1996); Gelvich *et al.* (1996); Rietveld *et al.* (1998); Tharp and Roemer, (1992); Stauffer *et al.* (1998)). An update of QA guidelines for superficial hyperthermic equipment dealing with current available antennae techniques and modelling capabilities is badly needed on short term. Only then can one properly exploit the possibilities of current and future state-of-the-art (superficial) hyperthermia techniques.

The first results from the use of FDTD-based modelling of superficial LCAs, as shown in this thesis (chapter 9), are promising. Consequently, clinically relevant set-ups in superficial hyperthermic applications can be modelled. In particular, the cross coupling between the different antennae can be studied and optimisation routines can be developed that enhance non-interactive handling of antennae in an array. Also the effect on local SAR from a finite waterbolus or tissue inhomogeneities can be studied in detail. When FDTD-modelling of smaller CSA becomes

available, more thorough analyses of the two superficial antenna types can be performed including modelled 3D-temperature distribution analyses.

The next steps in quality quantification hyperthermia research are:

- Incorporation of SAR/temperature modelling in the process of optimisation during treatment.
- The use of non-invasive MRI techniques in temperature monitoring which will validate current modelling results.

Despite the fact that still many problems have to be solved, the current status of hyperthermia research justifies its role in regular public health service in Europe.

10.5   References

ALFIERI, A.A. AND HAHN, E.W. 1978, An in situ method for estimating cell survival in a solid tumor. *Cancer Research*, 38, 3006-3011.

ARISTIZABAL, S.A. AND OLESON, J.R. 1984, Combined interstitial irradiation and localized current field hyperthermia: results and conclusions from clinical studies. *Cancer Research*, 44 (Suppl.), 4757s-4760s.

AUGER, E.A., GIACCIA, A.J. AND HAHN, G.M. 1993, Heat sensitivity of bleomycin-sensitive CHO derivatives is not due to improper initialization of heat shock response. *International Journal of Hyperthermia*, 9 (2), 275-284.

BERTSCH, F., MATTNER, J., STEHLING, M.K., MÜLLER-LISSE, U., PELLER, M., LOEFFLER, R., WEBER, J., MESSMER, K., WILMANNS, W., ISSELS, R. AND REISER, M. 1998, Non-invasive temperature mapping using MRI: comparison of two methods based on chemical shift and T1-relaxation. *Magnetic Resonance Imaging*, 16, 393-404.

BHUYAN, B.K. 1979, Kinetics of cell kill by hyperthermia. *Cancer Research*, 39, 2277-2284.

CAMPBELL, M.J. AND MACHIN, D. 1993, From sample to population. *Medical statistics a commonsense approach*. Anonymous Chichester: John Whiley & Sons Ltd.), pp. 60-68.

CARTER, D.L., MACFALL, J.R., CLEGG, S.T., WAN, X., PRESCOTT, D.M., CHARLES, H.C. AND SAMULSKI, T.V. 1998, Magnetic resonance thermometry during hyperthermia for human high-grade sarcoma. *International Journal of Radiation Oncology Biology Physics*, 40, 815-822.

COOPER, R.A., WEST, C.M., WILKS, D.P., LOGUE, J.P., DAVIDSON, S.E., ROBERTS, S.A. AND HUNTER, R.D. 1999, Tumour vascularity is a significant prognostic factor for cervix carcinoma treated with radiotherapy: independence from tumour radiosensitivity. *British Journal of Cancer*, 81, 354-358.

CORRY, P.M., JABBOURY, K., KONG, J.S., ARMOUR, E.P., MCCRAW, F.J. AND LEDUC, T. 1988, Evaluation of equipment for hyperthermia treatment of cancer. *International Journal of Hyperthermia*, 4, 53-74.

COX, R.S. AND KAPP, D.S. 1992, Correlation of thermal parameters with outcome in combined radiation therapy-hyperthermia trials. *International Journal of Hyperthermia*, 8, 719-732.

DAHL, O. 1982, Effect of hyperthermia on a neurogenic rat cell line (BT4A) in vivo. *Acta Radiology Oncology*, 21, 67-77.

DAHL, O., DALENE, R., SCHEM, B.C. AND MELLA, O. 1999, Status of clinical hyperthermia. *Acta Oncologica*, 38, 863-873.

DE WIT, G.A., DE CHARRO, F.T., VAN DER ZEE, J. AND VAN RHOON, G.C. 1994a, Economic evaluation of a new cancer treatment: hyperthermia in the management of advanced pelvic cancer. *Abstractbook, 10th Annual Meeting fo ISTAHC, Baltimore, Maryland USA*, Abstract

DE WIT, G.A., DE CHARRO, F.T., VAN DER ZEE, J. AND VAN RHOON, G.C. 1994b, Economic evaluation of hyperthermia in the management of advanced pelvic cancer. *Abstractbook, ESRB & ESHO joint Meeting, Amsterdam*, 24, Abstract

DELANNOY, J., CHEN, C.N., TURNER, R., LEVIN, R.L. AND LE BIHAN, D. 1991, Noninvasive temperature imaging using diffusion MRI. *Magnetic Resonance in Medicine*, 19, 333-339.

DENMAN, D.L., LEGORRETA, R.A., KIER, A.B., ELSON, H.R., WHITE, M.L., BUNCHER, C.R., LEWIS, G.C.J., BORN, A.M., SUNDARARAMAN, S. AND ARON, B.S. 1991, Therapeutic responses of spontaneous

canine malignancies to combinations of radiotherapy and hyperthermia. *International Journal of Radiation Oncology Biology Physics*, 21, 415-422.

DEWEY, W.C., HOPWOOD, L.E., SAPARETO, S.A. AND GERWECK, L.E. 1977, Cellular responses to combinations of hyperthermia and radiation. *Radiology*, 123, 463-474.

DEWHIRST, M.W., CONNOR, W.G. AND SIM, D.A. 1982, Preliminary results of a phase III trial of spontaneous animal tumors to heat and/or radiation: early normal tissue response and tumor volume influence on initial response. *International Journal of Radiation Oncology Biology Physics*, 8, 1951-1961.

DEWHIRST, M.W., PHILLIPS, T.L., SAMULSKI, T.V., STAUFFER, P., SHRIVASTAVA, P., PALIWAL, B., PAJAK, T., GILLIM, M., SAPOZINK, M., MYERSON, R. AND ET AL, 1990, RTOG quality assurance guidelines for clinical trials using hyperthermia. *International Journal of Radiation Oncology Biology Physics*, 18, 1249-1259.

DEWHIRST, M.W. 1996, Considerations for hyperthermia clinical trials design. *Thermoradiotherapy and thermochemotherapy*. edited by M.H. Seegenschmiedt, P. Fessenden and C.C. Vernon (Berlin: Springer-Verlag), pp. 361-372.

DEWHIRST, M.W., PROSNITZ, L., THRALL, D., PRESCOTT, D., CLEGG, S., CHARLES, C., MACFALL, J., ROSNER, G., SAMULSKI, T., GILLETTE, E. AND LARUE, S. 1997, Hyperthermia treatment of malignant diseases: current status and a view toward the future. *Seminars in Oncology*, 24, 616-625.

DIEDERICH, C.J. AND STAUFFER, P.R. 1993, Pre-clinical evaluation of a microwave planar array applicator for superficial hyperthermia. *International Journal of Hyperthermia*, 9 (2), 227-246.

EDELSTEIN-KESHET, L., DEWHIRST, M.W., OLESON, J.R. AND SAMULSKI, T.V. 1989, Characterization of tumour temperature distributions in hyperthermia based on assumed mathematical forms. *International Journal of Hyperthermia*, 5, 757-777.

EMAMI, B., MYERSON, R.J., SCOTT, C., GIBBS, F., LEE, C. AND PEREZ, C.A. 1991, Phase I/II study, combination of radiotherapy and hyperthermia in patients with deep-seated malignant tumors: report of a pilot study by the Radiation Therapy Oncology Group. *International Journal of Radiation Oncology Biology Physics*, 20, 73-79.

EMAMI, B.N., SCOTT, C.B., PEREZ, C.A., ASBELL, S.O., SWIFT, P., GRIGSBY, P.W., MONTESANO, A., RUBIN, P., CURRAN, W.J., DELROWE, J., ARASTU, H.H., FU, K.K. AND MOROS, E.G. 1996, Phase III study of interstitial thermoradiotherapy compared with interstitial radiotherapy alone in the treatment of recurrent or persistent human tumors: a prospectively controlled randomized study by the Radiation Therapy Oncology Group. *International Journal of Radiation Oncology Biology Physics*, 34, 1097-1104.

ENGIN, K., LEEPER, D.B., TUPCHONG, L. AND WATERMAN, F.M. 1995, Thermoradiotherapy in the management of superficial malignant tumors. *Clinical Cancer Research*, 1, 139-145.

FREW, D.G., DOBSON, J.M., STENNING, S.P. AND BLEEHEN, N.M. 1995, Response of 145 spontaneous canine head and neck tumours to radiation versus radiation plus microwave hyperthermia: results of a randomized phase III clinical study. *International Journal of Hyperthermia*, 11, 217-230.

GELVICH, E.A., MAZOKHIN, V.N. AND TROSHIN, I.I. 1996, An attempt at quantitative specification of SAR distribution homogeneity. *International Journal of Hyperthermia*, 12, 431-436.

GIBBS, F.A., JR. 1996, Thermoradiotherapy for genitourinary and gynecological tumors. *Thermoradiotherapy and Thermochemotherapy*. edited by M.H. Seegenschmiedt, P. Fessenden and C.C. Vernon (Berlin: Springer-Verlag), pp. 121-132.

HAND, J.W., LAGENDIJK, J.W., BACH ANDERSEN, J. AND BOLOMEY, J.C. 1989, Quality assurance guidelines for ESHO protocols. *International Journal of Hyperthermia*, 5, 421-428.

HAND, J.W., MACHIN, D., VERNON, C.C. AND WHALEY, J.B. 1997, Analysis of thermal parameters obtained during phase III trials of hyperthermia as an adjunct to radiotherapy in the treatment of breast carcinoma. *International Journal of Hyperthermia*, 13, 343-364.

HARISIADIS, L., HALL, E.J., KRALJEVIC, U. AND BOREK, C. 1975, Hyperthermia: biological studies at the cellular level. *Radiology*, 117, 447-452.

KANAMORI, S., NISHIMURA, Y., OKUNO, Y., HORII, N., SAGA, T. AND HIRAOKA, M. 1999, Induction of vascular endothelial growth factor (VEGF) by hyperthermia and/or an angiogenesis inhibitor. *International Journal of Hyperthermia*, 15, 267-278.

KAPP, D.S. AND COX, R.S. 1995, Thermal treatment parameters are most predictive of outcome in patients with single tumor nodules per treatment field in recurrent adenocarcinoma of the breast. *International Journal of Radiation Oncology Biology Physics*, 33, 887-899.

KONG, G. AND DEWHIRST, M.W. 1999, Review. Hyperthermia and liposomes. *International Journal of Hyperthermia*, 15, 345-370.

LAGENDIJK, J.J.W. 1983, A new coaxial TEM radiofrequency/microwave applicator for non-invasive deep-body hyperthermia. *Journal of Microwave Power*, 18, 367-376.

LAGENDIJK, J.J.W. 1990, Thermal models: principles and implementation. *An introduction to the practical aspects of clinical hyperthermia.* edited by S.B. Field and J.W. Hand (London, New York, Philadelphia: Taylor & Francis), pp. 478-512.

LEE, H.K., ANTELL, A.G., PEREZ, C.A., STRAUBE, W.L., RAMACHANDRAN, G., MYERSON, R.J., EMAMI, B., MOLMENTI, E.P., BUCKNER, A. AND LOCKETT, M.A. 1998, Superficial hyperthermia and irradiation for recurrent breast carcinoma of the chest wall: prognostic factors in 196 tumors. *International Journal of Radiation Oncology Biology Physics*, 40, 365-375.

LEOPOLD, K.A., DEWHIRST, M.W., SAMULSKI, T.V., DODGE, R.K., GEORGE, S.L., BLIVIN, J.L., PROSNITZ, L.R. AND OLESON, J.R. 1993, Cumulative minutes with T90 greater than TEMPindex is predictive of response of superficial malignancies to hyperthermia and radiation. *International Journal of Radiation Oncology Biology Physics*, 25, 841-847.

MCCHESNEY GILLETTE, S., DEWHIRST, M.W., GILLETTE, E.L., THRALL, D.E., PAGE, R.L., POWERS, B.E., WITHROW, S.J., ROSNER, G., WONG, C. AND SIM, D.A. 1992, Response of canine soft tissue sarcomas to radiation or radiation plus hyperthermia: a randomized phase II study. *International Journal of Hyperthermia*, 8, 309-320.

MEIJNDERS, P.J.N. 1998, The application of rat lung tumour models in experimental therapy of bronchial cancer. 1-176. Thesis

MYERSON, R.J., LEYBOVICH, L.B., EMAMI, B.N., GRIGSBY, P.W., STRAUBE, W.L. AND VON GERICHTEN, D. 1990a, Phantom studies and preliminary clinical experience with the BSD-2000. *International Journal of Hyperthermia*, 7, 937-951.

MYERSON, R.J., PEREZ, C.A., EMAMI, B., STRAUBE, W., KUSKE, R.R., LEYBOVICH, L. AND VON GERICHTEN, D. 1990b, Tumor control in long-term survivors following superficial hyperthermia. *International Journal of Radiation Oncology Biology Physics*, 18, 1123-1129.

MYERSON, R.J., SCOTT, C.B., EMAMI, B.N., SAPOZINK, M.D. AND SAMULSKI, T.V. 1996, A phase I/II study to evaluate radiation therapy and hyperthermia for deep-seated tumours: a report of RTOG 89-08. *International Journal of Hyperthermia*, **12**, 449-459.

NISHIMURA, Y., HIRAOKA, M., MITSUMORI, M., OKUNO, Y., LI, Y.P., MASUNAGA, S., KOISHI, M., AKUTA, K. AND ABE, M. 1995, Thermoradiotherapy of superficial and subsurface tumours: analysis of thermal parameters and tumour response. *International Journal of Hyperthermia*, **11**, 603-613.

OLESON, J.R., SIM, D.A. AND MANNING, M.R. 1984, Analysis of prognostic variables in hyperthermia treatment of 161 patients. *International Journal of Radiation Oncology Biology Physics*, **10**, 2231-2239.

OLESON, J.R. 1990, Prognostic parameters in clinical hyperthermia: is there a hyperthermia dosimetry? *Journal Cancer Research Clinical Oncology, Supplement*, **116**, (part II), 955, Abstract

OLESON, J.R., SAMULSKI, T.V., LEOPOLD, K.A., CLEGG, S.T., DEWHIRST, M.W., DODGE, R.K. AND GEORGE, S.L. 1993, Sensitivity of hyperthermia trial outcomes to temperature and time: implications for thermal goals of treatment. *International Journal of Radiation Oncology Biology Physics*, **25**, 289-297.

OVERGAARD, J., GONZALEZ GONZALEZ, D., HULSHOF, M.C., ARCANGELI, G., DAHL, O., MELLA, O. AND BENTZEN, S.M. 1995, Randomised trial of hyperthermia as adjuvant to radiotherapy for recurrent or metastatic malignant melanoma. European Society for Hyperthermic Oncology. *The Lancet*, **345**, 540-543.

OVERGAARD, J., GONZALEZ GONZALEZ, D., HULSHOF, M.C., ARCANGELI, G., DAHL, O., MELLA, O. AND BENTZEN, S.M. 1996, Hyperthermia as an adjuvant to radiation therapy of recurrent or metastatic malignant melanoma. A multicentre randomized trial by the European Society for Hyperthermic Oncology. *International Journal of Hyperthermia*, **12**, 3-20.

PAULSEN, K.D., GEIMER, S., TANG, J. AND BOYSE, W.E. 1999, Optimization of pelvic heating rate distributions with electromagnetic phased arrays. *International Journal of Hyperthermia*, **15**, 157-186..

PEREZ, C.A., GILLESPIE, B., PAJAK, T.F., HORNBACK, N.B., EMAMI, B.N. AND RUBIN, P. 1989, Quality assurance problems in clinical hyperthermia and their impact on therapeutic outcome: a report by the Radiation Therapy Oncology Group. *International Journal of Radiation Oncology Biology Physics*, **16**, 551-558.

PEREZ, C.A., PAJAK, T.F., EMAMI, B.N., HORNBACK, N.B., TUPCHONGA, L. AND RUBIN, P. 1991, Randomised phase III study comparing irradiation and hyperthermia with irradiation alone in superficial measurable tumors. *American Journal of Clinical Oncology: Cancer Clinical Trials*, **14**, 133-141.

PEREZ, C.A. AND EMAMI, B. 1989, Clinical trials with local (external and interstitial) irradiation and hyperthermia. Current and future perspectives. *Radiologic Clinics of North America*, **27**, 525-542.

PEREZ, C.A. AND SAPARETO, S.A. 1984, Thermal dose expression in clinical hyperthermia and correlation with tumor response/control. *Cancer Research*, **44**, 4818s-4825s.

RIETVELD, P.J.M., BROEKMEYER-REURINK, M.P., VERLOOP-VAN 'T HOF, E.M., STAKENBORG, J., VAN PUTTEN, W.L.J., VAN DER ZEE, J. AND VAN RHOON, G.C. 1996, 433 MHz lucite cone applicator: technical and clinical evaluations. *Hyperthermic Oncology 1996, Volume II. Proceedings of the 7th International Congress on Hyperthermic Oncology. Roma, Italy, April 9-13, 1996.* edited by C.F.G. Arcangeli and R. Cavaliere (Rome: Tor Vergata University of Rome, Italy), pp. 479-481.

RIETVELD, P.J.M., LUMORI, M.L.D., VAN DER ZEE, J. AND VAN RHOON, G.C. 1998, Quantitative evaluation of 2 x 2 arrays of Lucite cone applicators in flat layered phantoms using Gaussian-beam-predicted and thermographically measured SAR distributions. *Physics in Medicine and Biology*, **43**, 2207-2220.

RYAN, T.P., BACKUS, V.L. AND COUGHLIN, C.T. 1995, Large stationary microstrip arrays for superficial microwave hyperthermia at 433 MHz: SAR analysis and clinical data. *International Journal of Hyperthermia*, **11**, 187-209.

SCHLENGER, K., HÖCKEL, M., MITZE, M., SCHÄFFER, U., WEIKEL, W., KNAPSTEIN, P.G. AND LAMBERT, A. 1995, Tumor vascularity - a novel prognostic factor in advanced cervical carcinoma. *Gynecologic Oncology*, **59**, 57-66.

SEEGENSCHMIEDT, M.H. AND FELDMANN, H.J. 1996, Clinical rationale for thermoradiotherapy. *Thermoradiotherapy and thermochemotherapy*. edited by M.H. Seegenschmiedt, P. Fessenden and C.C. Vernon (Berlin: Springer-Verlag), pp. 3-24.

SHERAR, M., LIU, F.F., PINTILIE, M., LEVIN, W., HUNT, J., HILL, R., HAND, J., VERNON, C., VAN RHOON, G.C., VAN DER ZEE, J., GONZALEZ GONZALEZ, D.G., VAN DIJK, J., WHALEY, J. AND MACHIN, D. 1997, Relationship between thermal dose and outcome in thermoradiotherapy treatments for superficial recurrences of breast cancer: data from a phase III trial. *International Journal of Radiation Oncology Biology Physics*, **39**, 371-380.

SNEED, P.K., STAUFFER, P.R., MCDERMOTT, M.W., DIEDERICH, C.J., LAMBORN, K.R., PRADOS, M.D., CHANG, S., WEAVER, K.A., SPRY, L., MALEC, M.K., LAMB, S.A., VOSS, B., DAVIS, R.L., WARA, W.M., LARSON, D.A., PHILLIPS, T.L. AND GUTIN, P.H. 1998, Survival benefit of hyperthermia in a prospective randomized trial of brachytherapy boost ± hyperthermia for glioblastoma multiforme. *International Journal of Radiation Oncology Biology Physics*, **40**, 287-295.

STAUFFER, P.R., ROSSETTO, F., LEONCINI, M. AND GENTILLI, G.B. 1998, Radiation patterns of dual concentric conductor microstrip antennas for superficial hyperthermia. *IEEE Transactions on Biomedical Engineering*, **45**, 605-613.

STUBBS, M. AND GRIFFITHS, J.R. 1999, Monitoring cancer by magnetic resonance. *British Journal of Cancer*, **80 Suppl 1**, 86-94.

SULLIVAN, D.M., BEN-YOSEF, R. AND KAPP, D.S. 1993, Stanford 3D hyperthermia treatment planning system. Technical review and clinical summary. *International Journal of Hyperthermia*, **9**, 627-643.

THARP, H.S. AND ROEMER, R.B. 1992, Optimal power deposition with finite-sized, planar hyperthermia applicator arrays. *IEEE Transactions on Biomedical Engineering*, **39**, 569-579.

THRALL, D.E., ROSNER, G.L., AZUMAS, C., SAMULSKI, T.V., CASE, B.C., LARUE, S.M. AND DEWHIRST, M.W. 1999, Thermal dose quantified at CEM 43°C T90 can be delivered as prescribed. *Abstractbook, "18th Annual Meeting of the North American Hyperthermia Society", April 8-10, USA*, 23, Abstract

TURNER, P.F. 1984, Regional hyperthermia with an annular phased array. *IEEE Transactions on Biomedical Engineering*, **31**, 106-114.

TURNER, P.F. 1998, Development in deep EM phased array heating-BSD-2000.3D. *Abstractbook, "17th Annual Meeting of the European Society for Hyperthermic Oncology", September 2-5, Nancy, France*, 67, Abstract

VAN DER ZEE, J., TREURNIET-DONKER, A.D., THE, S.K., HELLE, P.A., SELDENRATH, J.J., MEERWALDT, J.H., WIJNMAALEN, A.J., VAN DEN BERG, A.P., VAN RHOON, G.C., BROEKMEYER-REURINK, M.P. AND REINHOLD, H.S. 1988, Low dose reirradiation in combination with hyperthermia: a palliative treatment for patients with breast cancer recurring in previously irradiated areas. *International Journal of Radiation Oncology Biology Physics*, **15**, 1407-1413.

VAN DER ZEE, J., VAN RHOON, G.C., VERLOOP-VAN 'T HOF, E.M., VAN DER PLOEG, S.K., RIETVELD, P.J.M. AND VAN DEN BERG, A.P. 1992, The importance of adequate heating techniques for therapeutic outcome.

Proceedings of the 6th International Congress on Hyperthermic Oncology, Tuscon, Arizona, April 27-May 1, 2, 349-352.

VAN DER ZEE, J., GONZALEZ GONZALEZ, D., VAN RHOON, G.C., VAN DIJK, J.D.P., VAN PUTTEN, W.L.J., HART, A.A.M., KOPER, P.C.M., DE WIT, G.A. AND DE CHARRO, F.T. 1996, Results of additional hyperthermia in inoperable pelvic tumours. *Hyperthermic Oncology 1996, Volume II. Proceedings of the 7th International Congress on Hyperthermic Oncology. Roma, Italy, April 9-13, 1996.* edited by C.F.G. Arcangeli and R. Cavaliere (Rome: Tor Vergata University of Rome, Italy), pp. 215-217.

VAN DER ZEE, J., VAN DER HOLT, B., RIETVELD, P.J., HELLE, P.A., WIJNMAALEN, A.J., VAN PUTTEN, W.L. AND VAN RHOON, G.C. 1999, Reirradiation combined with hyperthermia in recurrent breast cancer results in a worthwhile local palliation. *British Journal of Cancer*, 79, 483-490.

VAN DER ZEE, J., GONZALEZ GONZALEZ, D., VAN RHOON, G.C., VAN DIJK, J.D.P., VAN PUTTEN, W.L.J. AND HART, A.A.M. 2000, Comparison of radiotherapy alone with radiotherapy plus hyperthermia in locally in locally advanced pelvic tumours: a prospective, randomised, multicentre trial. *The Lancet*, 355, 1119 1125.

VAN DER ZEE, J. AND GONZALEZ GONZALEZ, D. 1995, Hyperthermia in in operable pelvic tumours. *Strahlentherapie und Onkologie*, 171, 11, Abstract

VERNON, C.C., HAND, J.W., FIELD, S.B., MACHIN, D., WHALEY, J.B., VAN DER ZEE, J., VAN PUTTEN, W.L., VAN RHOON, G.C., VAN DIJK, J.D., GONZALEZ GONZALEZ, D., LIU, F.F., GOODMAN, P. AND SHERAR, M. 1996, Radiotherapy with or without hyperthermia in the treatment of superficial localized breast cancer: results from five randomized controlled trials. International Collaborative Hyperthermia Group. *International Journal of Radiation Oncology Biology Physics*, 35, 731-744.

WUST, P., FÄHLING, H., HELZEL, T., KNIEPHOFF, M., WLODARCZYK, W., MÖNICH, G. AND FELIX, R. 1999, Design and test of a new multi-amplifier system with phase and amplitude control. *International Journal of Hyperthermia*, 14, 459-478.

Summary

In this thesis we have presented technical and clinical results from research in mainly superficial hyperthermia.

The basis for this research project was formed by the analyses of clinical superficial hyperthermia data obtained from two different heating techniques (**chapter 2**). The main conclusion from this study was that reirradiation with hyperthermia in recurrent breast cancer resulted in a worthwhile local palliation. The overall complete response (CR) rate was 58% for the original technique (2450 MHz) and 74% for the new technique, using water-filled waveguide applicators (WGAs) operated at 433 MHz. A remarkable difference in CR was found as function of maximum tumour diameter (≤ 3 cm or >3 cm): for the small tumours the CR was $\geq 87\%$, for large tumours the CR was 31% (2450 MHz) or 65% (433 MHz). We concluded that small tumours were properly heated, but even with the improved technical qualities of the 433 MHz system, the larger tumours responded less well. An additional technical improvement was needed. A research project proposal titled 'Clinical verification and optimisation of the quality of hyperthermic treatment of large superficial tumors of the chest wall' was granted by the Dutch Cancer Society (grant DDHK 93-603) and formed the backbone of this thesis.

The basic method used to monitor clinical hyperthermic quality is that of measuring the temperature during treatment. However, under clinical circumstances, practical limitations of invasive thermometry exist. They are discussed in **chapter 3** and the value of invasive thermometry for optimisation of the treatment appeared limited. Due to the relatively low number of temperature sites over the treatment volume, the calculated thermal dose parameters are considered to be of limited value. The problem of validation of thermal dose

calculations is addressed more extensively the General Discussion (**chapter 10**). To quantify antenna quality more accurately, a technical SAR-based evaluation of antenna characteristics was carried out first.

In **chapter 4** we presented the first results from a new type of 433 MHz antenna, the Lucite Cone Applicator (LCA). Quality was calculated from SAR distributions from antennae radiating in muscle-equivalent tissue. In an attempt to improve the quality of superficial hyperthermia treatments of larger tumours, we modified a conventional waveguide antenna (aperture 10x10 cm^2) which increased its effective field size (EFS) from 32 cm^2 to 100 cm^2. This was obtained through replacement of the diverging metal sidewalls that are parallel with the dominant E-field by Lucite and inserting a PVC cone in the aperture. During experiments with different dimensions of waterboli, which couple the radiation to the patient, strong influences on the EFS were found.

Based on this improvement, the SAR distributions from arrays of antennae were investigated by means of thermographical (TG) imaging and Gaussian beam (GB) modelling (**chapter 5**). Firstly, the SAR profiles along the principal planes were measured with a small dipole and compared with TG-measured SAR values. These dipole data were used as input for the GB modelling. The GB modelling is capable of calculating SAR distributions from 1D-layered structures, so its major drawback is the impossibility of modelling finite shaped water layers (i.e. waterboli). Using a large waterbolus in the TG-measured SAR distribution gave a proper match with the GB-predicted SAR distribution from a single LCA. Secondly, SAR distributions at 1 cm depth in muscle-equivalent tissue from 2x1 arrays of LCA were TG-measured, GB-predicted and compared. For clinical settings the differences between TG-measured and GB-predicted SAR distributions were acceptable although we measured some interaction between the LCAs in the array.

In **chapter 6**, we investigated 2x2 arrays of LCAs in different E-field orientated configurations. The GB model was used to predict SAR distributions from incoherently equally powered antennae. In the case of a clockwise-orientated E-field configuration, the maximum EFS was found that covered almost the entire aperture. Also the problem of antenna interaction was addressed. TG-measured SAR distributions showed that adjacent antennae moved the local maximum SAR towards the outer lucite aperture boundaries. The GB model does not take mutual interactions into account. However, the difference between TG-measured and GB-predicted SAR distributions was less equal than 15% on average and

dropped to 12% when an additional spacing of 2 cm was added to decrease antenna interactions. Especially in the more important EFS area, the difference decreased to 9% after implementing the 2 cm interspace in the clockwise-orientated E-field configured 2x2 LCA-array. From these (GB-modelled) results we concluded that the LCA was a technical better antenna than the WGA.

A second important item in the project was to find out the relevance of high spatial resolution in power control in optimising treatment quality. This can decrease penetration depth (PD). The Current Sheet Applicator (CSA) was developed into a clinical applicable antenna (aperture 6.6x7.5 cm²) and technically compared with the LCA (chapter 7). The CSA represented the small antenna capable of relative high spatial adaptation of power at the cost of 2 mm GB-predicted PD compared that of the LCA. Further technical comparison was based on field sizes (FS) of 50% (i.e. EFS), 75% and 25% SAR at either 1 cm depth in muscle-equivalent tissue or over a 3 cm deep volume covering the array aperture. For a single LCA and CSA, the EFS measured 69% respectively 57%. The SAR homogeneity coefficient (HC=FS_{75}/FS_{25}) for both single antennae was about equal. The comparison based on 2x2 LCA array and 3x3 CSA array GB predicted SAR distributions showed an increase of EFS to 75% respectively 72% and an increase of HC from 0.2 to 0.3. This indicated that a summation of single SAR distributions in an array application of both LCA and CSA resulted in constructively better SAR distribution. We concluded that the LCA and CSA performed technical equally well.

Based on the results from the GB-predicted SAR distributions from 2x2 LCA arrays, a clinical intra-patient study was set up in which the LCA was compared with the WGA to find out to what extent the technical improvements would be reflected in the power and temperature distributions. Although the EFS was about 3 times larger for the LCA compared to that of the WGA, the average power per LCA only increased by about 30%. The invasively measured temperatures increased by 0.27 °C on average. Since the main SAR difference between the two systems was found in the periphery of the antenna aperture, we analysed the temperature difference between the centre and the periphery of the aperture. For the WGA the average temperature in the centre of the aperture was 0.43 °C higher than in the periphery, while for the LCA this difference was –0.05 °C. This meant that the LCAs heated more uniformly than the WGAs. The minimum temperatures remained unchanged. From these

results we concluded that the LCA was clinically superior to the WGA. The LCA became therefore our new standard antenna for superficial hyperthermia.

From basic GB modelling of the LCA and basic temperature analyses of clinical data from LCA and WGA treatments we concluded that the LCA was superior. However, there are still questions to be answered: what is the optimal waterbolus size for clinical applications with the LCA, which problems generate mutual antenna interactions under clinical circumstances and why is the increase in temperature relatively small compared to the clinical results using the WGA? Since TG measurements of SAR are cumbersome and relatively slow when dealing with array applications of antennae, we started research on more sophisticated SAR modelling by means of Finite-Difference Time-Domain (FDTD) calculus. Chapter 9 presents the first results of modelling the LCA with FDTD. Special attention was paid to modelling the diverging metal sidewalls. The 'diagonally split cell model' was implemented on these sidewalls. Furthermore, it was found that modelling the Lucite cover in front of the antenna plays an important role for the calculations. Taking these two points into consideration, the FDTD-predicted SAR distribution of the LCA at 1 cm depth in a flat, homogeneous, muscle-equivalent phantom became comparable to that of the TG-measured SAR distributions.

The first FDTD results encouraged us to set up additional research in FDTD-calculations in the near future, which will include a thorough parameter study. Firstly, this study will be concerned with waterbolus size effects on the SAR distribution and typical side effects (e.g. mutual interaction) in array applications of the LCA and secondly it will concentrate more on clinically-orientated situations involving array applications on (curved) 3D tissue geometries. We expect that this study will push the quality of superficial hyperthermia treatments of especially the larger chest wall recurrences of breast cancer to a higher level and eventually will result in an improved CR rate comparable to that found for smaller lesions that are treated with low dose radiotherapy plus hyperthermia.

Samenvatting

In dit proefschrift worden technische en klinische resultaten gepresenteerd van onderzoek gedaan in voornamelijk oppervlakkige hyperthermie.

De basis voor dit onderzoek werd gevormd door de analyse van gegevens van oppervlakkige hyperthermiebehandelingen waarin twee verschillende verwarmingstechnieken werden vergeleken (hoofdstuk 2). De belangrijkste conclusie van dat onderzoek was dat de combinatie van een lage dosis bestraling en hyperthermie bij de behandeling van terugkomende borstkanker leidde tot waardevolle klachtenverminderingen. De gecombineerde behandeling sloeg aan (d.w.z. gaf een complete respons (CR)) bij 58% van de patiënten indien de oude techniek werd gebruikt (frequentie 2450 MHz) en bij 74% indien de nieuwe techniek werd gebruikt van Watergevulde GolfpijpAntennes (WGAs, frequentie 433 MHz). Een opmerkelijk verschil in CR werd gevonden als functie van de tumordiameter (kleiner gelijk dan 3 cm of groter dan 3 cm): voor de kleine tumoren was de CR 87%, voor de grote tumoren was de CR 31% (2450 MHz) of 65% (433 MHz). We concludeerden dat de kleine tumoren goed konden worden verwarmd maar dat zelfs met de verbeterde technische kwaliteiten van het 433 MHz systeem, de grotere tumoren slechter reageerden op de gecombineerde behandeling dan de kleine tumoren. Een aanvullende technische verbetering was gewenst. Een onderzoeksproject getiteld "Klinische verificatie en optimalisatie van de kwaliteit van hypertherme behandelingen van grote oppervlakkige tumoren van de borstkast" werd financieel gehonoreerd door de Nederlandse Kankerbestrijding-Koningin Wilhelmina Fonds (project DDHK 93-603). Dit project vormde de ruggengraat van dit proefschrift.

De eenvoudigste methode om de kwaliteit van de hyperthermiebehandeling te bekijken, is door temperaturen te meten tijdens de behandeling. Er zijn echter klinische omstandigheden die tot praktische beperkingen leiden bij inwendige temperatuurmetingen. We behandelen deze beperkingen in hoofdstuk 3. De waarde van inwendige temperatuurmetingen voor het optimaliseren van de behandeling bleken beperkt. Door het relatief lage aantal meetpunten in het behandelingsgebied, zijn de berekende hyperthermie dosisgetallen van beperkte waarde. Dit probleem wordt verder uitgewerkt in hoofdstuk 10. Om het gemis in kwaliteit van temperatuurmetingen in de kliniek te omzeilen, is gekozen om eerst een basale technische evaluatie van aanpassingen in de applicatie uit te voeren.

In hoofdstuk 4 hebben we de eerste resultaten gepresenteerd van een nieuw type 433 MHz antenne, de Lucite Cone Applicator (LCA) met een antenneopening van $10*10$cm^2. De kwaliteit van deze antenne werd berekend van SAR-verdelingen in materiaal met spierequivalente eigenschappen. In een poging de kwaliteit van oppervlakkige hyperthermiebehandelingen van grote tumoren te verbeteren, hebben we de WGA aangepast wat leidde tot een verhoging van de effectieve veldgrootte (EFS) van 32 cm^2 tot 100 cm^2. Dit werd bereikt door de metalen divergerende zijwanden welke parallel lopen aan het dominante elektrische veld te vervangen door perspex. Tevens werd een PVC kegel in de antenneopening geplaatst. Tijdens experimenten waarbij verschillende grootte waterbolussen werden gebruikt, die voor een koppeling zorgen van antenne naar patiënt, bleek dat deze variaties sterke invloed hadden op de EFS.

Gebaseerd op deze verbeteringen, werden thermografische (TG) gemeten en Gaussian beam (GB) berekende SAR distributies onderzocht (hoofdstuk 5). Eerst werden de SAR-profielen in de hoofdvlakken gemeten met een kleine dipoolantenne en deze waarden werden vergeleken met TG-gemeten SAR-waarden. De dipoolgemeten data diende als invoer voor de GB-berekeningen. GB-berekeningen kunnen informatie geven over SAR-verdelingen van 1-dimensionaal gelaagde structuren. De grootste tekortkoming van het GB-model is het gebrek om het effect van een eindige waterlaag (d.w.z. een waterbolus) in het model op te nemen. Door het gebruik van een grote waterbolus in de TG-gemeten SAR-verdelingen, werd een goede overeenkomst gevonden met de GB-berekende SAR-verdeling. Vervolgens werden de SAR-verdelingen op 1 cm diepte in spierequivalent weefsel gemeten (TG) en berekend (GB). Deze verdelingen werden vervolgens vergeleken. Onder klinische voorwaarden waren de verschillen tussen de TG- en GB-SAR-verdelingen acceptabel. Bij de TG-gemeten SAR verdelingen werd een interactie tussen de twee LCAs gevonden die de verdeling beïnvloedde.

In hoofdstuk 6 hebben we de eigenschappen onderzocht van een 2x2 array van LCAs die in onderling verschillende E-veld oriëntaties waren geconfigureerd. Het GB-model werd gebruikt om SAR distributies te berekenen van incoherente aangestuurde antennes met een gelijke vermogensinstelling. Indien de kloksgewijze E-veldconfiguratie werd toegepast, werd de maximale EFS voor een 2x2 array van LCAs gevonden. Dit effectieve veld bedekte bijna de gehele oppervlakte van de array. Ook werd het probleem van de onderlinge antennewisselwerking bestudeerd. TG-gemeten SAR verdelingen lieten zien dat bij aangrenzende antennes de lokale SAR maxima werden verschoven naar de perspexbuitenzijde van de antenneopening. Hoewel het GB-model geen rekening houdt met onderlinge antennewisselwerkingen,

was het verschil tussen de TG-gemeten en GB-berekende SAR verdelingen gemiddeld kleiner dan 15%. Het verschil verminderde tot 12% als een 2 cm grote tussenruimte tussen de antennes in de array werd toegevoegd om de wisselwerking te verminderen. In het SAR domein van de EFS werd het verschil 9% na de implementatie van de 2 cm tussenruimte voor de kloksgewijze E-veld configuratie van de 2x2 LCA array. Gebaseerd op deze resultaten concludeerden we dat de LCA technisch beter was dan de WGA.

Een tweede onderdeel binnen het project was het uitzoeken van het belang van een hoge ruimtelijke resolutie in vermogenssturing bij het optimaliseren van de behandeling. Dit gaat mogelijk ten koste van indringdiepte (PD) van de straling. De 'kleine' Current Sheet Applicator (CSA) werd geschikt gemaakt voor gebruik in de kliniek (antenneopening 6.6*7.5 cm^2) en vergeleken met de 'grote' LCA (hoofdstuk 7). De GB-berekende PD van de CSA bedroeg 2 mm minder dan die van de LCA. De technische vergelijking van de twee antennetypes was gebaseerd op veldgroottes (FS) van 50% SAR (EFS), 75% en 25% SAR op ofwel 1 cm diepte in spierequivalent weefsel ofwel over een volume van 3 cm diep opgespannen door de array. Voor één LCA en CSA bedroeg de EFS respectievelijk 69% en 57%. De SAR homogeniteitcoëfficiënt (HC=FS$_{75}$/FS$_{25}$) was voor beide antennes nagenoeg gelijk. De vergelijkingen gebaseerd op GB-berekeningen van een 2x2 LCA-array en een 3x3 CSA-array toonden een verhoging in de EFS tot 75% respectievelijk 72% en een verhoging in de HC van 0.2 tot 0.3. Dit geeft aan dat een sommatie van individuele SAR distributies in een array-applicatie voor zowel de LCA als de CSA leidde tot een constructief verbeterde SAR verdeling. We concludeerden dat de LCA en CSA technisch gelijkwaardige antennes zijn.

Gebaseerd op de resultaten van de GB-berekende SAR verdelingen van 2x2 LCA arrays, werd een klinisch intra-patiënten onderzoek opgezet waarbij de LCA werd vergeleken met de WGA (hoofdstuk 8). Hieruit moest duidelijk worden in hoeverre een technische verbetering zou leiden tot gewijzigde vermogens- en temperatuurverdelingen. Hoewel de EFS van de LCA ongeveer 3 maal zo groot is als die van de WGA, nam het gemiddelde vermogen per LCA slechts toe met ongeveer 30%. De gemiddelde invasief gemeten temperatuur werd 0.27°C hoger. Omdat het verschil in de SAR-verdeling van de twee systemen voornamelijk in de buitenrand van de antenneopening zit, hebben we het temperatuurverschil tussen centrum en periferie onder de antenneopening geanalyseerd. Voor de WGA was de gemiddelde temperatuur in het centrum 0.43°C hoger dan in de periferie terwijl voor de LCA het temperatuurverschil - 0.05°C bedroeg. Dit betekent dat de LCAs meer uniform verwarmen dan de WGAs. De minimum temperatuur bleef echter ongewijzigd. Een statistische analyse van deze gegevens resulteerde in een significant verschil dus de LCA was klinisch superieur aan de WGA. De LCA werd dan ook tot standaardantenne gekozen voor oppervlakkige hyperthermie.

Middels eenvoudige GB-modelberekeningen aan de LCA en middels temperatuuranalyses van klinische data verkregen met LCAs of WGAs, hebben we geconcludeerd dat de LCA beter was dan de WGA. Er zijn echter nog een aantal vragen die moeten worden beantwoord: wat is de optimale afmeting van de waterbolus bij gebruik van de LCA, welke problemen in de kliniek worden veroorzaakt door onderlinge wisselwerkingen tussen de antennes en waarom is de verhoging van de gemiddelde invasief gemeten temperatuur bij gebruik van de LCAs relatief klein t.o.v. de WGAs? Omdat TG-metingen van de SAR relatief moeilijk zijn en langzaam gaan indien klinische applicaties worden gesimuleerd, hebben we onderzoek gestart naar het gebruik van een meer geavanceerd SAR-bepalend rekenmodel, de Finite-Difference Time-Domain (FDTD) methodiek. In hoofdstuk 9 presenteren we de eerste resultaten voor de LCA van deze berekeningstechniek. Er werd speciale aandacht besteed aan het correct modelleren van de divergerende metalen wanden. Het 'diagonally split cell model' werd toegepast om een optimale representatie te krijgen. Ook bleek dat de perspex plaat in de antenneopening een grote invloed had op de berekende SAR distributie. Rekeninghoudend met deze twee specifieke problemen, bleken de FDTD-berekende SAR distributies op 1 cm diepte in spierequivalent fantoom van een LCA goed overeen te komen met de TG-gemeten SAR distributies.

De eerste FDTD-resultaten hebben ons bemoedigend om het FDTD-onderzoek verder uit te werken in de nabije toekomst in de richting van een gedetailleerd onderzoek. In deze studie zullen we ons eerst richten op het effect van de waterbolus op de SAR verdeling als functie van de afmetingen, de onderlinge antennewisselwerkingen in een array applicatie van de LCA en vervolgens zullen we ons concentreren op meer klinisch-relevante situaties waarin de antenne arrays stralen op (gekromde) 3D-weefseldistributies. We verwachten dat deze studie de kwaliteit zal verhogen van oppervlakkige hyperthermische applicaties van grotere terugkomende borstkanker op de borstwand. Mogelijk kan dit leiden tot een verbeterde complete respons welke vergelijkbaar is met die van kleinere borstkankertumoren die behandeld worden met een lage dosis radiotherapie en hyperthermie.

Word of thanks

Completion of this thesis could not have been successful without the help and support of many people. I will mention the persons who were closely involved in the presented work.

First of all I thank you Peter Levendag for having the courage to enter the fields of hyperthermic physics and guide me to and through the clinical landscape I found myself in and mould the subjects we found on our way into this booklet.

Cobi, hours of discussions on the various subjects closely related to hyperthermia or otherwise, provided an environment in which a physicist can do his hyperthermic research and can find a meaning behind the numbers he generates. Your motto as I perceived it 'Anything to benefit the patient' was always a great motivating force.

Gerard, as co-promoter, you were the key to this project. You never seem to have a lack of ideas on how to tackle a problem. As a colleague your critical attitude towards results obtained, although seeming to slow down the process, actually gave extra impetus to progress.

Jeff Hand, Mikaya Lumori and Mike Prior, you took the trouble to spend time in explaining to me how to use the Gaussian beam model. I never thought that I would be able to exploit its possibilities to this extent. It was an important contribution to this thesis.

Tom Cetas, we could quickly design a clinically reliable CSA thanks to your involvement. The project could not have been finished in time without your support.

To all my other colleagues, the fact that you have been able to cope with all my hyperthermic-products-in-progress and with me as me, has been of great help to get the work done. It is your flexibility together with your enthusiasm for hyperthermia that has made us as a group so successful.

Mum and dad, you were always there in the background, stimulating me to continue on the road of progress from secondary school onwards. Your encouragement paid off eventually. Thank you so much for having faith in me.

Dear Annette, the transfer of research results from a logbook into a peer-reviewed article is an essential and sometimes troublesome part of the work a scientist has to do. You helped me to formulate clear and concise manuscripts with improved readability. It made all the difference to the reviewers and me. Thanks a lot.

Curriculum vitae

Naam	Rietveld, Paulus Johannes Maria
Geboortedatum	12 juli 1959
Geboorteplaats	Rotterdam

OPLEIDING

1971 – 1975	MAVO-4 aan de RKSG Sint-Montfort te Rotterdam
1975 – 1977	HAVO aan de RKSG Sint-Montfort te Rotterdam
1977 – 1979	Atheneum B aan de RKSG Sint-Montfort te Rotterdam
1979 – 1987	Experimentele Fysica aan de Rijks Universiteit Utrecht (RUU) Grootonderzoek: Onderzoek naar objektieve meetkriteria voor de klankkwaliteit van een concertpauk

WERKERVARING

1987	Medewerker sectie Centrale Computergroep van de Faculteit Natuur- en Sterrenkunde - RUU
	Onderzoek naar ogenmotoriek bij (niet-)dyslectische kinderen aan de afdeling Biomedische Natuurkunde en Technologie van de Medische Faculteit van de Erasmus Universiteit Rotterdam
1989 –	Onderzoek in oppervlakkige en diepe hyperthermie in de sectie Hyperthermie van de afdeling Radiotherapie van het Academisch Ziekenhuis Rotterdam-Daniel
1989 – 1991	Nederlandse Kankerbestrijding (NKB) project RRTI 87-9
1991 – 1992	NKB project DDHK 91-8
1992 – 1993	OG-project 89-32
1993 – 1997	NKB project 'Clinical verification and optimisation of the quality of hyperthermic treatment of large superficial tumours of the chest wall' (DDHK 93-603)
1997 – heden	NKB project '3D-SAR optimisation and quality assurance for the BSD2000 system in clinical practice' (DDHK 97-1497)